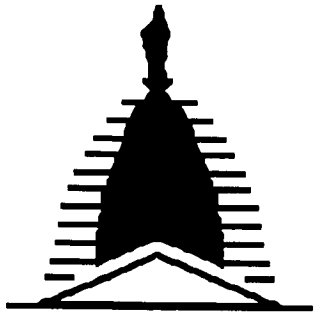

UNIVERSITY of
NOTRE DAME

NASA/USRA UNIVERSITY ADVANCED DESIGN PROGRAM 1988-1989

Final Design Proposal

THE SPiRiT

An RPV Designed to Investigate
the Pressure Distribution on a Lifting Surface

Department of Aerospace and Mechanical Engineering
University of Notre Dame
Notre Dame, IN 46556

SPiRiT

A Proposal for an Aerodynamic Testing

Remotely Piloted Vehicle

Design Team:

Team Leader Tyrus Soares
Ken Ancerewicz
Sarah Cantu
Keith Ebner
Paul Edwards
Jennifer Kreykes
Eric Lewis
Sam Siewert
Nick Simon
Markus Wenninger

UNIVERSITY OF NOTRE DAME
DEPARTMENT OF AEROSPACE
AND MECHANICAL ENGINEERING
AEROSPACE DESIGN
AERO 441-SPRING SEMESTER 1989

TABLE OF CONTENTS

NOMENCLATURE

ac	aerodynamic center
A/D	analog-to-digital
AR	aspect ratio
a_w	lift curve slope of wing
b	wing span
B	number of propeller blades
c	wing mean chord
cg	center of gravity
C_D	total drag coefficient
$C_{D\pi}$	flat plate drag coefficient
C_{do}	parasitic drag coefficient
C_f	fuselage correction factor
CG	center of gravity
C_l	section lift coefficient
C_L	wing lift coefficient
C_{Lmax}	maximum lift coefficient
C_{Lo}	lift coefficient at zero angle of attack
C_{Lt}	tail lift coefficient
C_{Ltrim}	aircraft lift coefficient to trim
$C_{L\alpha}$	lift curve slope
$C_{L\alpha t}$	tail lift curve slope
$C_{L\alpha v}$	vertical tail lift curve slope
$C_{L\alpha w}$	wing lift curve slope
C_{mo}	pitching moment intercept
$C_{m\alpha}$	pitching moment slope
$C_{m\alpha w}$	wing pitching moment slope
$C_{n\beta}$	yawing moment curve slope
$C_{n\delta r}$	rudder control effectiveness coefficient
C_P	power coefficient
C_T	thrust coefficient
d	diameter
D	drag force
$dC_{Lt}/d\delta_e$	elevator effectiveness
$dC_{Lv}/d\delta_r$	rudder effectiveness

$dC_m/d\alpha$	aircraft pitching moment slope
e	span efficiency
f	fuselage
HT	horizontal tail
i	incidence angle
Ix	mass moment of inertia
Iy	mass moment of inertia
Iz	mass moment of inertia
J	advance ratio
k_f	wing correction factor
k_n	wing-body interference factor
k_{RI}	Reynolds number correction factor
L	lift force
l_f	length from center of gravity to tail plane
M_t	tip Mach number
n	revolutions per second
S	wing area
SFC	specific fuel consumption
S_{fs}	projected side area of fuselage
SHT	horizontal tail area
S_w	wing area
t	tail
t	thickness
T_o	static thrust
ts	test specimen
V	velocity
V_{to}	takeoff velocity
VH	horizontal tail volume ratio
V_V	vertical tail volume ratio
VT	vertical tail
w	wing
W	weight
w_f	maximum width of fuselage
x_{cg}	distance to center of gravity of aircraft
x_{ac}	distance to wing aerodynamic center
α	angle of attack

δ_{trim}	elevator angle to trim
Γ	dihedral angle
η_p	propeller efficiency
η	tail to wing velocity ratio parameter
ρ	ambient density
τ	elevator or rudder effectiveness parameter

EXECUTIVE SUMMARY

Typically, most aerodynamic data is obtained from the use of a windtunnel. There are both advantages and disadvantages to using a wind tunnel to collect aerodynamic data. It is simple to control model position and flow speed, however at the same time wall interference and free stream turbulence are almost impossible to control. Wind tunnels can also be limited by the ability to achieve dynamic similarity between the test and actual flight conditions. To alleviate some of these problems, it would be desirable to actually collect the data in-flight; very much like a "flying wind tunnel." Remotely Piloted Vehicles (RPVs) can be readily adapted to this task. The goal of this project is to design an RPV capable of taking in-flight aerodynamic data on a lifting surface.

The Surface Pressure Readings and Testing (SPiRiT) aircraft is designed to measure the surface pressure distributions about a two and three dimensional lifting surface at Reynolds numbers ranging from 4.0×10^4 to 1.0×10^6. The RPV will be able to accomodate lifting surfaces with spans ranging from 1 to 5 feet and chords ranging from 4 to 16 inches. The test specimen itself will be able to rotate in flight to angle of attacks ranging from -20° to 40°.

To meet these mission objectives, it was necessary to define and prioritize the mission goals. The foremost goal of this design is to be able to make accurate measurements of the pressure field on the test specimen. While this would seem to be an obvious goal, the ramifications are quite subtle in themselves. Because the flow conditions about the test specimen cannot be adequately controlled during flight, it is necessary to measure all points of the pressure field simultaneously (or as close to simultaneous as possible).

Assuming that this can be accomplished, the next consideration is the influence the RPV has on the flow around the test specimen. To minimize the disturbance, a push-propeller, high-wing configuration was selected. Furthermore, the test specimen was mounted as far forward as possible to minimize the effects of the wing and propeller. Views of the final configuration are given in the '3-View Configuration' in Figure 1.

The secondary design goals generally involved optimization of the performance parameters, maximization of stability and control authority, and minimizing weight. To maximize the amount of time in the air it is necessary to reduce the drag and weight of the RPV while at the same time increasing lift and power. These goals led to a high aspect ratio wing and a relatively large power plant. The test specimen mounted forward of the main fuselage will create large aerodynamic forces significantly altering the the stability and control characteristics. Thus in order to control these high forces a large tail and control surface will be required. At the same time, because an automatic flight control system will be incorporated into the design, it is felt that the RPV should be as statically and dynamically stable as possible. This will reduce the work load of the flight control system

The actual test specimen itself should be easily interchangeable with other test specimens. This will make the entire RPV a more versatile and easy to use experimental tool. For ease of operation two people at most should be needed for operation. One person controls the data acquisition and the other person controls the flight systems.

The current design has met all these goals. The A/D system collects one pass of data in .2 seconds and stores the data on board for later retrieval. The RPV will fly for a maximum of thirty minutes and collect data for twenty minutes. It can be operated by two people in a 45.7 meter (150 foot) radius clearing. A

complete summary of all the design specifications is given in the 'Design Specifications' following the aircraft 3-view.

The design itself, however, is incomplete in several key areas. The stability analysis has shown a static margin of 75%. By appropriately shifting the location of the internal components of the RPV, it is possible to move the center of gravity to a more desirable location. Similarly, the weight estimations are not as exact as can be and thus calculations dependent on these weight estimations will be inexact as well.

One other aspect that needs to be examined further deals with the overall lift forces created by the test specimen, tail section and wing when the test specimen is at a positive angle of attack. The lift generated by all three surfaces combined is much greater than the weight of the aircraft and results in load factors as high as 9.5. A preliminary design concept to correct this is to have the wing rotate on its pylon so as to produce a downward force instead of lift. This wing rotation will be coordinated with the test specimen angle of attack and flight velocity to ensure steady level flight of the aircraft. This will be accomplished by the automatic flight control system (AFCS). Perhaps an even more simple solution would be to mount the specimen inverted for positive angle of attack testing, and thus really put the specimen through a negetive angle of attack as far as the aircraft is concerned, yet provide high positive angle of attack conditions for the specimen. Although such a strategy means that positive and negative angle of attack tests must be completed in separate missions.

Before this RPV can go into production, several key technologies must be developed. The data acquisition system uses four parallel processing A/D converters to increase the frame sample rate. Parallel processing is a

complicated and very expensive concept. It requires much electronic support that has not been considered in this design. Until parallel processing technology develops to the point where the supporting electronic circuitry is not needed, the space limitation on the boards makes the concept of parallel processing A/D converters unfeasible. Similarly, the Automatic Flight Control System utilizes a closed loop feedback system to regulate the airspeed and angle of attack of the test specimen. To save space and weight the RPV was not equipped with this processing capability, therefore the pertinent information must be radioed to the ground and the correction signals radioed back to the RPV. There is a distinct possibility that the telemetry system will take too long to encode, transmit, and decode the data. If the telemetry system does take too long, then the controls will not respond to the changing environment as desired and the acquired data will be useless.

It is generally recognized that the design of this RPV is still in its preliminary stages. Another iteration of the design process should bring the final design of this concept into a much sharper perspective.

FIGURE 1. THREE VIEW CONFIGURATION

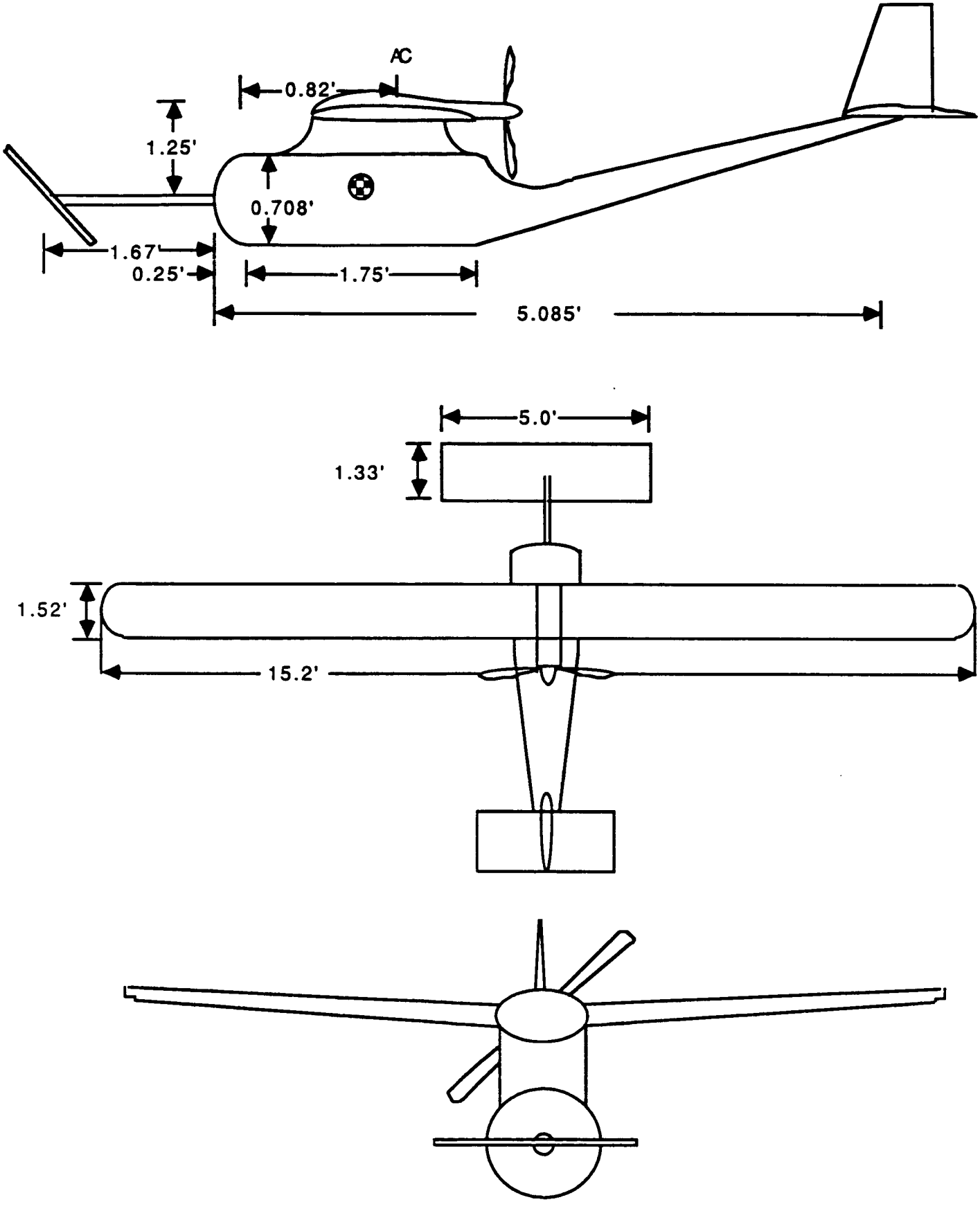

DESIGN SPECIFICATIONS

OVERALL SPECS:

WEIGHT TOTAL	30 lb	
(see chapter 4 for detailed breakdown)		
Drag		
Cd0 (dirty, test @ 0°)	.0395	
Cd0 (dirty, test @ 30°)	.0995	
Cd0 (worst case)	.1295	
Lift		
CLmax	0.916	
Stall Angle	6°	
Flight Velocity Range	11 m/s - 44 m/s	36.1 ft/s - 144.4 ft/s
Center of Gravity	30% mean aerodynamic chord	

FUSELAGE

Cross Sectional Shape	circular	
diameter	0.172 m	6.77 inches
Length	1.55 m	5.09 ft
Fineness Ratio	7.2	

WING:

Airfoil Section	Gottingen 797	
Planform shape	Rectangular	
Area	2.15 m2	23.12 ft^2
Aerodynamic Center	25% mean aerodynamic chord	
Aspect Ratio	10	
Wing Loading		1.3 psft
Span	4.64 m	15.2 ft
Sweep	0°	
Chord	.46m	1.52 ft
Load Factor	4.5	
Oswald Efficiency	.91	

Dihedral Angle	5° (Total)	
Zero Lift Angle	-7°	
$C_{l_{max}}$ (section at 12°)	1.11	
$C_{l_{max}}$ (wing)	1.0	
C_{l_α}	(section)	5.3 rad^{-1}
C_{m_α}	-.2176	
C_{d_0} (section)	.015	

CONTROL SURFACES:

Area Ratio:	
Horizontal	1.0
Vetical	0.2
Total Deflection Angle	10° to -10°

VERTICAL TAIL:

Airfoil Section	NACA 0009
Tail Volume Ratio	0.374
Tail Area	0.28 m^2
C_{l_α} (tail)	6.3 rad^{-1}
Chord	0.3 m
Span	0.917 m

HORIZONTAL TAIL:

Airfoil Section	NACA 0009	
Area	.7503 m^2	8.073ft^2
Aspect Ratio	2	
Sweep	0°	
Taper Ratio	1	
Tail Volume Ratio	.7 - 1.0	
Zero Lift Angle	-3.3°	
$C_{l_{MAX}}$ (tail at 10°)	.5311	
$C_{l_{MAX}}$ (section at 10°)	1.2	
C_{l_α} (section)	6.3 rad^{-1}	
C_{l_α} (htail)	3.043 rad^{-1}	

TEST BED:

Load Factor (specimen)	5.48
Geometry	Flat plate

TEST BOOM:

Length	.5 m	1.67 ft
Outer Diameter	5.08 cm	2 in
Wall Thickness	2.5 mm	.0984 in

PROPULSION:

# Propeller Blades	3
Advance Ratio	0.4 to 0.6
Propeller Diameter	0.58 m 23 inches
Propeller Section	Clark Y
Propeller Efficiency	0.912 (0.46 advance ratio)
Amount of Fuel	2.27 Kg 5 lb
Power plant	7.5 hp gas engine
P_{av} (range)	2.8 to 7 hp
P_{req}	0.5 to 7 hp
SFC	1.38 lb/hp hr

INSTRUMENTATION:

DAQ Package Weight	6.67 N	1.5 lb_f
DAQ Volume Required	368.7 cm^3	22.5 in^3
DAQ Power Supply	.5 A*h	
DAQ Voltage Range	1 Volt Bipolar	
Input Channels	120	
Maximum Sample Rate	400 Hz	
Frame Sample Rate	5 Hz	
Pressure Measurements:		
Total Weight	31.1 N	7 lb_f
Telemetry System	Remtron RTS-1 Telemetry System	
Size	86.5 cm2	13.4 in^2
Weight	2.2 N	.5 lb_f
Channels	8	
Power	12 VDC	

MISSION DEFINITION

SPiRiT is a Remotely Piloted Vehicle (RPV) capable of obtaining in-flight aerodynamic data on a test specimen. Before each flight the pressure transducers will be calibrated and the data acquisition system checked for faults in addition to the standard pre-flight inspection of the flight controls and telemetry systems. After the pre-flight check, the RPV will be ready for take-off.

The RPV is designed to take off and land using conventional landing gear. The flight operations controller will control the take-off of the RPV. Immediately after take-off, the landing gear will retract into the RPV and climb to a cruise altitude of 60.9 m (200 feet). Once at the cruise altitude, the flight operations controller will fly the RPV approximately one half mile down range and then turn the RPV back up range in a 2g turn. Once this turn is executed, the flight operations controller will turn on the ground based Automatic Flight Control System (AFCS). The AFCS will fly the RPV in a continuous figure-eight pattern with one mile long legs and 35.4 m (116 ft) radius turns. This flight pattern is programmed into the AFCS and can easily be interchanged with other flight patterns between flights.

Once the AFCS in engaged, the systems controller will activate the Data Acquisition System (DAS). All the data acquisition parameters such as the sample rate and number of channels are preprogrammed into an EEPROM (Electrically Erasible Read Only Memory) on the A/D board itself. The EEPROM can be reprogrammed on site by the systems controller prior to flight.

The systems controller will continually receive telemetry from the DAS in the RPV indicating data acquisition battery voltage, angle of attack of the specimen, and the air speed. If the voltage level falls below the minimum operating range, manual control of the RPV can be regained and the RPV landed to recharge the data acquisition batteries. Integrated into the AFCS is the Automatic Attitude Control (AAC). By comparing the angle of attack of the specimen and the air speed to the pre-set nominal values, the AAC will automatically correct for changes in the angle of attack of the test specimen or the airspeed as needed. The RPV will continue to sample data for a maximum of 20 minutes. During the data acquisition, the propellor will be disengaged from the engine and feathered back to reduce the interference on the test specimen. The data collected will be stored on board the RPV and retrieved after the RPV has landed. After the memory banks are full, the flight operations controller will switch back to manual control, extend the landing gears, and land the RPV. After the RPV has landed, the engine batteries and data acquisition batteries will be recharged. The data stored in memory on-board the RPV will be transferred to the ground control computer through an RS-232 serial interface port. The raw voltage data be duplicated on disk and then reduced to yield the desired quantities. The total turn around time for the RPV will be dictated by the time required to recharge the batteries. It is expected that this will take between 30 minutes to one hour.

CHAPTER I
INDIVIDUAL CONCEPT DESIGNS

1.1 SPiRiT Configuration Selection Study

The following discussion represents three of the major configurations considered in the choice of the configuration of the SPiRiT. The configurations are first described, the operation strategy and test specimen mounting discussed, and then the stability and structural problems are considered for each prototype. The prototype configurations were studied by every member of the group and through an argumentation process, the SPiRiT configuration was determined with the attempt to include positive attributes from each and to limit the disadvantages of each of the proposed configurations.

1.2 Markus' Concept

Figure 1.1 shows the three view drawings of a preliminary conceptual design of an RPV capable of performing the pressure measurement mission. In general the configuration is a twin tail boom, single engine pusher propeller, low wing, pear shaped fuselage aircraft. The pusher propeller is to be mounted aft of the wing on the tip of the pear shaped fuselage. The blunt nose is to carry all equipment for data acquisition and flight control. The fuel tank will be at the wing root near the center of gravity so that retrimming due to fuel depletion will be minimal. The main wing will have no sweep and it will be located at the narrowing part of the fuselage. The low wing design will minimize interference with local airflow over the test specimen at positive high angle of attack.

igure 1.1 shows the three view drawings of a preliminary conceptual design of an RPV capable of performing the pressure measurement mission. In general the configuration is a twin tail boom, single engine pusher propeller, low wing, pear shaped fuselage aircraft. The pusher propeller is to be mounted aft of the wing on the tip of the pear shaped fuselage. The blunt nose is to carry all equipment for data acquisition and flight control. The fuel tank will be at the wing root near the center of gravity so that retrimming due to fuel depletion will be minimal. The main wing will have no sweep and it will be located at the narrowing part of the fuselage. The low wing design will minimize interference with local airflow over the test specimen at positive high angle of attack.

Again, this configuration is designed to operate at low speeds. A realistic speed range for this type of aircraft with a takeoff weight of 25 to 35 pounds is between 11 m/s (36 ft/sec) to 44 m/s (144 ft/sec). Such a flight velocity range leads to a maximum Reynold's number of 1.46×10^6 for the 16 inch chord specimen and a minimum of 9.127×10^4 for the minimum specimen chord of 4 inches. The Reynold's number range asked for in the RFP can not be met for the entire size range of specimens, but the entire Reynold's number range is attainable using larger specimens at high velocity and smaller at low velocity to obtain the range quoted here. The aircraft is to operate within line-of-sight, the landing and take off to be conventional with fixed tricycle gear, and the mission pattern to be a figure eight pattern. The figure eight mission pattern with a maximum bank angle of 40 degrees will result in a load factor of 1.3 for a maximum turning speed of 35 m/s (115 ft/sec).

The test specimen is to be mounted on top of two flat plates. There, it can be rotated as well as translated in the horizontal. This makes control of the aircraft in some flight regimes easier. The fact that both the elevator and the test specimen can

be translated before each flight should solve most of the stability problems associtated with this configuration. The major drawback to this mounting strategy is that the mount will interfere with the flow at the specimen wing tips. Structurally, no major problems with such a mount are foreseen.

A major problem with the low speed designs is the destabilization that will result from the large specimens needed to obtain high Reynold's number. To compensate for the large destabilizing affect of the specimen, again the strategy is to locate the specimen near the center of gravity. Also, this configuration includes a longitudinally adjustable large all-moving stabilator. The configuration includes a conventional lifting surface arrangement. Two tail booms support the all-moving stabilator. Further, it is movable along the boom so that the operator can adjust for the wide range of moments caused by different test sections. Such adjustment would be made on the ground prior to flight. In flight, the entire control surface can pitch up or down. This strategy will allow compensation for the destabilization of the large specimens with the stabilator.

1.3 Paul's Concept

Figure 1.2 shows the three view drawings of another preliminary conceptual design of an RPV capable of performing the pressure measurement mission. This configuration consists of a high mounted wing with vertical stabilators, single boom tail, single engine pusher propeller, and vertically mounted specimen. The engine is to be located forward and slightly lower than the main wing to allow the center of gravity to be moved further forward so as to lessen any tendency of the aircraft to veer to one side due to the pusher propeller design. The instrumentation is to be located in

the nose of the aircraft beneath the vertically mounted specimen. The engine, control equipment, and fuel tank are to be located directly beneath the overhead wing. The tail boom will have to have a small cross section and protrude from the base of the main fuselage to allow for proper clearance for the pusher propeller. The small cross section tail boom will result in very high stress levels and stress concentrations at the joining of the boom with the main fuselage and thus will be a structural difficulty.

The prototype has been designed to achieve a maximum Reynold's number of 500,000 for the 4 inch chord specimen. The RPV should then be able to allow testing over the entire Reynold's number range for the larger specimens up to the 16 inches in chord. To attain the range specified, the aircraft will have a maximum flight speed of approximately 150 miles per hour. For low Reynold's number and thus low velocity testing, flaps can be deployed to allow cruise at low speeds. Finally, the propeller will have the ability to change pitch to allow good performance over the wide range of flight velocities required. The operation will be line-of-sight and the flight pattern a circular or figure eight route.

The test specimens are to be interchangeable and mounted vertically in a vice like device to allow variously sized specimens to be tested. With this vertical mounting strategy, a total maximum half span length of 2.5 feet will be allowed. The testing therefore is limited to half span testing of specimens. The device that the test specimens will be mounted in will further be capable of rotating the lifting surfaces through the entire 60 degree angle of attack range and through the total sweep range of 50 degrees. This mounting strategy of course will also lead to significant yaw instability and require significant rudder trim.

The vertical specimen will cause significant side forces and weathercock instability as well as large bending moments about the axis normal to the wing plane.

To account for the side force generated from the test section arrangement, the main wing will include two vertical stabilators mounted downwards approximately at one third of the half span on each side. These panels will be capable of rotating by means of a control servo to provide the necessary side force to counteract the test specimen side force when it is at an angle of attack. The test specimen will also cause weathercock instability because it will be located in front of the center of gravity. To minimize this affect, the location of the center of gravity is to be put as close to the specimen location as possible. Further, the rear vertical tail will be made large to compensate for this instablility. The large moments created by the specimen in the wing plane is an uncommon loading for aircraft, and will require special consideration. Specifically, a structural weak point in the configuration will be where the tail boom joins the main fuselage. Further, a high bending moment will exist at this point due to the side forces. The use of the wing mounted vertical stabilators versus trimming with a rudder should at least reduce this moment.

1.4 Sam's Concept

Figure 1.3 shows the three view drawings of another preliminary conceptual design of an RPV capable of performing the pressure measurement mission. This configuration incorporates a tractor propeller, a twin tail boom, single engine, overhead elevated wing, and a hung test bed for specimen mounting. The engine is mounted in the center of the wing structure. An overhead wing with dihedral was chosen for its stability characteristics as well as roll control authority and simplicity. The test specimen itself is mounted on a test bed that is affixed underneath the wing/engine assembly. One of the major drawbacks to this configuration is the high profile of the wing/engine assembly. This may result in severe instability during the ground roll phase of take-off and landing unless landing gear with a wide base is

used.

One of the underlying restrictions on this project is that the RPV must be operated by line-of-sight. To operate the RPV with a small test section, the RPV must fly at a higher velocity to achieve the same Reynolds number as compared to a slow flying, large test specimen case. Using the smallest test specimen at the largest Reynolds number at sea level, the RPV must travel 120 m/s. Clearly at this speed, line-of-sight operation of the RPV is not possible. Thus for high speed applications, a tracking system must be used. To eliminate the need for a tracking system and simplify the design overall, the RPV will be designed for slow-speed and short range missions.

Test specimen mounting will be modular and specimens will be mounted on a test bed horizontally at mid span to provide fully three dimensional flow with minimum disturbance. The hung test bed will house all of the data acquisition equipment and the specimen control equipment. Internal in the test bed are servo-mechanisms that will allow the RPV to alter the angle of attack of the test specimen during the flight. This will facilitate the data collection and eliminates the need to land the RPV after each test run to change the angle of attack. Further, to meet specimen sweep angle requirements the specimens themselves must be constructed with sweep for each testing condition desired. The design of the interface between the test specimens and the test bed will provide significant design complication. Further, to minimize the aerodynamic interference of the test bed, the cross-section of this structure should be as low as possible which presents significant structural and logistics problems. The wing is mounted high on the fuselage to increase stability and decrease the flow interference effects on the test specimen.

An important effect of the low speed configuration is that the test specimen must be larger to achieve the Reynold's number range. Due to its increased size, the test specimen will generate significant aerodynamic loads which will affect the RPV's in-flight stability as well as induce significant structural loads on the RPV itself. To minimize the destabilizing affects of the large aerodynamic loads on the specimen, the goal of this configuration is to place the specimen as close as possible to the aircraft center of gravity. With the raised wing/engine design, the specimen won't be far from the center of gravity longitudinally. Further, the center of gravity should fall somewhere in between the engine and the specimen location vertically. Finally, the large twin boom tail should be able to counteract the destabilizing effects of the specimen. The most critical areas structurally are the wing structure that joins the lower fuselage to the wing/engine assembly, and the test bed itself. The stress levels and stress concentrations will be high in these areas due to the high loads that will be induced from the specimen.

1.5 Incorporation Into Final Configuration

The final SPiRiT configuration decided upon as shown in the 3-view SPiRiT configuration. includes various aspects of each one of the preceeding configuration proposals. The configuration includes an overhead elevated wing to minimize wing flow interference with the test specimen. This provides a structural challenge to support the wing sufficiently, but it was felt this could be achieved, and the raised wing would help significantly in reducing flow interference with the specimen. A pusher propeller with engine mounted in the wing was decided upon to minimize the propeller wash interference with the flow over the specimen. A single tail boom was decided

upon to eliminate structural problems associated with a twin boom. Further, the main fuselage is to hang below the wing at the same level as the test boom. The single tail boom then is angled up after the propeller location to ensure that when the specimen is deflected at high angles of attack the flow over the tail surfaces is not too disrupted. The raised wing/engine provides the propeller clearance required and allows for a tail boom with sizeable cross section reducing the structural problems associated with the tail boom fuselage joint.

Due to the importance placed on obtaining three dimensional pressure distribution in the request for proposal, it was decided that the specimen be mounted horizontally with full span on a test boom connecting at mid span and half chord. Further, the group decided that the structural problems that would result from such a strategy could be overcome through the use of a high strength metal such as heat treated aluminum alloy or a titanium alloy. The logistics problem of the measurement device to data acquisition equipment interface is solved by mounting the transducers in the specimen and the data acquisition equipment in the fuselage with simply a wire link through the test boom. Further, the servo mechanisms for specimen angle of attack changes are also to be mounted within the specimen. The specimen is to pivot on an axial secured in the specimen structure and then mounted to the boom through a bearing pivot point. This strategy requires that each specimen tested requires all of the measurement devices and servo mechnisms which is a drawback, but simplifies the interface a great deal and meets the main objective of uninterfered three dimensional flow very well.

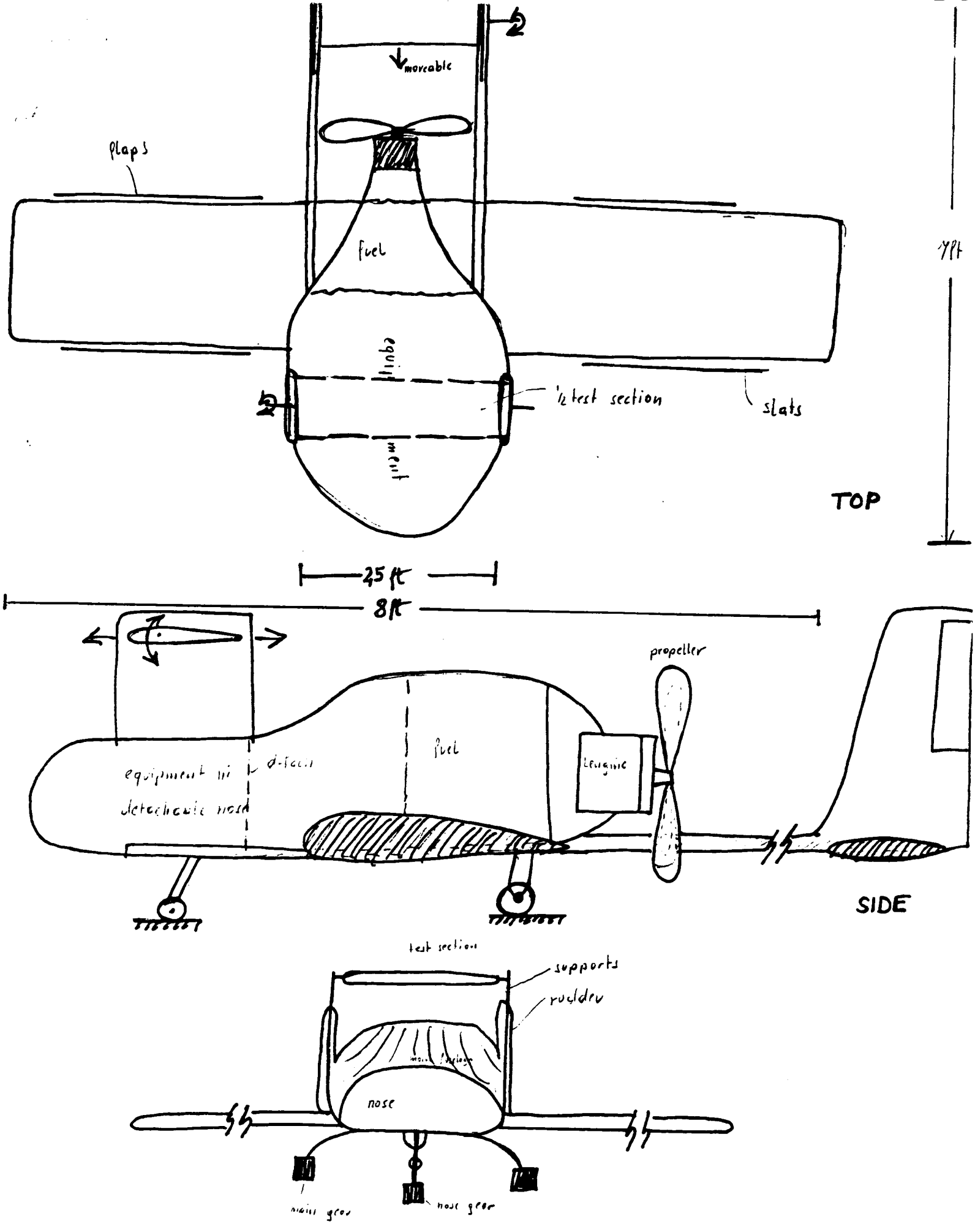
movable
flaps
fuel
engine
½ test section
slats
TOP
25 ft
8 ft
propeller
fuel
equipment in
detachable nose
engine
SIDE
test section
supports
rudder
nose
nose gear
FRONT

FIGURE 1.1

PRELIMINARY RPV SKETCH

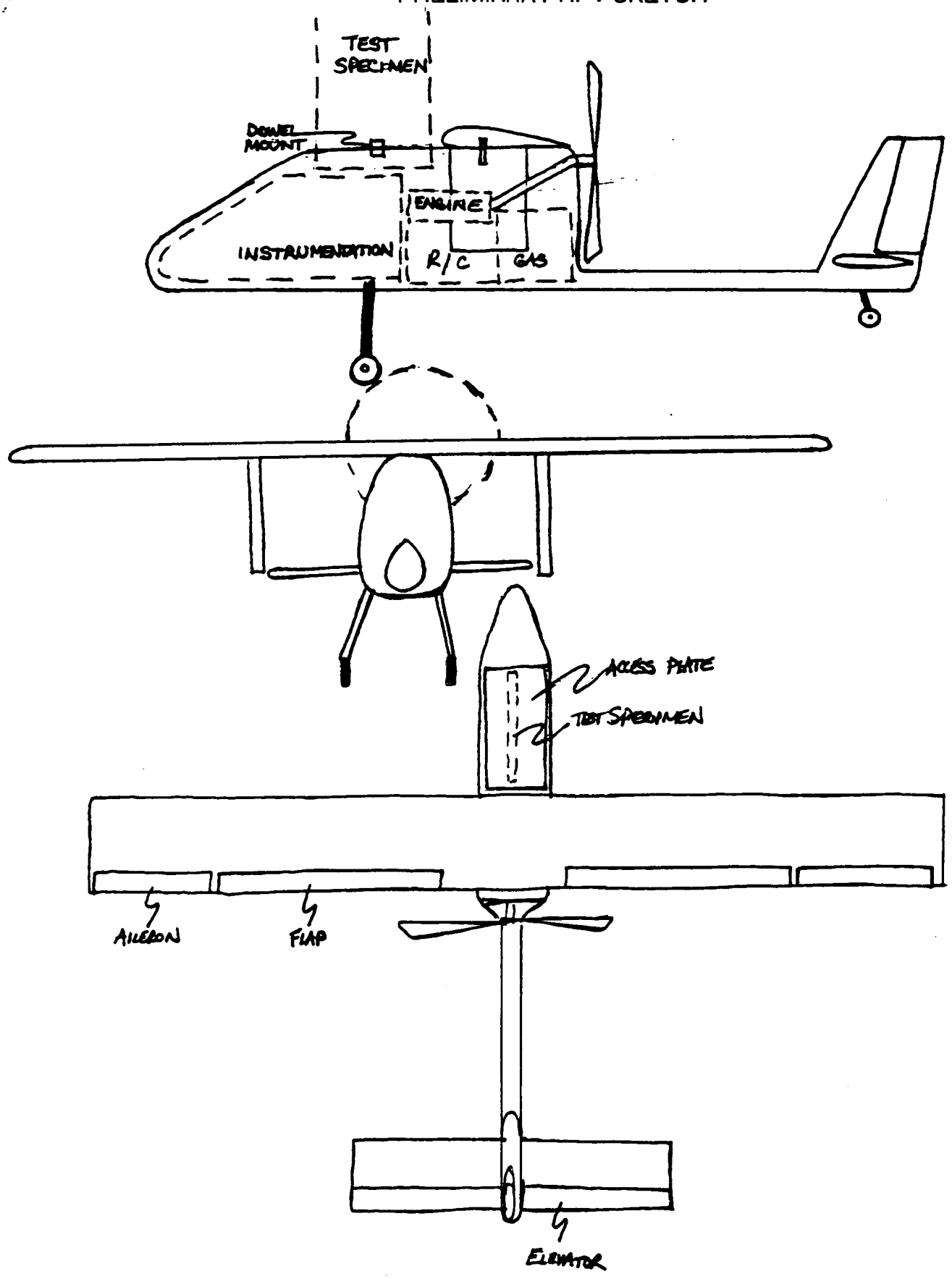

FIGURE 1.2

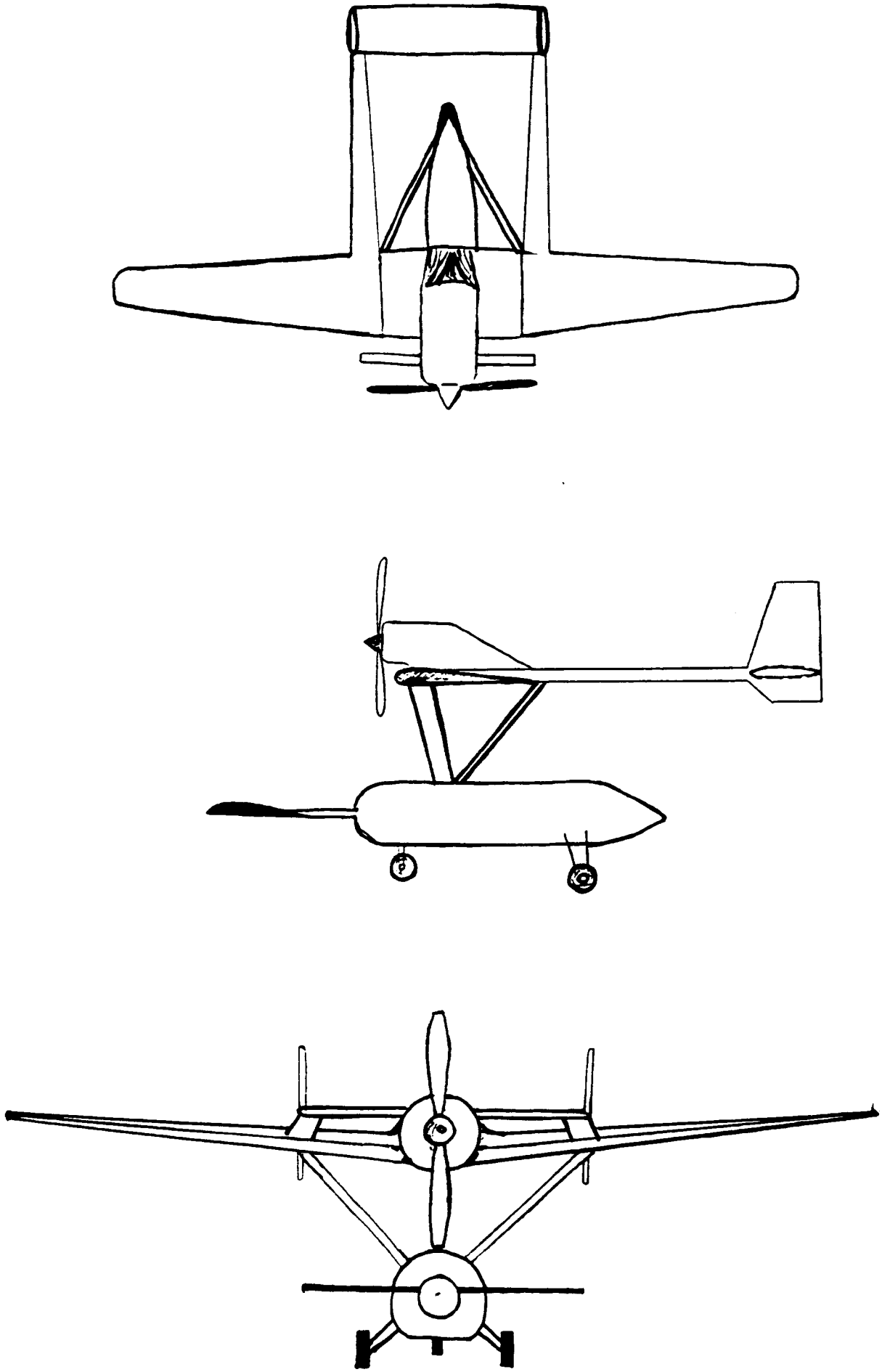

FIGURE 1.3

CHAPTER II
AERODYNAMIC DESIGN

2.1 AIRFOIL SELECTION

The selection of the airfoil for the aircraft is paramount in the wing design. Primary concerns in the choice of the airfoil were performance at the required Reynolds numbers, high lift, and ease of fabrication. For the design of the wing, we looked at thick, flat-bottomed airfoils in order to achieve the high lift required to complete the mission and to simplify the wing construction.

The airfoils that were considered were the Gottingen 700 series. The Gottingen 797 was chosen over the 799 or 796, as an acceptable compromise between the two concerning high lift and drag. The lift curve for this airfoil can be seen in Figure 2.1. The airfoil has a lift curve slope Cl_α = 5.3/rad, a maximum lift coefficient Cl_{max} = 1.36 at α=12°, a zero-lift angle of attack $\alpha_{L=0}$ =-7°, and a lift coefficient at zero angle of attack C_{l0}=0.6475. It delivers high lift at relatively low angles of attack, which will be the orientation of the aircraft during flight, and the 19° range between zero lift and stall angles of attack provide a comfortable cushion to account for gusts, pilot errors, and maneuvers. This airfoil also promotes a relatively simple fabrication process due to a gentle camber and the flat bottom.

Since high forces on the tail are undesirable, a thin symmetric airfoil was selected for its design. The NACA 0009 airfoil (Figure 2.2) was chosen for this purpose. It has Cl_α=6.3/rad, Cl_{max}=1.2 at α=10°, $\alpha_{L=0}$=-3.3°, and C_{l0}=0.363. These characteristics are summarized in Table 2.1.

2.2 WING DESIGN

For the initial size estimates of the wing, the wing was assumed to be of rectangular planform. Although an elliptical planform has the most desirable spanwise load distribution and excellent aerodynamic qualities, it is difficult to build and even more difficult to incorporate into simple calculations, and was therefore not considered. The rectangular planform was also chosen because of its "safe stall," that is it is known to stall first at the root.

For the initial wing sizing, the weight of the aircraft was estimated at 30 lbs., the aircraft was assumed to take off at V_{TO}=11.3 m/s (37 ft/s), and a conservative CL_{max}=0.8 was used. The initial wing size was then calculated as shown in Table 2.3 to be S=7.04m^2 (23.12 ft^2) . A high aspect ratio AR=10 was chosen in order to decrease the induced drag, and this value was used to obtain the span and chord of the wing, b=4.64m (15.2 ft) and c= 0.46 m (1.52 ft). These values give a wing loading of 1.3 lb/ft^2.

An empirical rule of thumb was used to determine the initial tail sizes. This rule states that the horizontal tail area is 17-30% of the wing area, and that the vertical tail is 7-10% of the wing size. However, since a large lifting surface is being attached to the aircraft during its mission, the performance of the aircraft will be greatly altered. Therefore, in calculating the sizes of the tail surfaces, the area of the largest possible test section was added to the area of the wing, and this total reference area was used for the sizing of the tail surfaces (see Table 2.3). We took the high ends of these ranges as the limiting values, and obtained a horizontal tail area S_{HT}= 0.83 m^2 (8.97 ft^2) and a vertical tail area of S_{VT}= 0.92 m^2 (3.01 ft^2). Initially using aspect ratios for the tail surfaces as AR_{HT}=2.0 and AR_{VT}=3.0, the span and chord for those surfaces were

determined to be b_{HT}=1.29 m (4.23 ft), c_{HT}= 0.65 m (2.12 ft), b_{VT}= 0.91 m (3.0 ft), and c_{VT}=0.30 m (1.0 ft). These results are summarized in Table 2.2. Later, however, these values were varied slightly to increase the stability of the aircraft, and will be discussed in Chapter 5.1.

After the initial sizes were determined, a lifting line program as shown in Appendix A for the Apple II system was used to determine general lift characteristics of the aircraft. Using the airfoil section characteristics and lifting surface geometries listed in Tables 2.1 and 2.2, the program was used to determine the lift characteristics for the lifting surfaces and their efficiencies. Assuming the wing will stall at the same angle of attack as its section, and assuming that $\alpha_{L=0}$ remains the same for the section and the lifting surface, lift curves were generated for the wing and tail (Figures 2.3 and 2.4). These lift curves were generated from the program outputs for the wing and tail surfaces listed in Appendices B and C by plotting the angle of attack against the total wing lift coefficient. The important characteristics of these lift curves are summarized in Table 2.4.

From the same program outputs, the maximum section lift coefficients for the primary lifting surfaces were determined. At the stall angle of attack (12° for the wing), the spanwise lift distribution shows a maximum section lift coefficient of Cl_{max}=1.009 at the root of the wing. Thus it was determined that at no section of the wing should that lift coefficient be exceeded. The same analysis was performed on the tail, revealing a Cl_{max}=0.642.

Since the lifting line analysis only takes into account the geometric parameters of twist, taper, span, and chord of the lifting surface, another program was used to model sweep, taper, incidence, and dihedral. LinAir 1.2 for the Macintosh, an extended lifting line program which allows for the simultaneous modeling of several panels, was used for this purpose. In order to

validate the results of both analyses, it must be shown that both methods agree in their results. By modeling a simple, rectangular, untapered, unswept wing in the LinAir program (a wing equivalent in geometry to the one used in the previous lifting line program), a lift curve was produced in a similar fashion as before. By comparing the lift curves from both methods of analysis (Figure 2.5), it can be seen that both sets of results are in reasonable agreement, and therefore can be used in conjunction with one another and can be compared on a fairly equal basis.

Using the LinAir program, the constraint that the section lift coefficient cannot, at any point across the span, exceed 1.01 for the wing or 0.64 for the tail was imposed on an analysis to study the effects of sweep, taper, incidence and dihedral on the lifting performance of the aircraft. It was discovered that sweep and taper do not significantly affect the efficiency of the aircraft, but do affect the spanwise lift distribution across the wing (Figure 2.6). The addition of either taper or sweep tends to decrease the amount of lift at the root of the wing and increase it at the tips, creating less evenly distributed loads and resulting in stall at lower angles of attack, and therefore are not implemented in the wing design.

Variations in the incidence of the wing change the total and section lift coefficients at different rates (Figure 2.7). A wing incidence of -3° was chosen in order to insure the maximum section lift coefficient was not exceeded while still maximizing CL, the total lift coefficient.

Finally, the effects of dihedral on the lifting performance of the aircraft were studied. It was previously determined that some amount of dihedral should be implemented to improve dynamic stability, and by looking at data bases to obtain a preliminary range of dihedral, angles between 5° and 8° were studied. Several dihedral schemes were considered (Figure 2.8), and based on an extensive trade study constrained by a high CL, and appropriate Cl, and

high efficiency, a four panel wing with the break at 0.5-semi-span was chosen. Also based on this criteria, it was determined that the inner panel dihedral should be Γ_1=3.5° and an outer dihedral angle of Γ_2=5.8°, which corresponds to an equivalent dihedral of 5°.

The final wing design is sketched in Figure 2.9, and its load distribution is shown in Figure 2.10.

2.3 DRAG PREDICTION

In determining a drag estimate for the aircraft, a drag breakdown technique was used to calculate Cd_0, the zero lift drag (Ref: Flight Mechanics Text and Handout from 3/31/88). The airplane was broken down into the basic components listed in Table 2.5, and each component was transformed into an "equivalent flat plate" based in the characteristic lengths of the individual component. The area of that "equivalent flat plate" was then used in conjunction with an equivalent flat plate turbulent boundary layer analysis stating

$$C_{D\pi} = C_f = 0.074 Re_L^{-1/5},$$

where Re_L is the Reynolds number based upon the length of the "equivalent" flat plate. The estimate

$$C_{D0} = \Sigma(C_{D\pi} A_\pi)/S_{wing}$$

may be used to determine the total C_{D0} for the aircraft, where $C_{D\pi}$ is found as shown above, A_π is the area of the "equivalent" flat plate, and S_{wing} is the wing surface area. C_{D0} was calculated to be C_{D0} =0.0236, and a 15% roughness factor was added, increasing the value to C_{D0}=0.0271.

The fuselage was modeled with a paraboloid nose, a straight circular mid-section with a constant diameter, and a conical tail. The test specimen was

modeled as a flat plate, as were the wing, tail surfaces, and the strut attaching the wing to the fuselage.

Next, the airplane efficiency factor was estimated. The following equation

$$1/e = 1/e_{wing} + 1/e_{fuselage} + 1/e_{other}$$

where span efficiency factors, e_{wing} and $e_{fuselage}$, were obtained from Figure 2-28 of (Flight Mechanics text, p. 2-50), and e_{other} is assumed to be 0.05. This analysis resulted in a span efficiency factor of e=0.74, which is in close agreement with the e=0.78 obtained from the LinAir analysis. This value was then used to calculate the airplane efficiency factor,

$$k=1/(\pi eAR)=0.0430$$

which was used in calculating the drag polar.

The drag of the aircraft is estimated as

$$C_D=C_{D0} + kC_L^2 = 0.027 + 0.043C_L^2,$$

and the drag polar (Figure 2.11) was plotted with the values shown in Table 2.6.

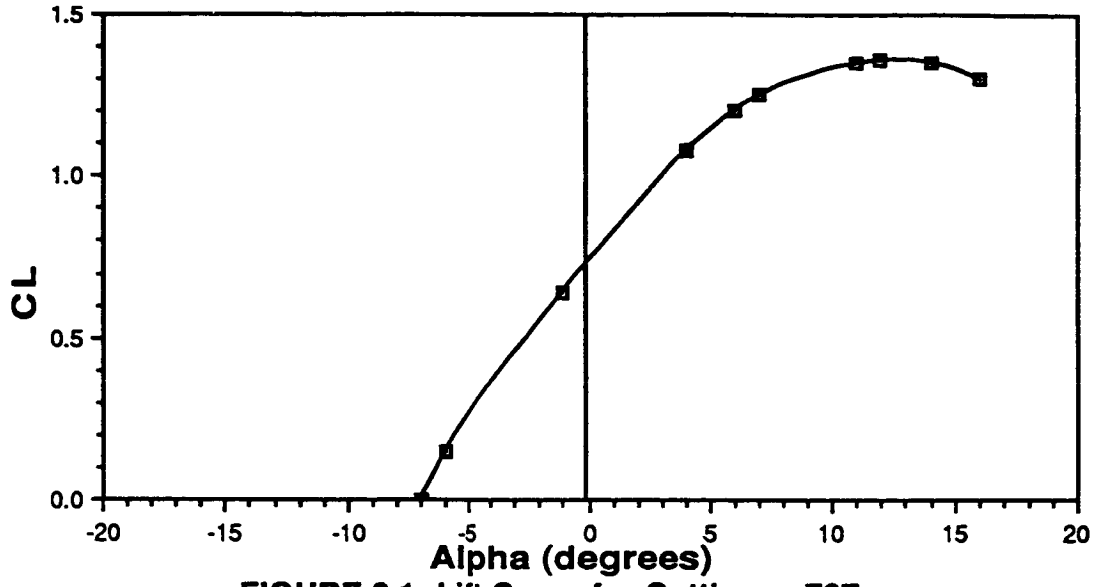

FIGURE 2.1: Lift Curve for Gottingen 797

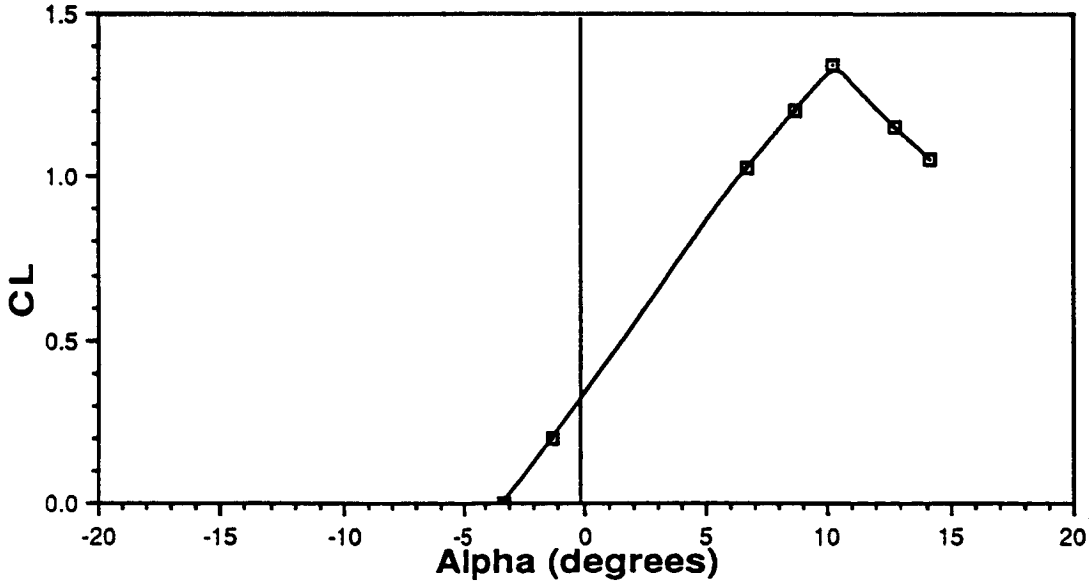

FIGURE 2.2: Lift curve for NACA 0009

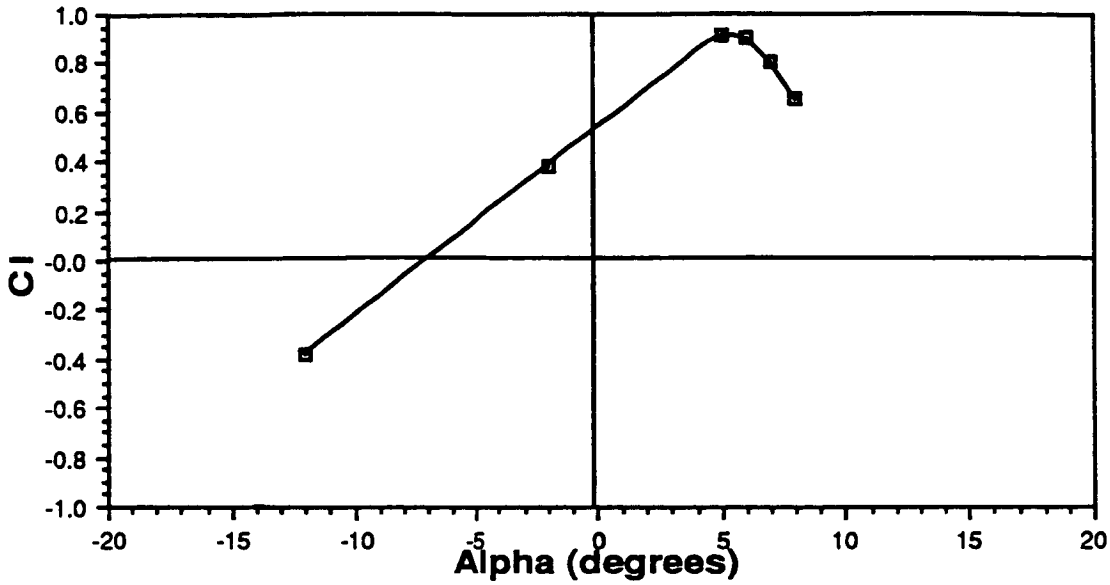

FIGURE 2.3: Wing lift curve, from lifting line program

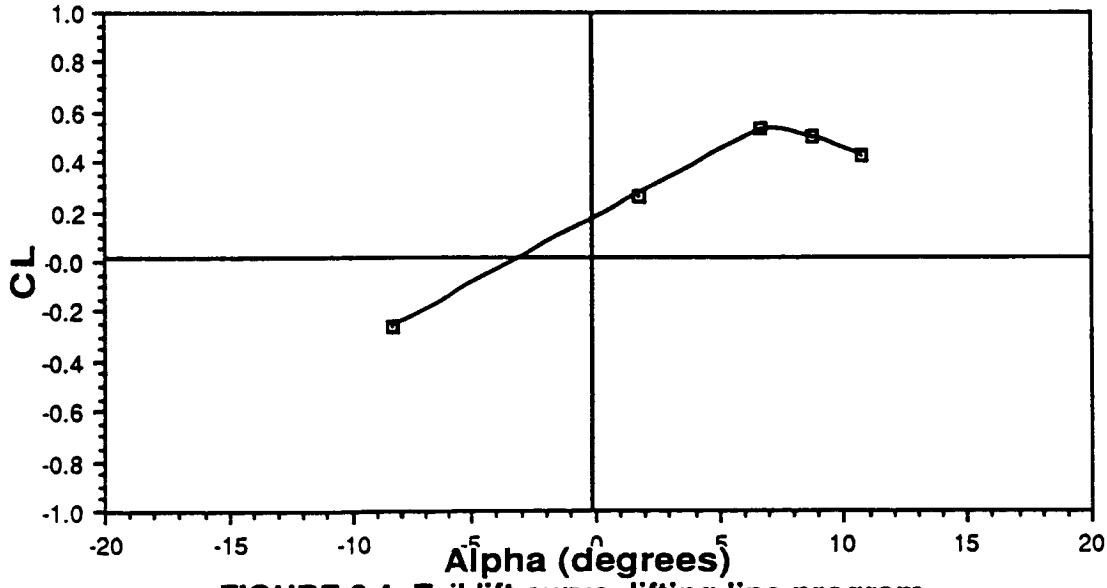

FIGURE 2.4: Tail lift curve, lifting line program

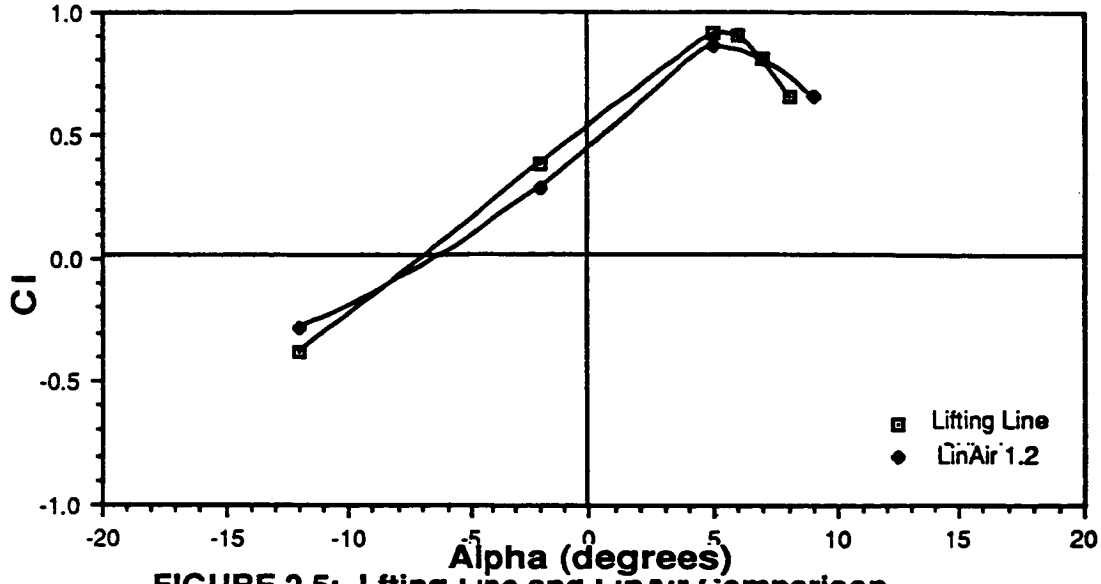

FIGURE 2.5: Lfting Line and LinAir Comparison

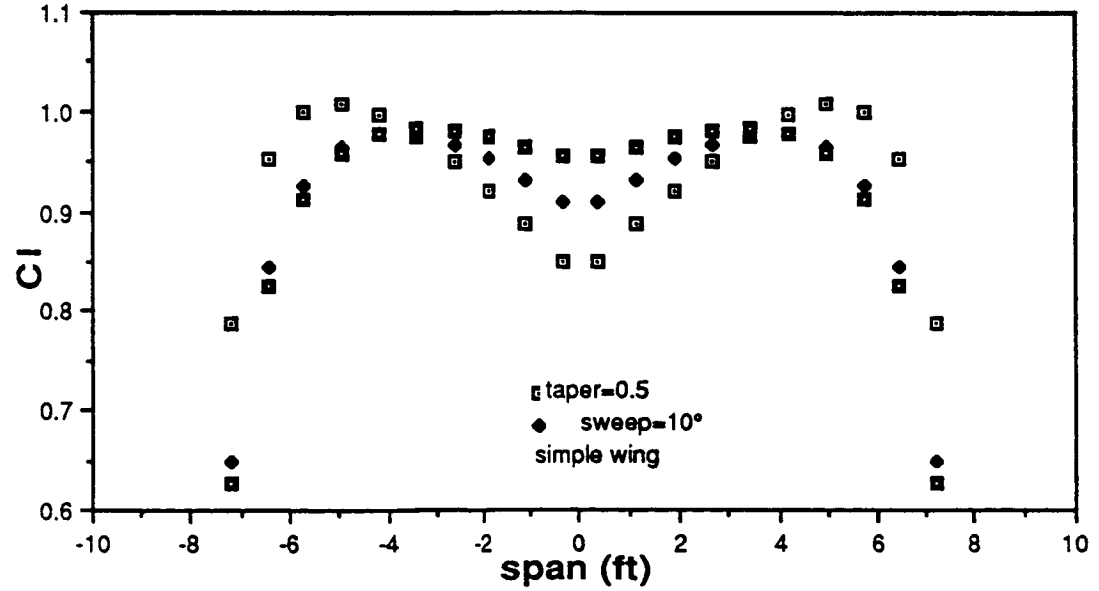

FIGURE 2.6: Spanwise lift distribution

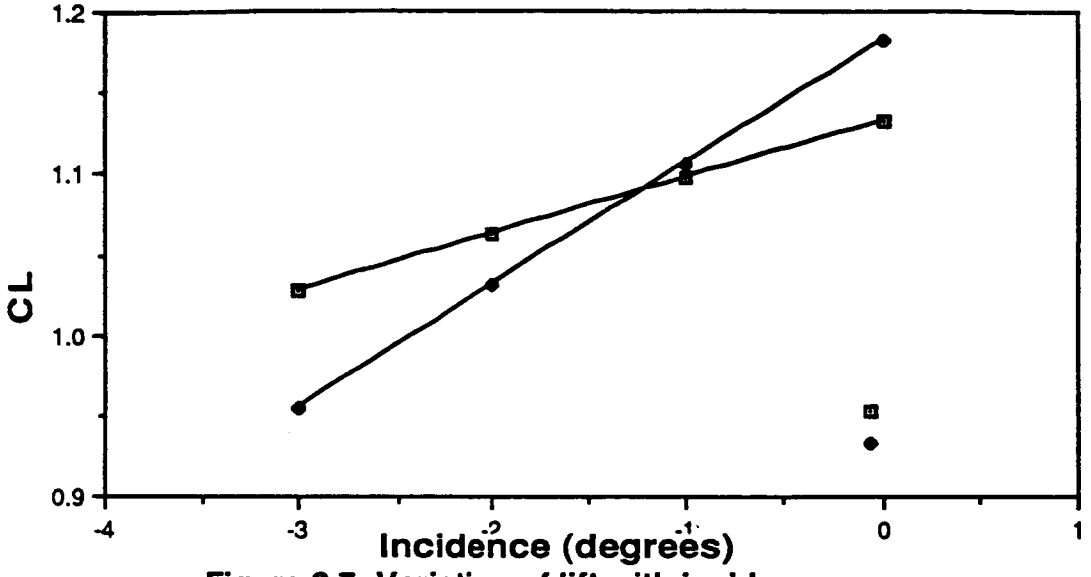

Figure 2.7: Variation of lift with incidence

FIGURE 2.8 DRAWING OF DIHEDRAL SCHEMES

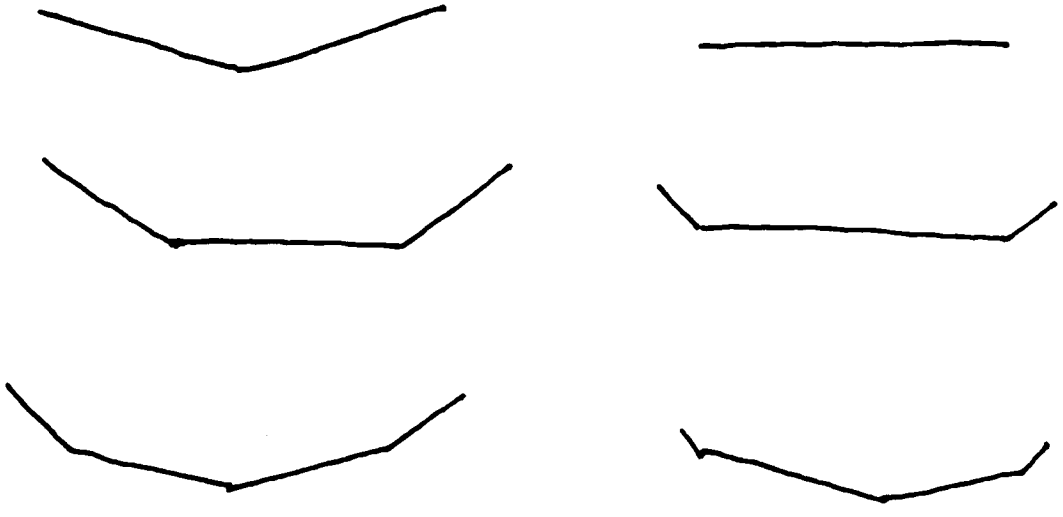

FIGURE 29

DRAWING OF FINAL WING DESIGN

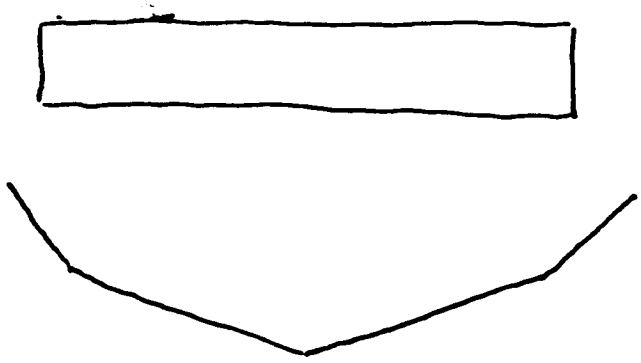

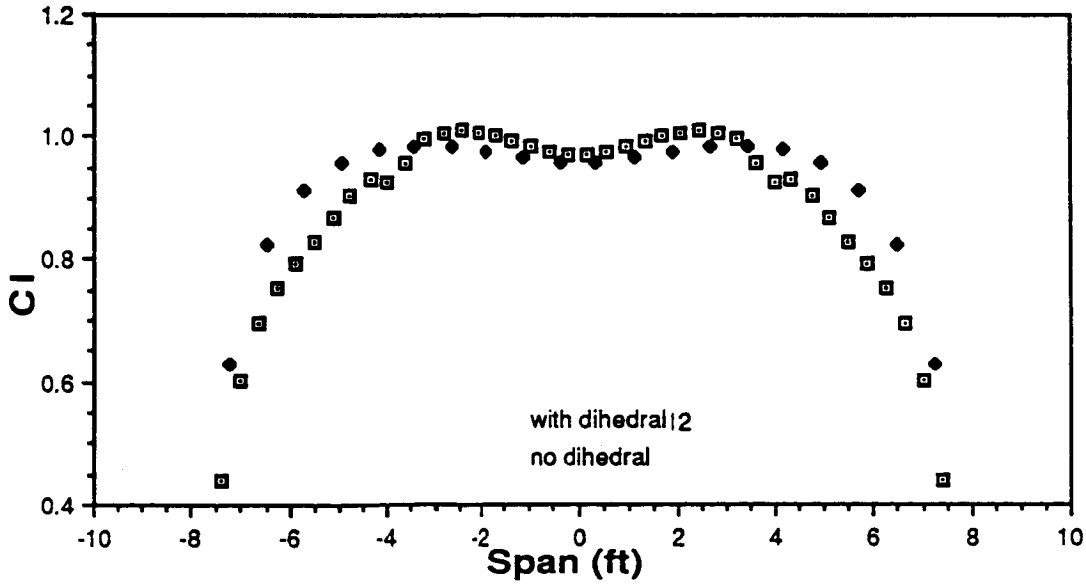

Figure 2.10: Spanwise lift distribution over the wing

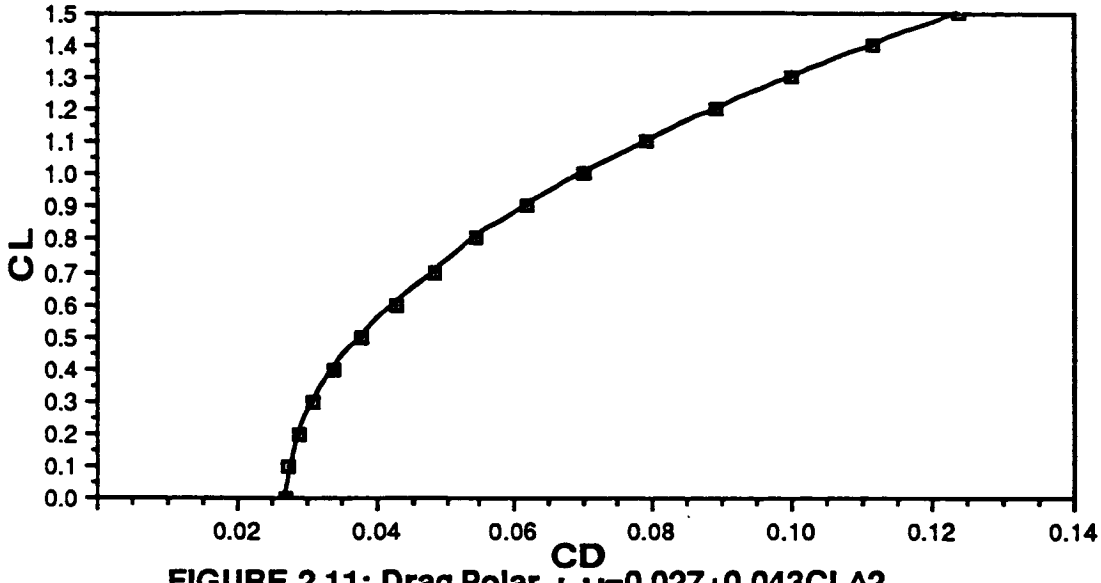

FIGURE 2.11: Drag Polar, CD=0.027+0.043CL^2

TABLE 2.1: AIRFOIL SECTION CHARACTERISTICS:

	Gottingen 797	NACA 0009
CL_α (rad^{-1})	5.3	6.3
CL_{max}	1.36 (at α=12°)	1.2 (at α=10°)
$\alpha_{L=0}$	-7°	-3.3°
C_{L0}	0.6475	0.363

TABLE 2.2: SIZES OF LIFTING SURFACES:

	WING	HORIZONTAL TAIL	VERTICAL TAIL
AR	10	4	3
S (ft^2)	23.12	8.07	3.01
b (ft)	15.2	5.68	3.0
c (ft)	1.52	1.42	1.0

TABLE 2.3: INITIAL SIZING OF LIFTING SURFACES

WING:

CL=0.8

V_{TO}=37 ft/s

W=30 lb.

AR=10

CL=W/(0.5*r*V^2*S) => S=W/(0.5*r*V^2*CL)

S=30/(0.5*0.00237*37^2*0.8)

S=23.12 ft^2

AR=b^2/S => b=SQRT(AR*S)

b=SQRT(10*23.12)

b=15.2 ft

S=b*c => c=S/b = 23.12/15.2

c=1.52 ft

HORIZONTAL TAIL:

$S_{tot}=S_{wing} + S_{test}$ = 6.66 ft^2 + 23.12 ft ^2 = 29.78 ft^2

AR=2.0

$S_{HT}=0.3*S_{tot}$ => SHT=0.3*29.78

S_{HT}=8.97 ft^2

AR = b^2/S_{HT} => b=SQRT(AR*S)

b=SQRT(2.0*8.97)

b_{HT}=4.23 ft

S=b*c => c=S/b

c=9.87/4.23

c=2.12 ft

TABLE 2.4: Lifting surface characteristics

	WING	TAIL	WING	PLANE
	Lifting Line		LinAir	
CL_α	4.375	3.043	4.67	5.39
CL_{max}	0.916 (at 5°)	0.531 (at 6.7°)	0.856(at 5°)	1.029 (9°)
$\alpha_{L=0}$	-7°	-3.3°	-6.8°	-1.8°
C_{L0}	.54	.175	0.44	0.18
e	0.91	0.99	------	0.783

Cdo estimation as of April 22, 1989

	0.000018
rho=	1.225
velocity=	11
sref=	2.1344

Table 2.5

component	n	p	length	diam	chord	span	surf area	y	Leq	Cdpi	CdpiApi
fus,nose	0.666	1	0.0762	0.2155	-----	-----	0.034340	-----	-----	-----	-----
fus,mid	1	1	0.5335	0.2155	-----	-----	0.361003	-----	-----	-----	-----
fus,tail	-----	-----	0.9146	0.2155	-----	-----	0.309441	-----	-----	-----	-----
fuselage	-----	-----	1.5243	-----	-----	-----	0.704785	0.67667	1.041549	0.004907	0.003458
wing,up	-----	-----	-----	-----	0.46	4.64	2.1344	4.64	0.46	0.005571	0.011892
wing,low	-----	-----	-----	-----	0.46	4.64	2.1344	4.64	0.46	0.006042	0.012896
wing	-----	-----	-----	-----	-----	-----	-----	-----	-----	0.011614	0.024789
htail,up	-----	-----	-----	-----	0.433	1.73	0.74909	1.73	0.433	0.005639	0.004224
htail,low	-----	-----	-----	-----	0.433	1.73	0.74909	1.73	0.433	0.006115	0.004581
htail	-----	-----	-----	-----	-----	-----	-----	-----	-----	0.011755	0.008805
vtail	-----	-----	-----	-----	0.31	0.9165	0.56823	0.9165	0.62	0.005443	0.003093
nac.nose	0.666	1	0.07	0.254	-----	-----	0.037182	-----	-----	-----	-----
id	1	1	0.2	0.254	-----	-----	0.159512	-----	-----	-----	-----
na.,tail	-----	-----	0.075	0.254	-----	-----	0.029908	-----	-----	-----	-----
nacelle	-----	-----	0.345	-----	-----	-----	0.226602	0.79756	0.28412	0.006363	0.001441
strut	-----	-----	-----	-----	0.46	0.305	0.2806	0.305	0.92	0.005030	0.001411
test,up	-----	-----	-----	-----	0.4065	1.524	0.619506	1.524	0.4065	0.005711	0.003538
test,low	-----	-----	-----	-----	0.4065	1.524	0.619506	1.524	0.4065	0.006193	0.003837
testspec	-----	-----	-----	-----	-----	-----	-----	-----	-----	0.011904	0.007375

CdpiApi total =	0.050375
Cdo,smooth=	0.023601
Cdo=	0.027142

Table 2.6a

Drag Polar as of April 22, 1989

do=	0.027142
e=	0.74
AR=	10
k=	0.043036
V(m/s)=	11
V(m/s)=	40
Sref(m2)=	2.1344
rho=	1.225

		For V = 11 m/s		For V = 40 m/s	
Cl	Cd	D (N)	L (N)	D (N)	L (N)
0	0.027142	4.293476	0	56.77324	0
0.1	0.027572	4.361554	15.81857	57.67345	209.1712
0.2	0.028863	4.565788	31.63714	60.37405	418.3424
0.3	0.031015	4.906177	47.45571	64.87507	627.5136
0.4	0.034027	5.382722	63.27428	71.17649	836.6848
0.5	0.037901	5.995423	79.09286	79.27832	1045.856
0.6	0.042635	6.744279	94.91143	89.18055	1255.027
0.7	0.048229	7.629292	110.7300	100.8832	1464.198
0.8	0.054685	8.650459	126.5485	114.3862	1673.369
0.9	0.062001	9.807783	142.3671	129.6897	1882.540
1	0.070178	11.10126	158.1857	146.7935	2091.712
1.1	0.079216	12.53089	174.0042	165.6978	2300.883
1.2	0.089114	14.09668	189.8228	186.4024	2510.054
1.3	0.099873	15.79863	205.6414	208.9075	2719.225
1.4	0.111493	17.63673	221.4600	233.2130	2928.396
1.5	0.123974	19.61099	237.2785	259.3189	3137.568
1.6	0.137315	21.72140	253.0971	287.2252	3346.739
1.7	0.151517	23.96797	268.9157	316.9319	3555.910
1.8	0.166580	26.35070	284.7342	348.4390	3765.081
1.9	0.182504	28.86958	300.5528	381.7465	3974.252
2	0.199288	31.52462	316.3714	416.8545	4183.424

CHAPTER III
PROPULSION SYSTEM

The SPiRiT remotely piloted aircraft needs a reliable, light-weight propulsion system. The system under consideration consists of the engine and fuel supply necessary to accomplish the RPV's mission. An acceptable design will allow the RPV to accomplish the mission goals specified in the preliminary design request without extending beyond the obvious constraints of this system. The engine package is designed for reliability, accessibility, and power. The system proposed is the Quadra 80 engine. The following are some of the factors and methods taken into consideration when designing the propulsion system.

An acceptable system will allow the RPV to travel at speeds of up to 40 m/s, in order to test a wide variety of test specimens. It must be able to fly for up to 30 minutes at an average cruise velocity of 30 m/s. The mass of the engine itself should not exceed 3.18 kg (7.0 lb), which is approximately 25% of the entire aircraft mass. The engine should be serviceable and must also conform to noise regulations.

3.1 Engine Performance

The Quadra 80 is a 3.5 kg (7.7lb) engine that produces 5595 Watts (7.5 sbhp) of power. It has a specific fuel consumption of 1.38 lb/Hp-hr, with a fuel load of 2.27 kg (5 lb.), which is approximately a gallon of fuel. This allows for 15 minutes of flight at 30 m/s, and 30 minutes of flight at 22 m/s. The engine is 20 cm high and 17.1 cm long with a displacement of 82cc. The engine

produces power to reach speeds of up to 39 m/s. The power available is shown in Figure 3.1. The specific fuel consumption of the engine was estimated from data in Reference 1 which has been reproduced in Figures 3.2 and 3.3. The Quadra 80 can be easily fitted with a muffler, thus eliminating potential problems with noise.

The most important relationship considered in choosing the propulsion system is that of the power required to that of power available. In Figure 3.4, The power required for increasing velocity is graphed for various values of C_{do}. Initial estimates of C_{do} were around .09, which necessitates a power of approximately 7460 Watts (10 hp). Taking into account losses due to propeller inefficiencies, the system would need at least a 13 hp engine. The power to weight correlations in Figures 3.5 and 3.6 show that engine weight increases at approximatly a pound per horsepower, which in case of a 13 hp engine would be 5.9 kg. This is far heavier than the 3.18 kg limitation.

Two things can be done. The C_{do} can be lowered, so that the power requirement is not so great, or the maximum velocity required can be lowered. For instance, lowering the velocity required from 40 m/s to 36 m/s brings down the power required to 5595 Watts (7.5 hp). This type of tradeoff between design parameters and mission requirements is central to this system design.

Reference 2 gives a good rule of thumb which says that one should have 1 cubic inch of engine displacement for every 10-12 pounds of aircraft weight. Figure 3.7 shows that since the SPiRiT needs at least 3 cubic inches of displacement, any engine under 4 hp will not be powerful enough. Engines producing under 4 hp are discarded immediately, which for all practical purposes rules out electric engines, which need heavy battery packs and

produce less power. The data base in Table 1 as well as data from reference 1 are considered when looking for a suitable propulsion system. Also, in order to remain close to the presupposed weight standards, only engines from 4 to 9 horse power are considered.

The C_{do} of the RPV was reduced to .06, which gives a power required curve as shown in Figure 3.8, which still requires a heavy engine in order to reach speeds of 40 m/s. In order to further clarify some of the necessary tradeoffs, the endurance of the RPV is considered. In Figure 3.9, using SFC data from Reference 1, the endurance of the RPV is graphed for three values of power produced by engines from the data base. The entire required endurance can be achieved with a 4.4 hp engine, but only half of the required flight range. The entire flight range can be covered with the powerful 9 hp engine, but only half of the proposed endurance. The endurances of the RPV were calculated using a 2.26 kg (5 lb) fuel load which was the limit in terms of the possible fuel payload.

In order to further clarify the intricate trade-offs, a more qualitative analysis is undertaken. The percent of mission requirement achieved is calculated for engines between 4.4 and 9 lb. The results of this are graphed in Figure 3.10. Three trends can be observed. As the power of the system increases, more of the flight range can be covered, and consequently, a greater percent of the mission is fulfilled. As the power of the system increases, the endurance decreases, and thus less of the mission is fulfilled. The weight of the system does not become an extremely important factor until it begins to exceed the imposed restrictions, and then, a percentage of the

mission is not fulfilled. These three tradeoffs are averaged together, and the results are in Figure 3.11.

The percentages in Figure 3.11 are calculated with each part of the mission weighted differently. The power necessary to cover the flight range is considered most important, and is weighted doubly in the average. The endurance is averaged normally, and the weight is only considered when it began to adversely affect the mission. The result of this weighted average is a peak in mission accomplishment percentage. The peak is around 82%, which is for a 7.5 to 8 hp engine. Obviously there will be limitations in all areas of performance as a result of the trade-offs. The engine that best matches the requirements of this study is the Quadra 80.

3.2 Propeller

The SPiRiT RPV uses a three bladed propeller with a .5842 m (23") diameter. Each of the blades uses a Clark-Y airfoil section with a 16% thickness ratio. The operating velocity range is selected as 36-147 fps. At a design shaft speed of 9000 RPM, the advance ratio range is calculated for a given blade diameter. Table 3 shows the desired advance ratio range for the blade diameters examined.

The propeller has six primary variables: the airfoil section, the number of propeller blades, the diameter of the blade, the chord distribution, thickness distribution, and the pitch distribution. In order to maximize the propeller design, one must determine the best combination of these variables to yield the most efficient propeller for the mission.

Although there are many influencing factors to consider, the mission performance is most important. Other factors taken into consideration include airfoil selection, blade number selection, blade diameter ,thickness distribution, and chord and pitch distribution.

The airfoil was the first design variable considered. Using a chord and pitch determined from the first computer code, various airfoils were analyzed with a thickness-to-chord ratio of 16%. The airfoil selection was resticted to the airfoils supplied in the existing computer code: the inviscid flat plate (providing a worst case scenario), symmetrical, Clark-Y, and RAF-6 airfoils. The preliminary design propeller used was a three-bladed, 23 in. diameter propeller. Figure 3.12 clearly indicates that the Clark-Y airfoil performs significantly better than either the inviscid flat plate (a worst case scenario), symmetrical, or RAF-6 airfoils. The Clark-Y airfoil section was thus selected for the SPiRiT.

The number of blades used posed a little more difficulty. Although the number of blades does not affect the efficiency or tip speed of the propeller blade, it does influence its thrust coefficient and solidiy. Figure 3.13 shows the affect of blade number on these parameters. A three-bladed propeller was selected in preference to two or four-bladed configurations as a compromise between high thrust coefficient values and low solidity values. The significance of the number of propeller blades used also arises in the consideration of the noise levels which the propeller emits. A study was conducted by Barry et al (Reference 4) which concluded that for low noise levels, propellers should operate at the lowest possible tip speed and use a large diameter propeller and a greater number of blades (three to five blades as opposed to two blades).

Noise limitations restrict the blade tip speed from exceeding 0.9*M. The blade diameter thus limits the revolution rate which governs the advance ratio boundaries. The effect of blade diameter on the advance ratio parameters as well as the propeller efficiency and thrust coefficient is shown in Figure 3.14. Although the thrust coefficient increases with decreasing blade diameter, the minimum allowable advance ratio is also increased. The 23" diameter propeller provides for the widest desirable advance ratio range while maintaining adequate thrust coefficient values and propeller efficiency results over its range.

The study of the effect of blade thickness on the propeller performance yielded a selected thickness ratio of 16%. The entire thickness ratio range was studied from 6%-21% and the results are shown in Figure 3.15. The 16% thickness ratio was chosen over the 21% thickness ratio due to its better performance characteristics at lower advance ratios, a range morecommon in SPiRiT's mission.

The chord and pitch distribution was the most difficult to analyze. In order to obtain different distributions, an optimization program was run for various design speeds over the desired velocity range. The computer code used outputs the optimum chord and pitch distribution for the prescribed input conditions from the Quadra engine block. Like the thickness ratio, the chord and pitch distribution affect the advance ratio range. The distribution associated with the 50 MPH design speed was found to cover the desired advance ratio range with the most efficiency as shown in Figure 3.16.

FORTRAN programs were run on both the Macintosh SE and PRIME computing systems. Cricket Graph and Techtronix programs were used for graphing. Computer programs for power, range, and endurance calculations can be found in the attached Appendices D and E. Two computer programs are used in the propeller analysis. The first of these which was adapted from a program written by David Dingeman, determines the optimal design of the blade, including the chord and pitch distribution, for a given engine and design velocity. However, the analysis program is not valid for three or four-bladed propellers. A second program developed by Barry N. Young is thus used to determine the performance of the propeller design once the chord and pitch distributions have been determined. This program accounts for tip losses and is valid for three and four-bladed propellers as well as the standard two-bladed propeller. The computer code determines the maximum rotational speed for a given blade diameter as well as the advance ratio limits and calculates the resulting performance of the propeller.

References

1. RPV's - Aerodynamics and Related Topics. Von Karman Institute for Fluid Dynamics, lecture series 101, B-1640 Rhode Saint Genese, Belgium,1977.

2. John d. AndersonIntroduction to Flight, McGraw-Hill Book Company, New York, 1985.

3. Bocci, A.J., A New Series of Airfoil Sections Suitable for Aircraft Propellers, Aeronautical Quarterly, Feb. 1977.

4. F.W. Barry and B. Magliozzi, "Noise Detecability Prediction Method for Low Tip Speed Propellers," AFAPL-TR-71-37, Wright-Patterson AFB, OH, June1971.

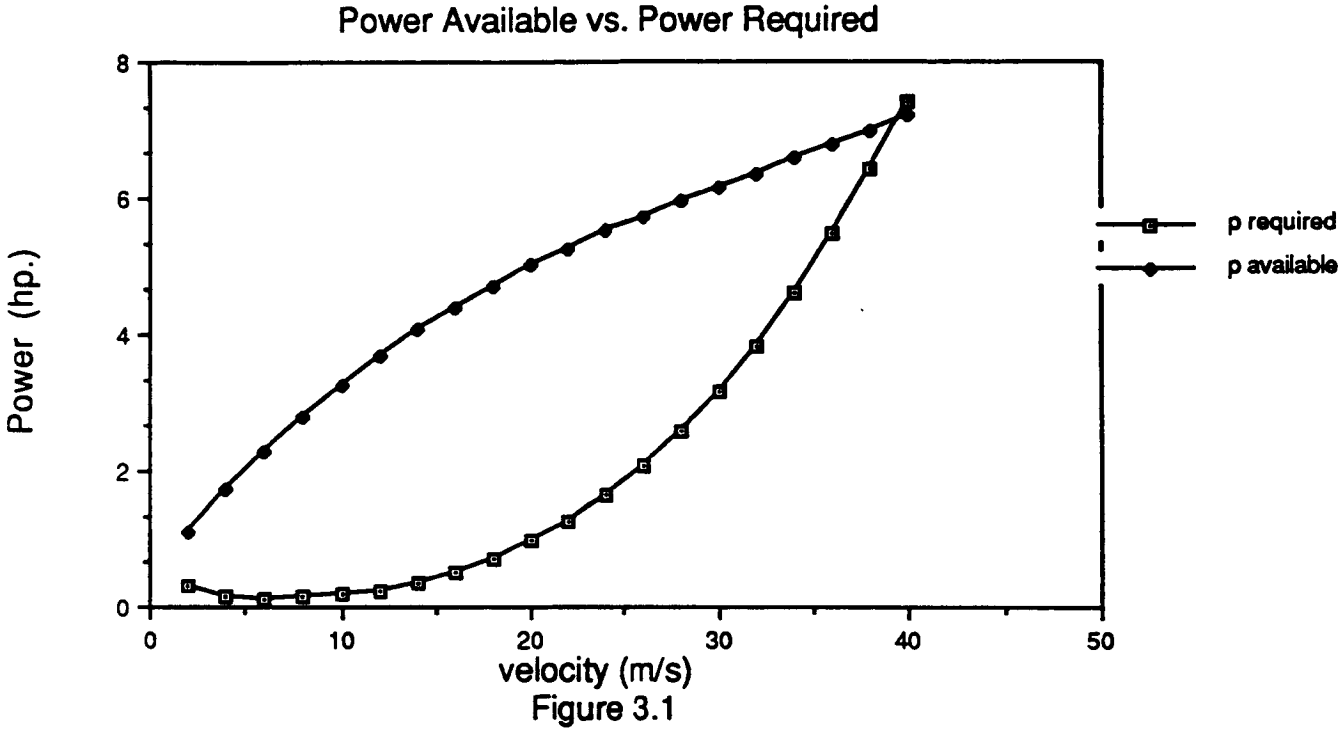
Power Available vs. Power Required
Power (hp.)
velocity (m/s)
p required
p available
0
2
4
6
8
0
10
20
30
40
50
Figure 3.1

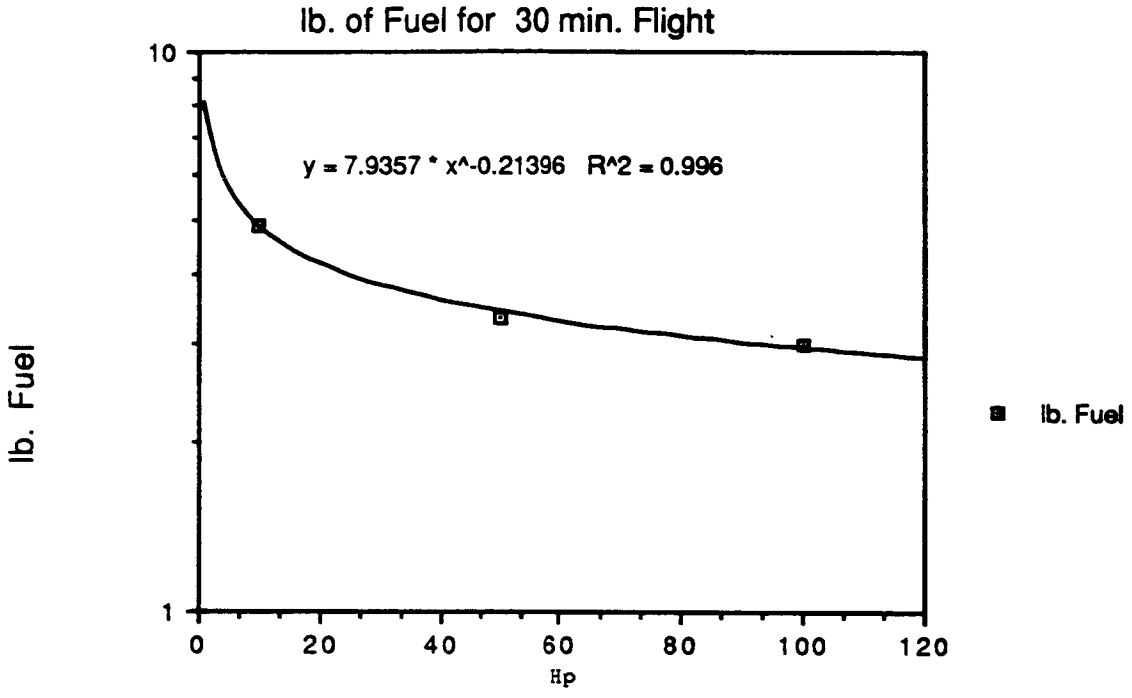

Figure 3.2

(Extracted from Reference 1)

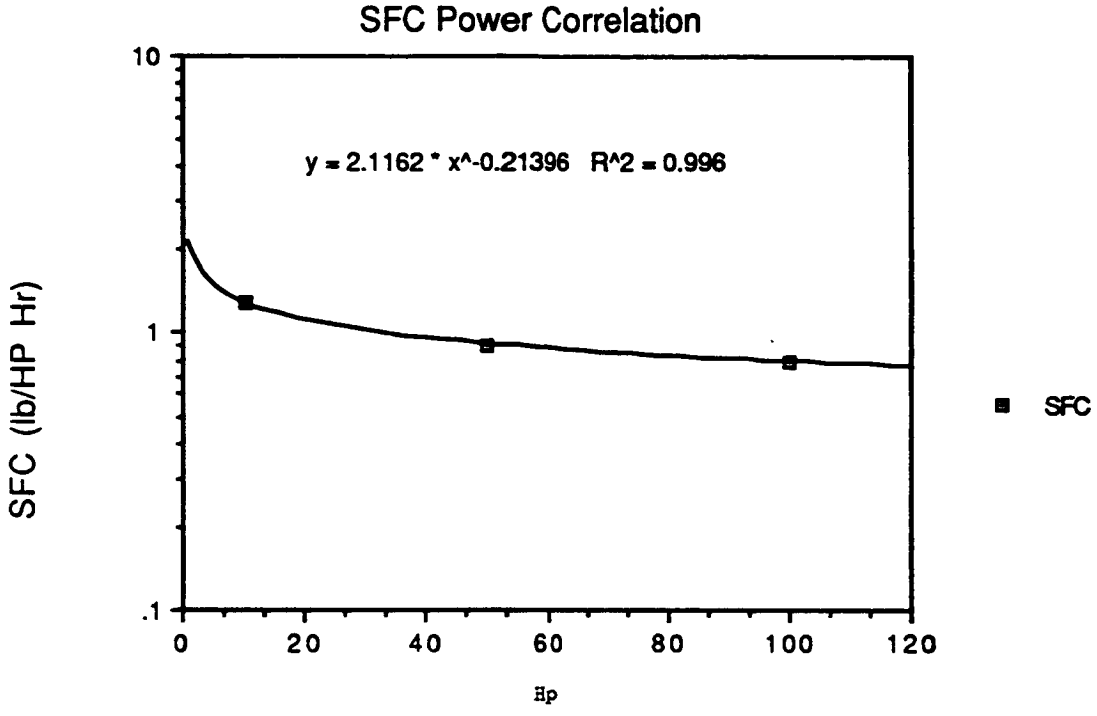
SFC Power Correlation
y = 2.1162 * x^-0.21396 R^2 = 0.996
SFC (lb/HP Hr)
10
1
.1
0
20
40
60
80
100
120
Hp
SFC

Figure 3.3

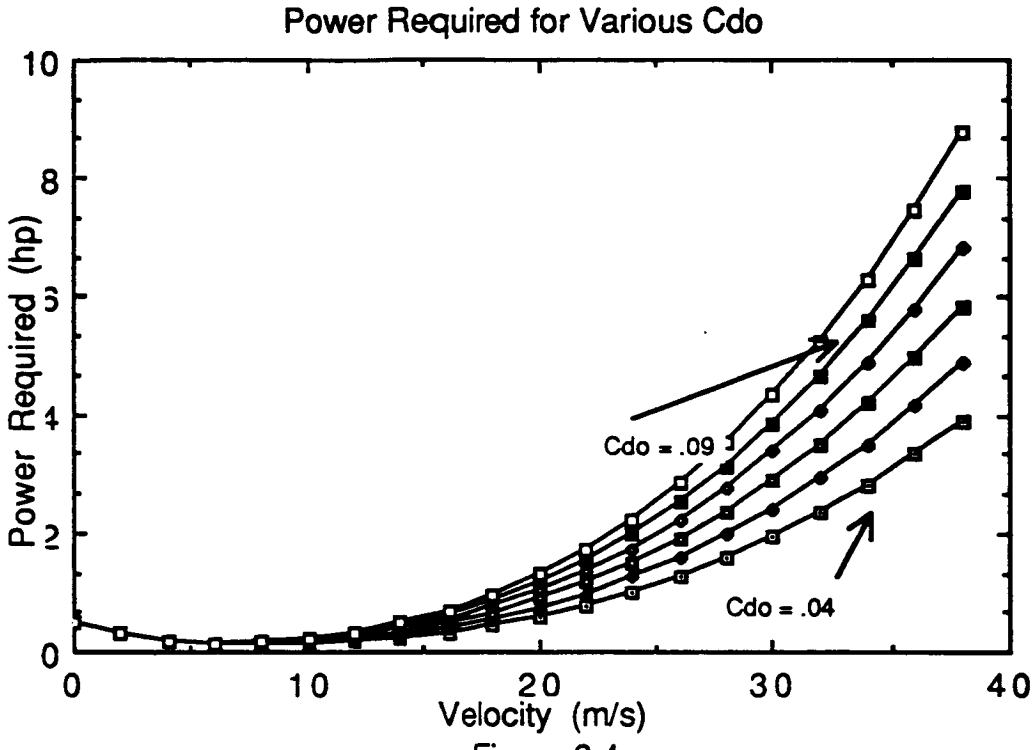
Power Required for Various Cdo
Power Required (hp)
Velocity (m/s)
Cdo = .09
Cdo = .04
0
2
4
8
10
0
10
20
30
40
Figure 3.4

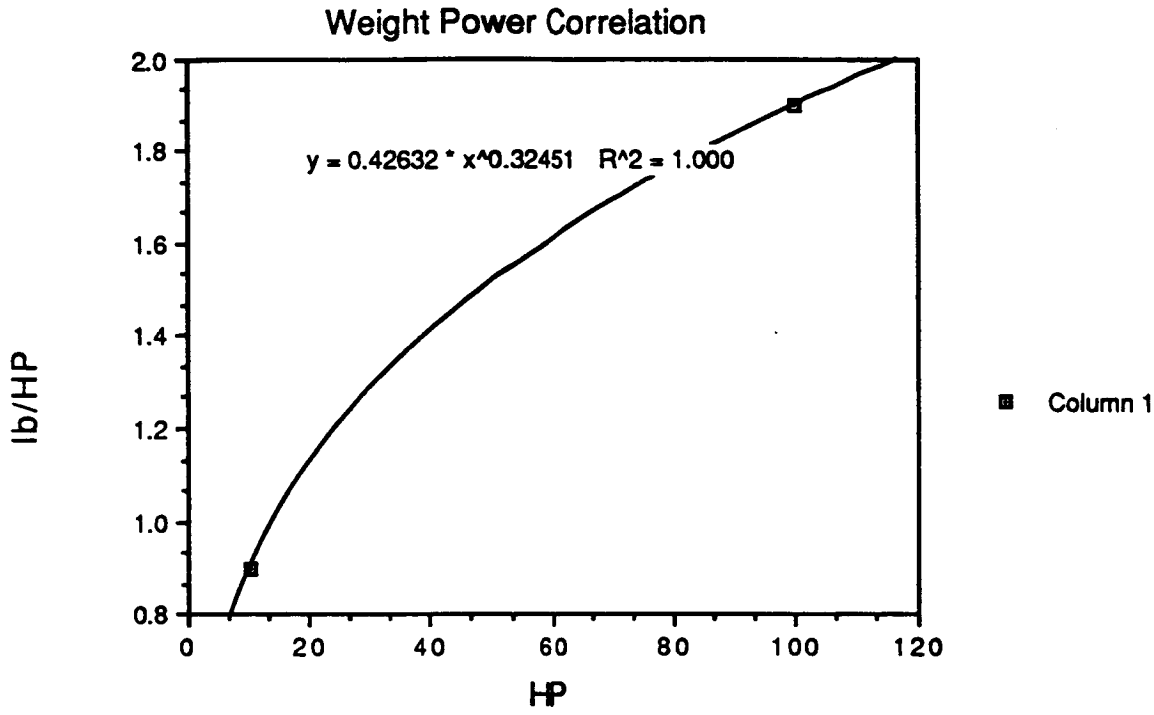

Figure 3.5
(Extracted from reference 1)

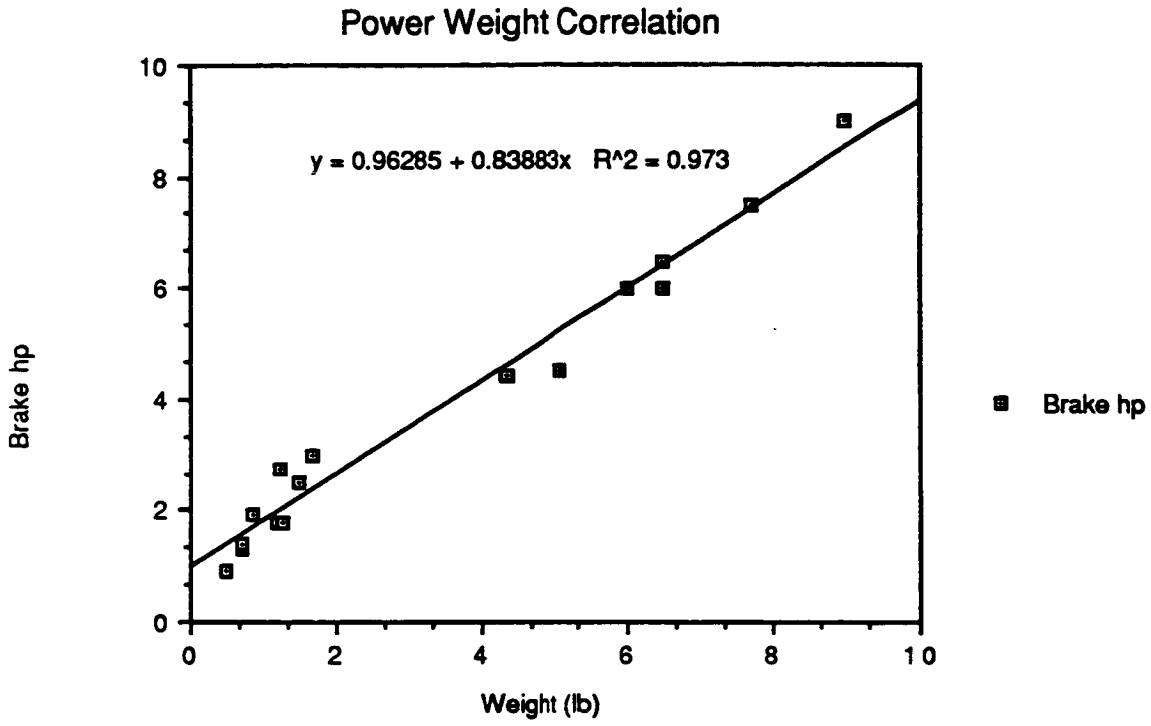
Power Weight Correlation
y = 0.96285 + 0.83883x R^2 = 0.973
Brake hp
Weight (lb)
Brake hp
0
2
4
6
8
10

Figure 3.6

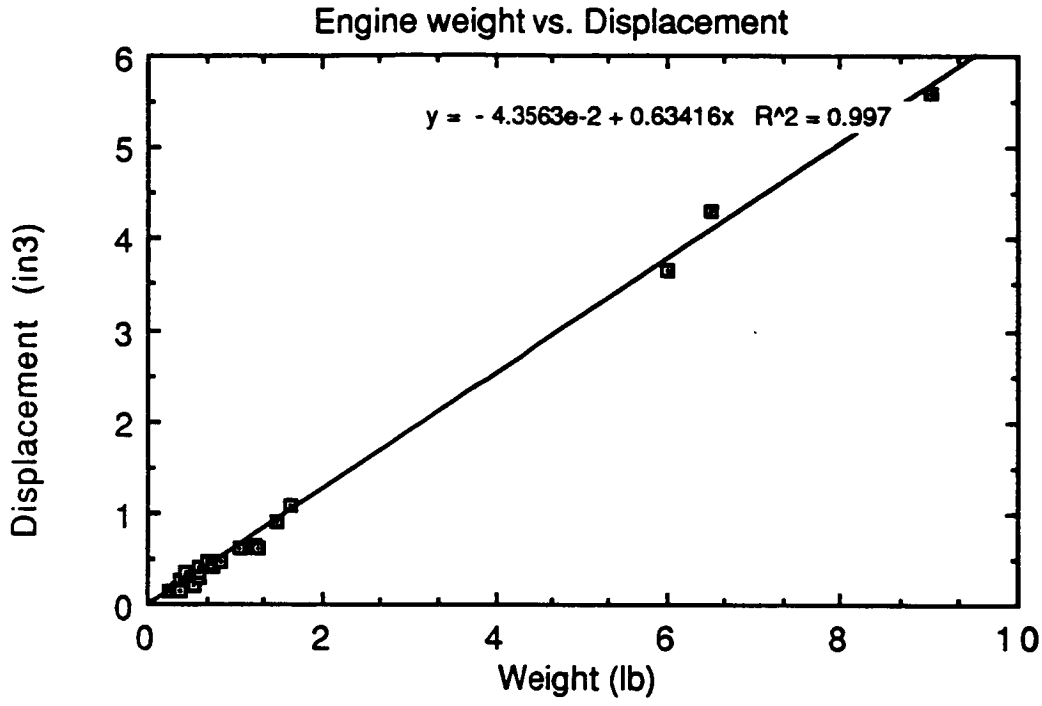
Engine weight vs. Displacement
y = - 4.3563e-2 + 0.63416x R^2 = 0.997
Displacement (in3)
Weight (lb)
0
1
2
3
4
5
6
0
2
4
6
8
10

Figure 3.7

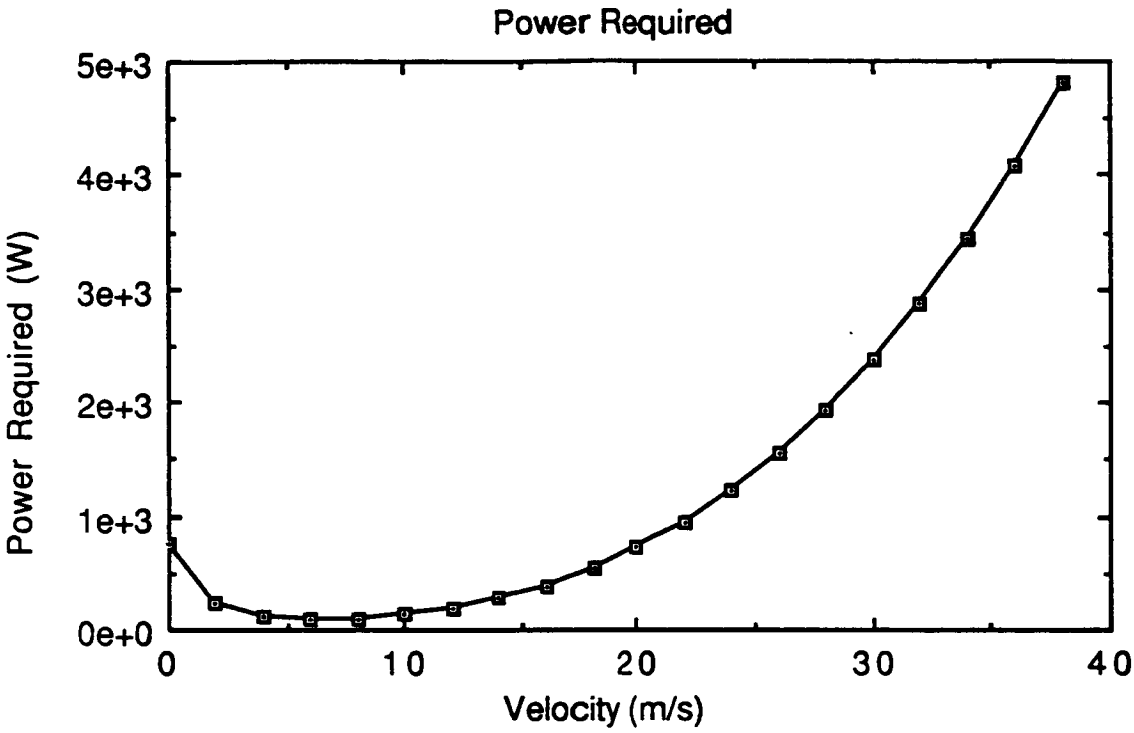
Power Required
5e+3
4e+3
3e+3
2e+3
1e+3
0e+0
Power Required (W)
0
10
20
30
40
Velocity (m/s)

Figure 3.8

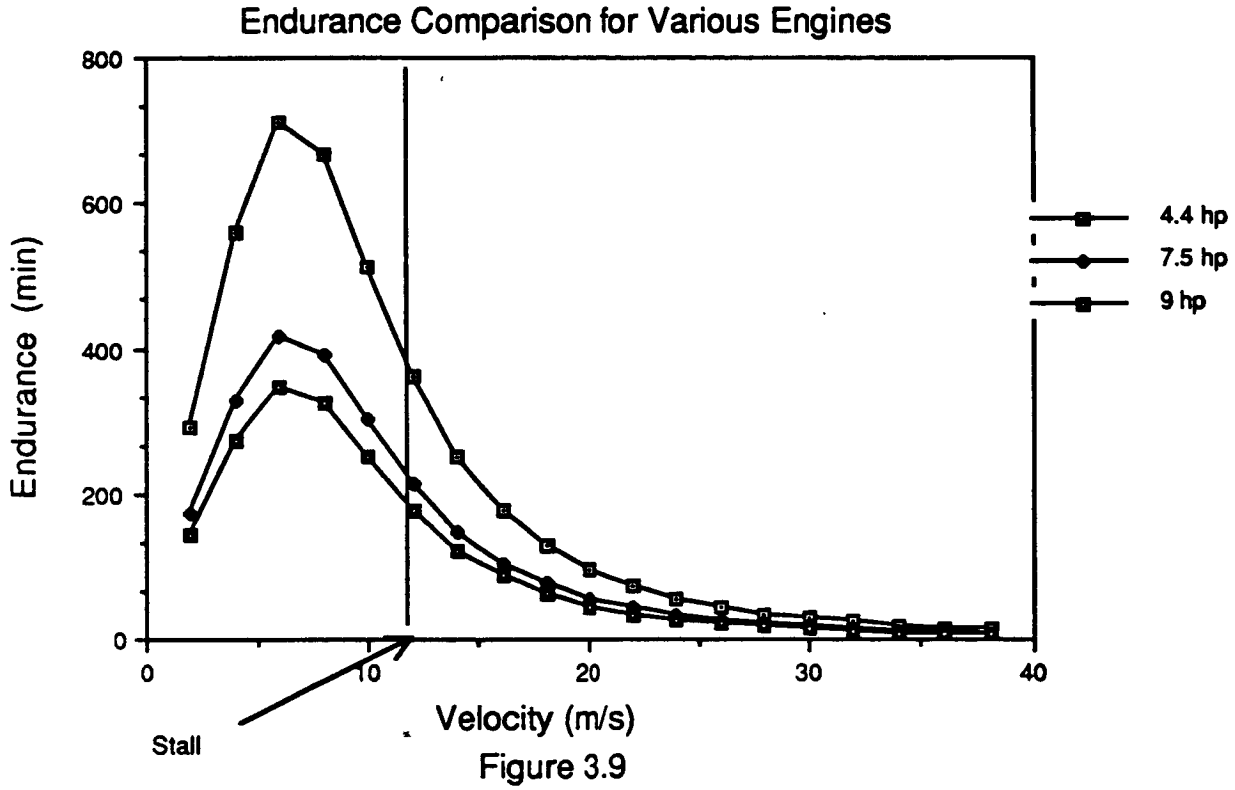
Endurance Comparison for Various Engines
800
600
400
200
0
Endurance (min)
0
10
20
30
40
Velocity (m/s)
Stall
4.4 hp
7.5 hp
9 hp

Figure 3.9

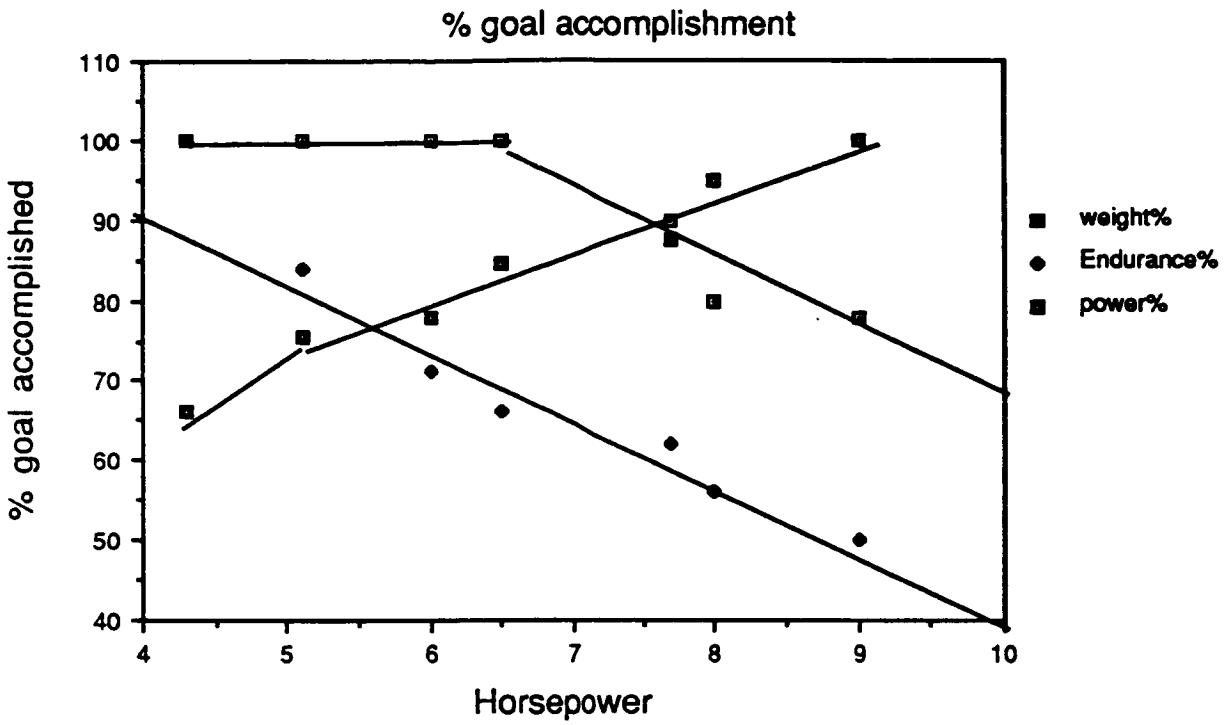
% goal accomplishment
% goal accomplished
110
100
90
80
70
60
50
40
4
5
6
7
8
9
10
Horsepower
weight%
Endurance%
power%

Figure 3.10

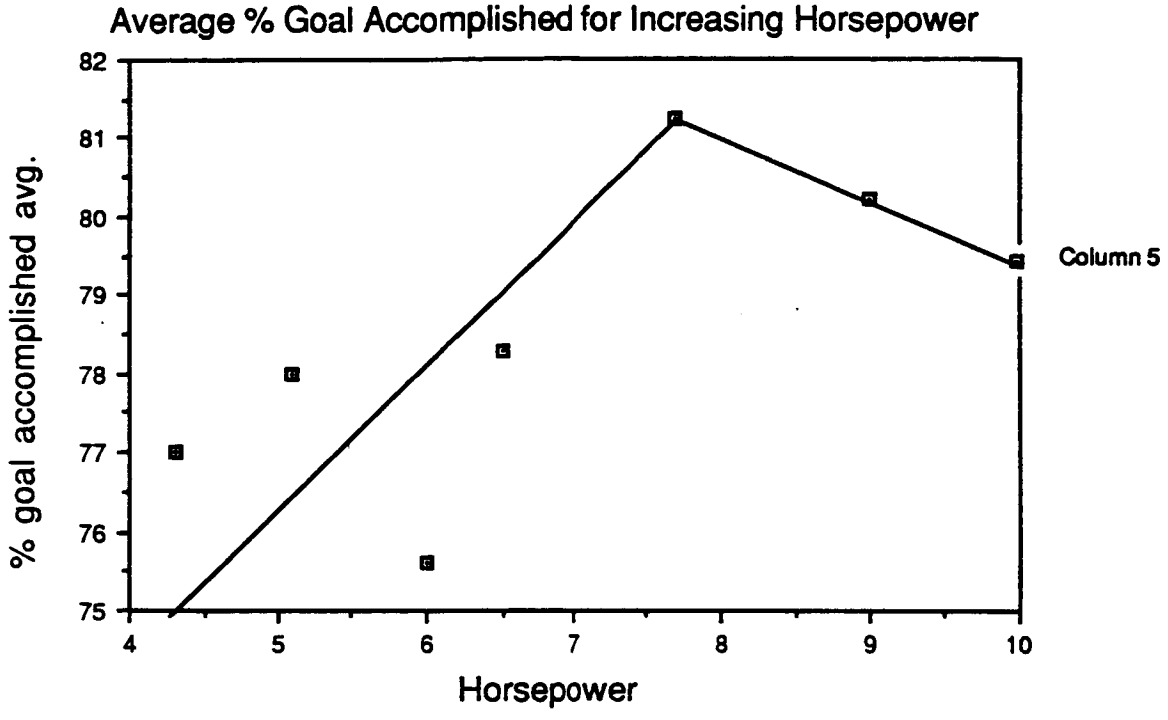
Average % Goal Accomplished for Increasing Horsepower
% goal accomplished avg.
82
81
80
79
78
77
76
75
4
5
6
7
8
9
10
Horsepower
Column 5

Figure 3.11

Figure 3.12

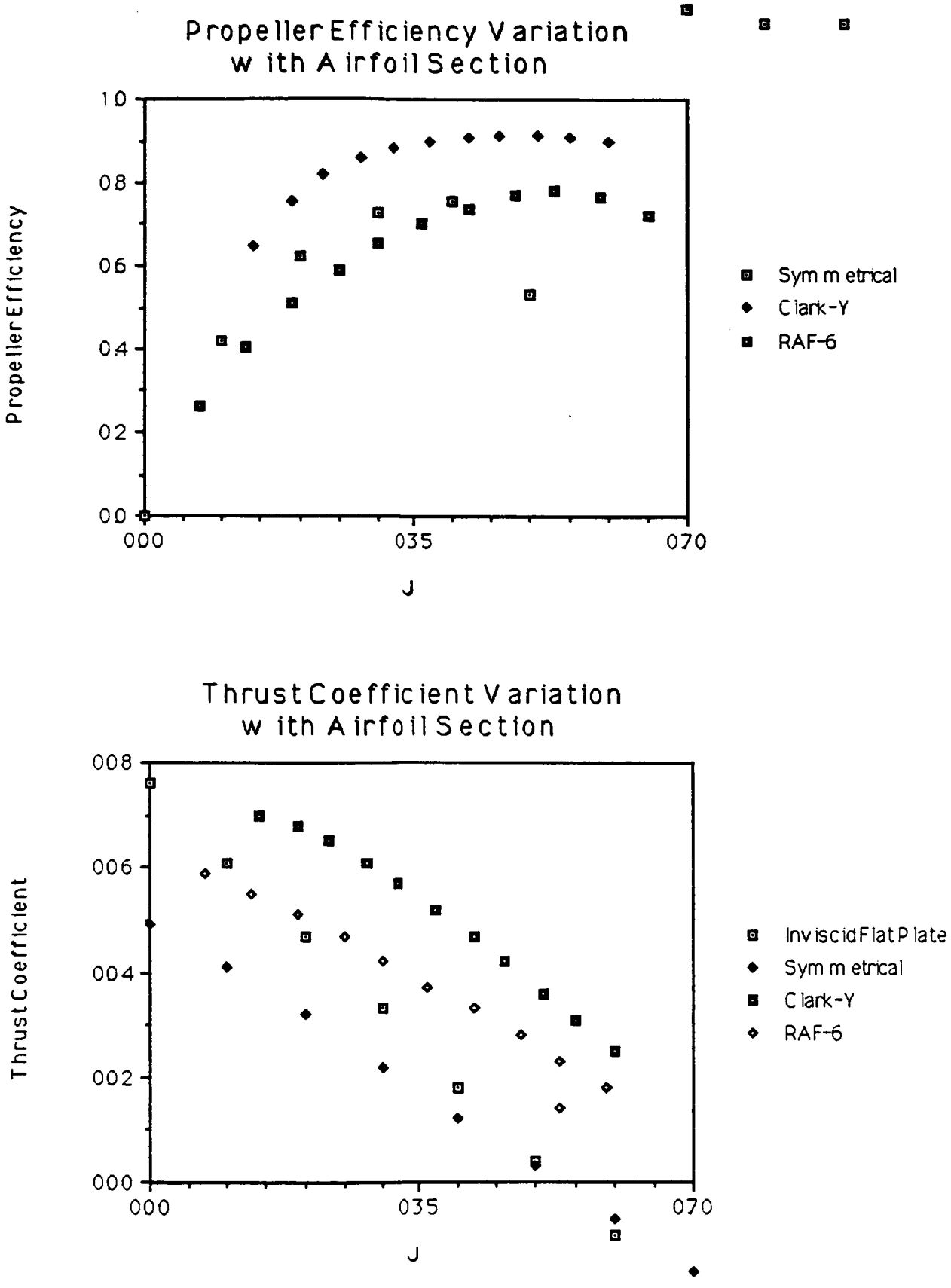
Propeller Efficiency Variation
w ith A irfoil Section
Propeller Efficiency
10
08
06
04
02
00
000
035
070
J
Sym m etrical
Clark-Y
RAF-6
Thrust Coefficient Variation
w ith A irfoil Section
Thrust Coefficient
008
006
004
002
000
000
035
070
J
Inv iscid Flat P late
Sym m etrical
Clark-Y
RAF-6

Figure 3.13

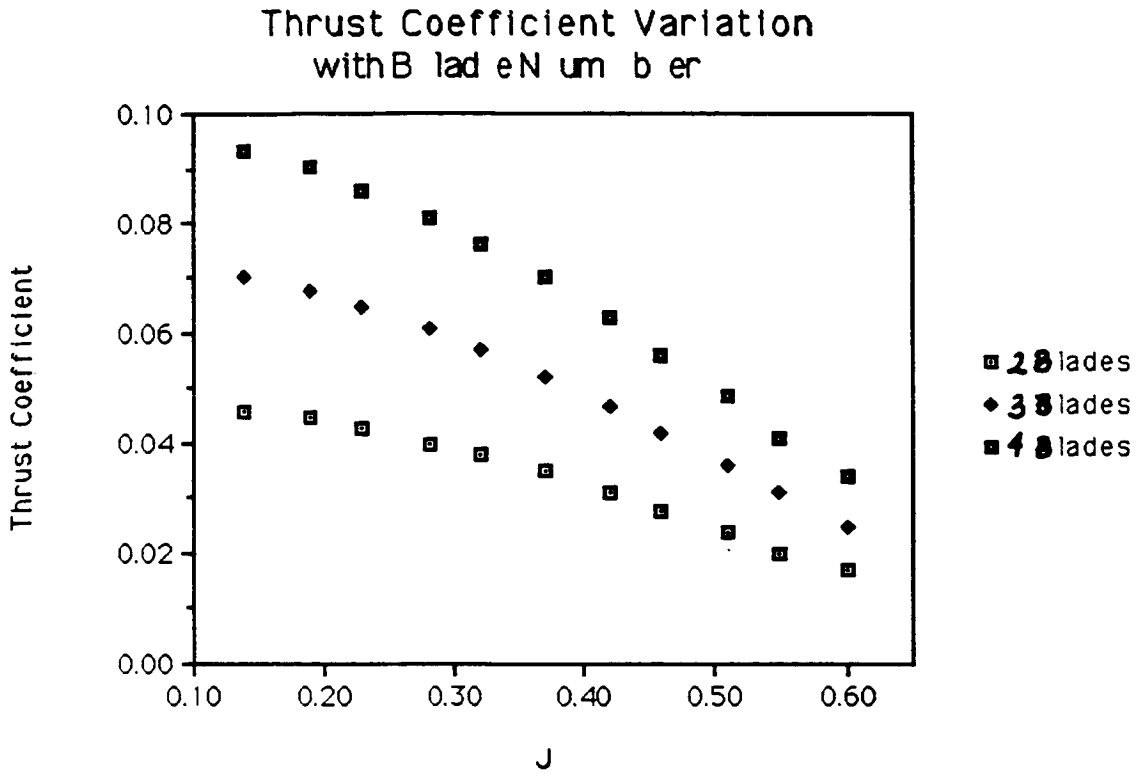
Thrust Coefficient Variation
with Blade Number
Thrust Coefficient
0.10
0.08
0.06
0.04
0.02
0.00
0.10
0.20
0.30
0.40
0.50
0.60
J
2 Blades
3 Blades
4 Blades

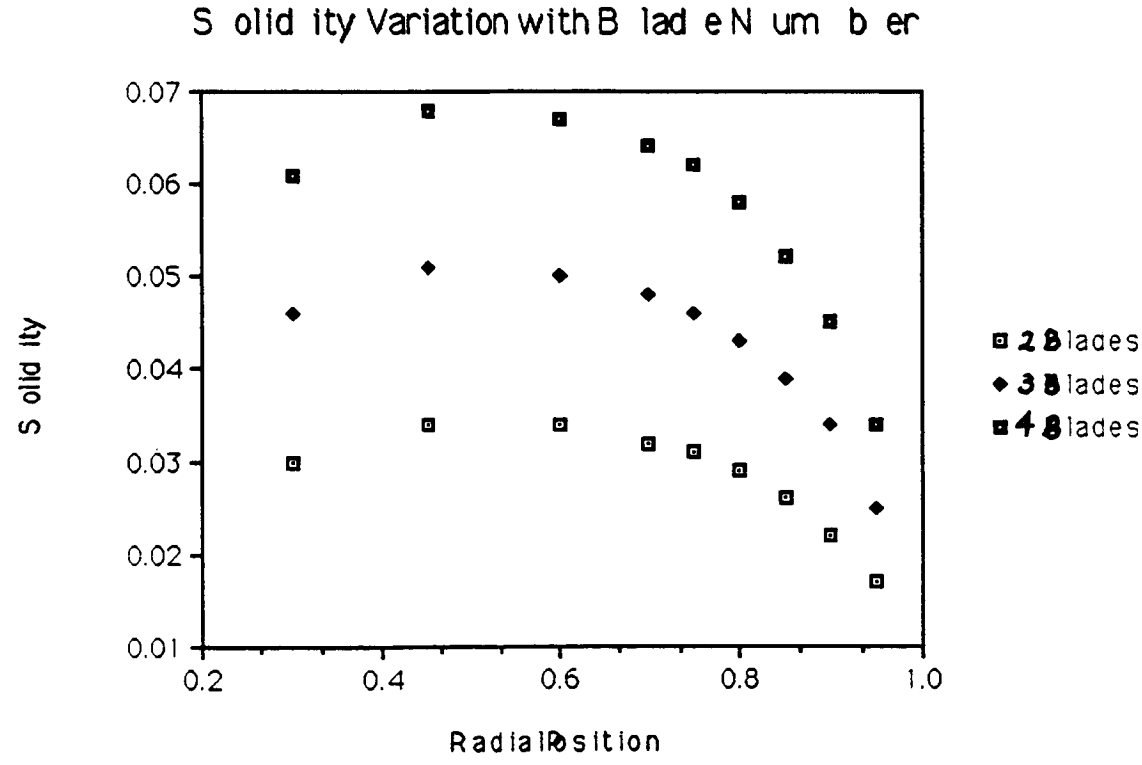
Solidity Variation with Blade Number
Solidity
0.07
0.06
0.05
0.04
0.03
0.02
0.01
0.2
0.4
0.6
0.8
1.0
Radial Position
2 Blades
3 Blades
4 Blades

Figure 3.14

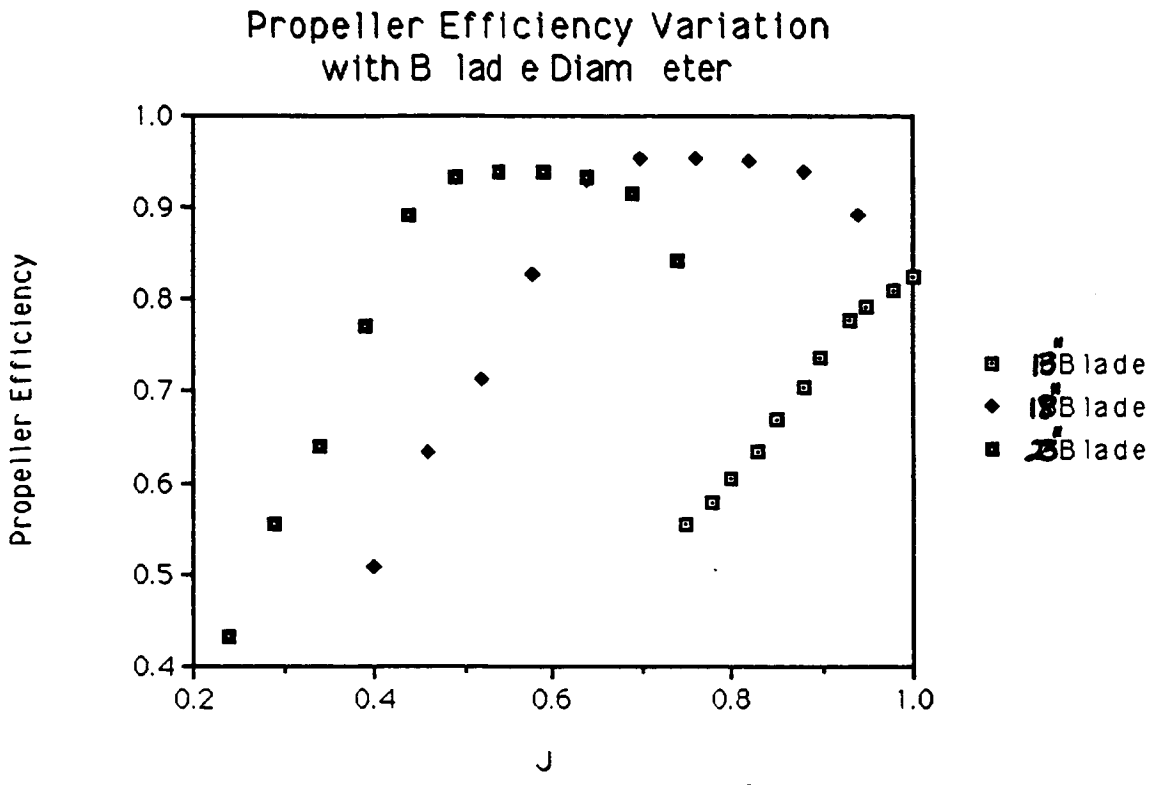
Propeller Efficiency Variation
with B lad e Diam eter
Propeller Efficiency
1.0
0.9
0.8
0.7
0.6
0.5
0.4
0.2
0.4
0.6
0.8
1.0
J
B lade
B lade
B lade

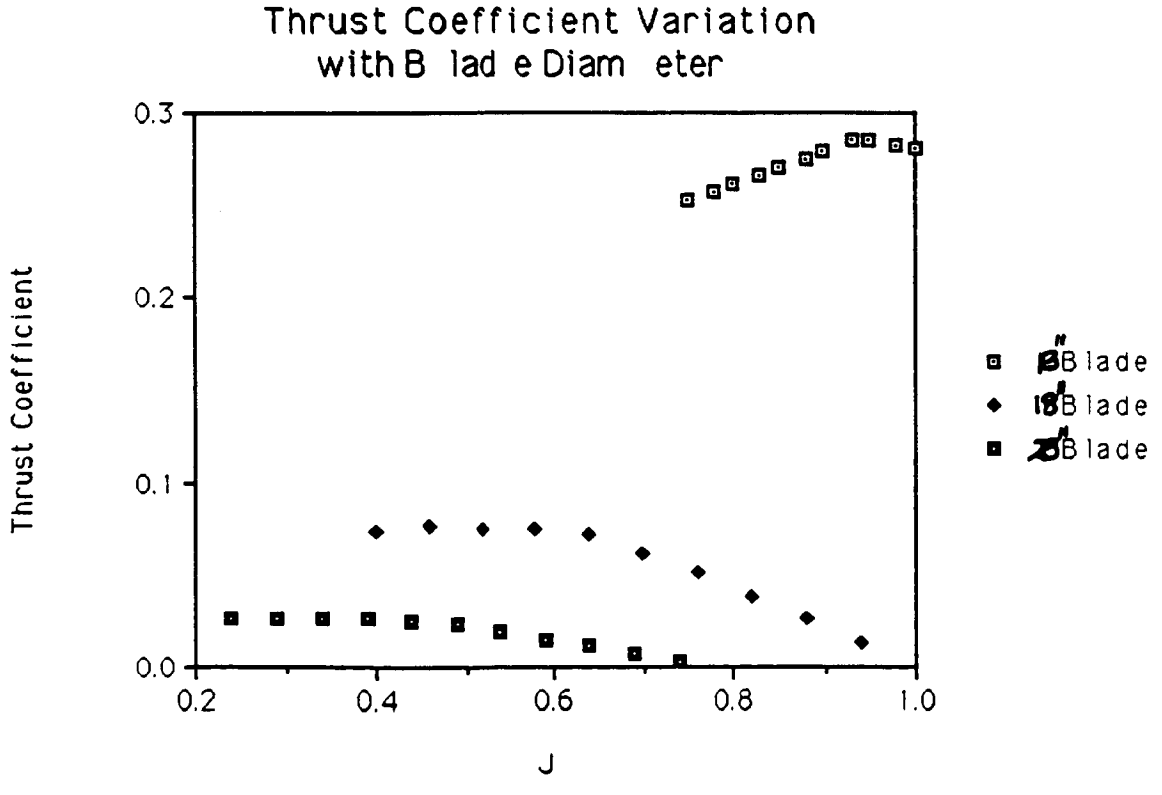
Thrust Coefficient Variation
with B lad e Diam eter
Thrust Coefficient
0.3
0.2
0.1
0.0
0.2
0.4
0.6
0.8
1.0
J
B lade
B lade
B lade

Figure 3.15

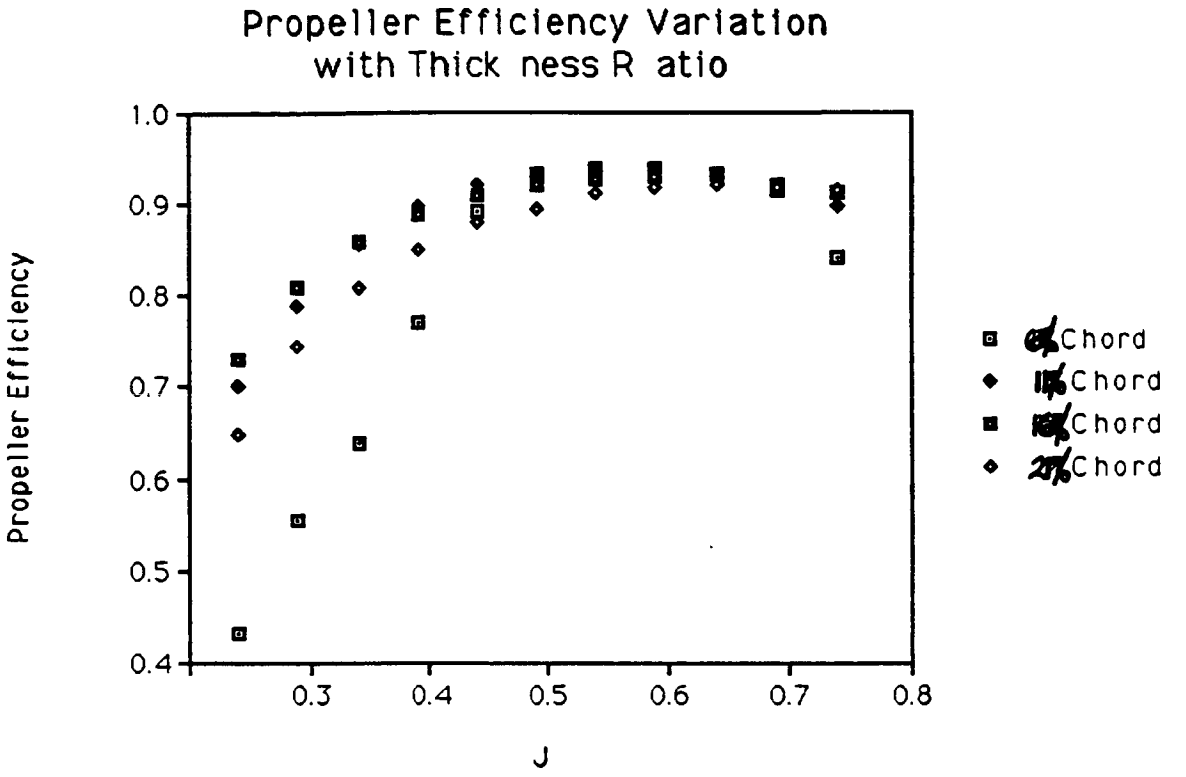
Propeller Efficiency Variation
with Thick ness R atio
Propeller Efficiency
1.0
0.9
0.8
0.7
0.6
0.5
0.4
0.3
0.4
0.5
0.6
0.7
0.8
J
Chord
Chord
Chord
Chord

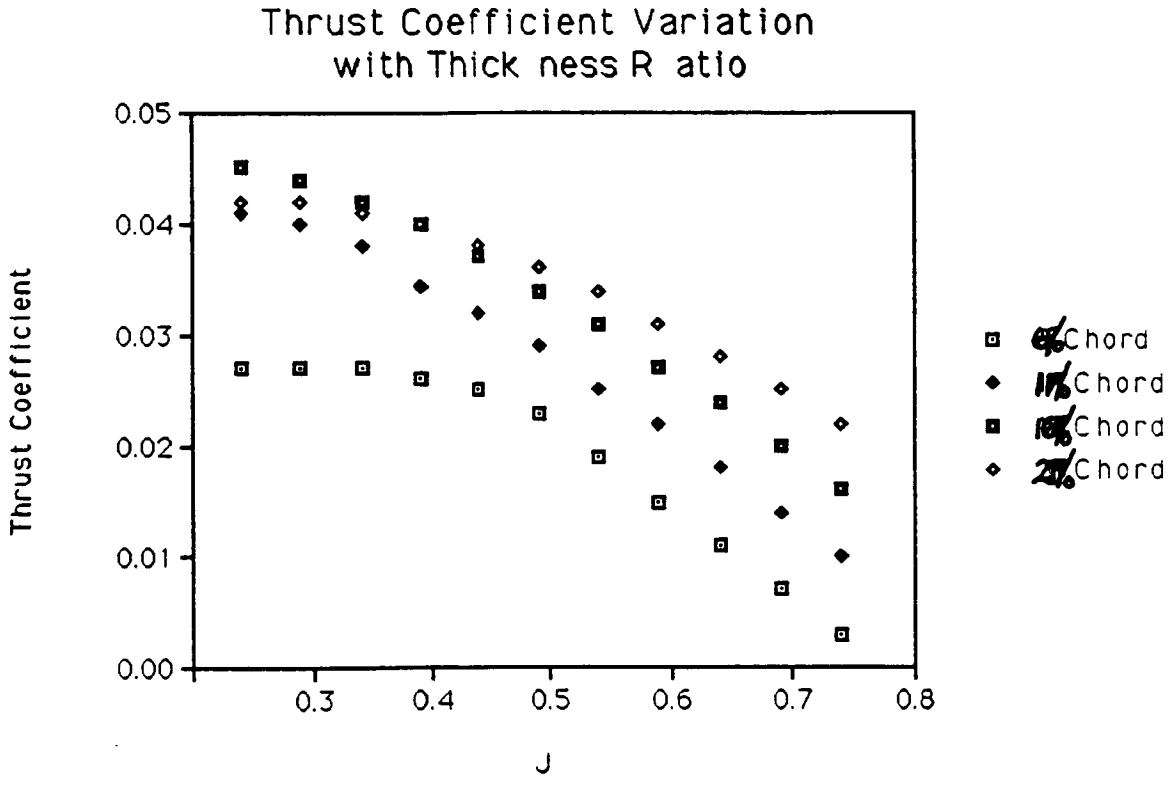
Thrust Coefficient Variation
with Thick ness R atio
Thrust Coefficient
0.05
0.04
0.03
0.02
0.01
0.00
0.3
0.4
0.5
0.6
0.7
0.8
J
Chord
Chord
Chord
Chord

Figure 3.16

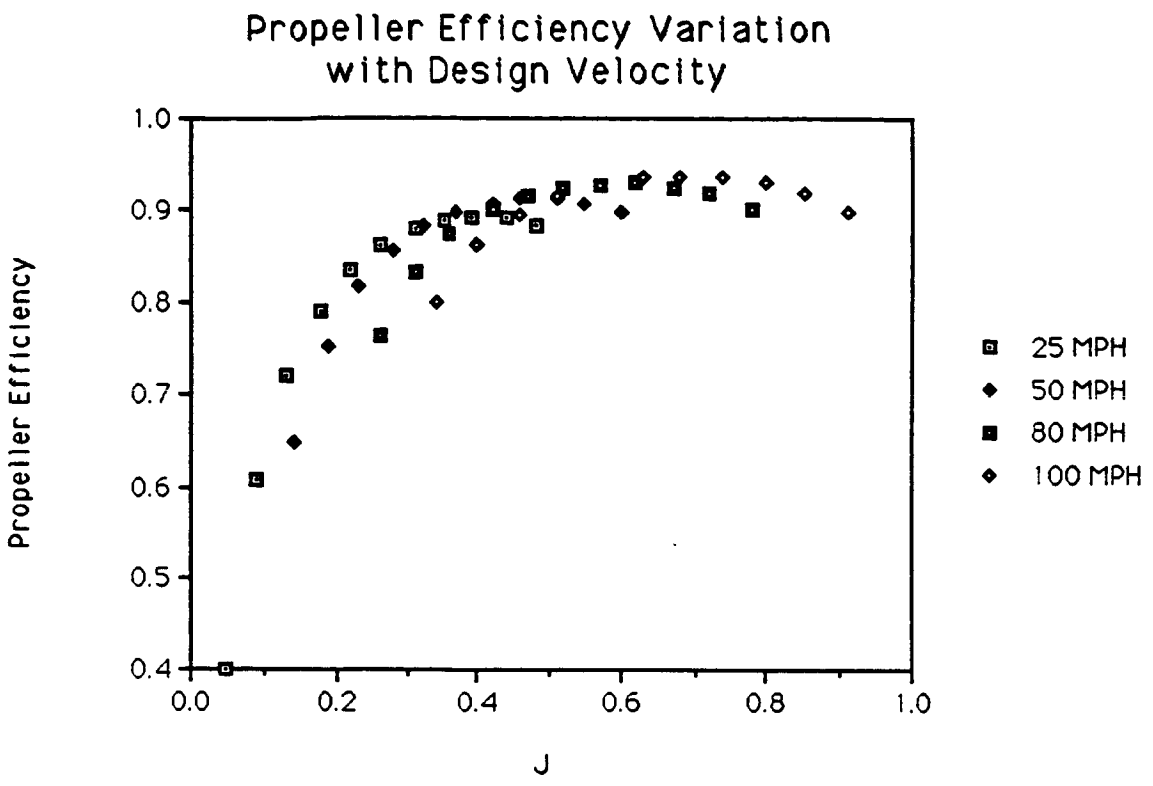
Propeller Efficiency Variation
with Design Velocity
Propeller Efficiency
1.0
0.9
0.8
0.7
0.6
0.5
0.4
0.0
0.2
0.4
0.6
0.8
1.0
J
25 MPH
50 MPH
80 MPH
100 MPH

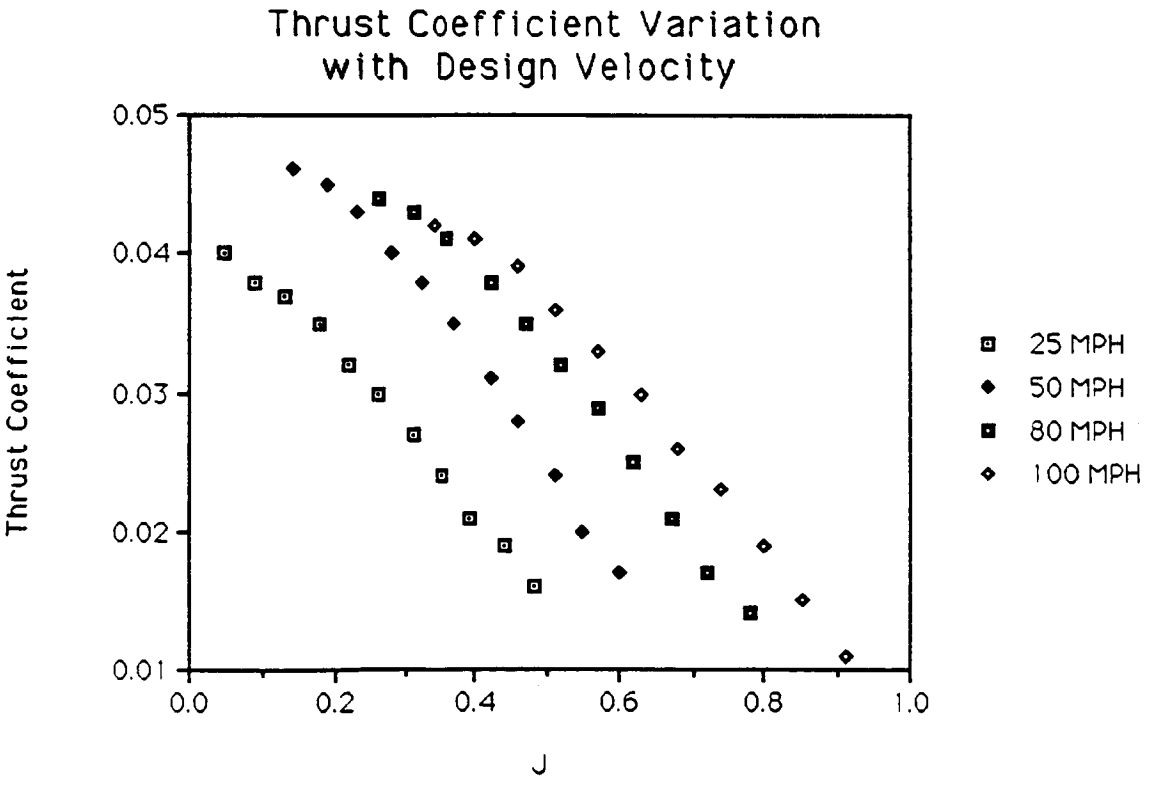
Thrust Coefficient Variation
with Design Velocity
Thrust Coefficient
0.05
0.04
0.03
0.02
0.01
0.0
0.2
0.4
0.6
0.8
1.0
J
25 MPH
50 MPH
80 MPH
100 MPH

TABLE 1.

Engine Data Base

Wed, May 3, 1989 5:35 AM

	Engine Name	Weight (lb)	Brake hp	Displacement	RPM	oz/min	fuel
1	fox 15x	0.250		0.150	12000.000		0.250
2	fox 15	0.375		0.150	14000.000		0.300
3	fox 19	0.344		0.190	15000.000		0.350
4	fox 19 s	0.516		0.199	17000.000		0.400
5	fox 25 bushing	0.375		0.250	12000.000		0.400
6	fox 29 s	0.594		0.290	11000.000		0.450
7	fox 35 stunt	0.438		0.352	9500.000		0.500
8	Fox 36 s	0.594		0.360	12000.000		0.600
9	Fox compact 40	0.594		0.400	14500.000		0.700
10	fox 40 bb	0.750		0.400	13500.000		0.800
11	Fox 45 bb	0.750		0.450	14000.000		0.900
12	fox eagle III	1.062		0.610	13000.000		1.250
13	Max 108fsr	1.652	3.000	1.089	16000.000		
14	Max 90fsr	1.491	2.500	0.909	16000.000		
15	max 65vr-df-abc	1.233	2.750	0.649	22000.000		
16	Max 61 vf abc	1.198	1.800	0.607	17000.000		
17	Max 61 vr-abc	1.267	1.800	0.607	17000.000		
18	Max 46vr-df-abc	0.835	1.900	0.455	23000.000		
19	Max 45fsr abc	0.694	1.400	0.456	16000.000		
20	max 45 fsr	0.692	1.300	0.456	16000.000		
21	Max 28 F	0.491	0.900	0.279	16000.000		
22	Quad 505	5.100	4.500		11000.000		
23	Quad 50x	4.300	4.400		11000.000		
24	Quad 65	6.500	6.000		11000.000		
25	Quad 80	7.700	7.500		11000.000		
26	RM Titan	6.500	6.500	4.300			
27	Kioritz 3.65	6.000	6.000	3.650			
28	Kioritz 5.6	9.000	9.000	5.600			

CHAPTER IV

WEIGHT ESTIMATION

4.1 Component Weight Fractions

The following is a breakdown of component weights in percent of equipped gross weight of 30 lb. Note that at weights above 40 lb AMA permission for operation is required.

	percent of total,(%)	weight, (lb)
structure	48.58	14.50
power plant	29.44	8.83
fixed equipment	10.31	3.01
test specimen	6.64	2.00
empty weight	95.00	28.50
payload	5.00	1.50
<u>Structure</u>		
wing	13.23	3.98
empenage	4.42	1.33
fuselage(s. below)	22.08	6.63
nacelle	1.47	0.44
gear	7.36	2.22
<u>fuselage</u>		
platform	0.91	0.27
tail boom	7.36	2.21
main fuselage	12.30	3.68
test specimen boom	1.54	0.46

4.2 Center of Gravity Location and Travel

A Fortran program given in Appendix F was written that determines the center of gravity location (CG) along the longitudinal and yaw axis as well as an incremental CG travel with an incremental component location shift. This program also calculates mass moments of inertia (Ix, Iy along longotudinal and lateral axis respectively). The design CG location is at 30% of the mean aerodynamic chord (MAC). A change from this location has negligible effect on dynamic stability . The phugoid, Dutch roll and short period damping ratios (Zp, Zdr, Zsp) as well as the Dutch roll undamped natural frequency (Wndr) and the Dutch roll product (W*Zdr) are plotted at 35ft/s, 75ft/s, and 115ft/s versus CG location from 10% to 40% MAC (see Appendix G for the graphing program and Figures 4.1, 4.2, 4.3).

Although a CG shift constitutes a change in tail volume ratio, the above dynamic stability criteria remain nearly constant throughout the range of CG locations. Therefore, handling characteristics will remain constant throughout a mission as fuel is depleted and the CG moves forward or aft.

The effect of changing I_x and I_y was also plotted (see Figures 4.4, 4.5). It is estimated that they could be changed by 10% without changing the CG location. The above mentioned CG program can be used to rearrange the mass distribution without shifting the CG. Figures 4.4 and 4.5 show that a change in Ix has virtually no effect on the plotted dynamic stability characteristics, while a 10% increase in I_y reduces the Dutch roll product and increases the short period

damping, both by only 5%. Since other, more effective means can be used to change dynamic characteristics, mass redistribution in the fuselage is not used for this purpose. Any component location changes have negligible effects on dynamic stability.

Similarly, static stability is not influenced by any reasonable CG shift. The neutral point is well aft of any location where the CG can reasonably be expected to move. In addition, the large tail gives a stick fixed static margin of 0.75, which is much larger than what is normally used on conventional aircraft. Thus, minor CG shifts can be performed in the field (changing servos, batteries etc.) without changing the stability and handling characteristics of the RPV.

Fig. 4.1 Zp,Zsp,Zdr,Wndr,W*Zdr vs. CG Location

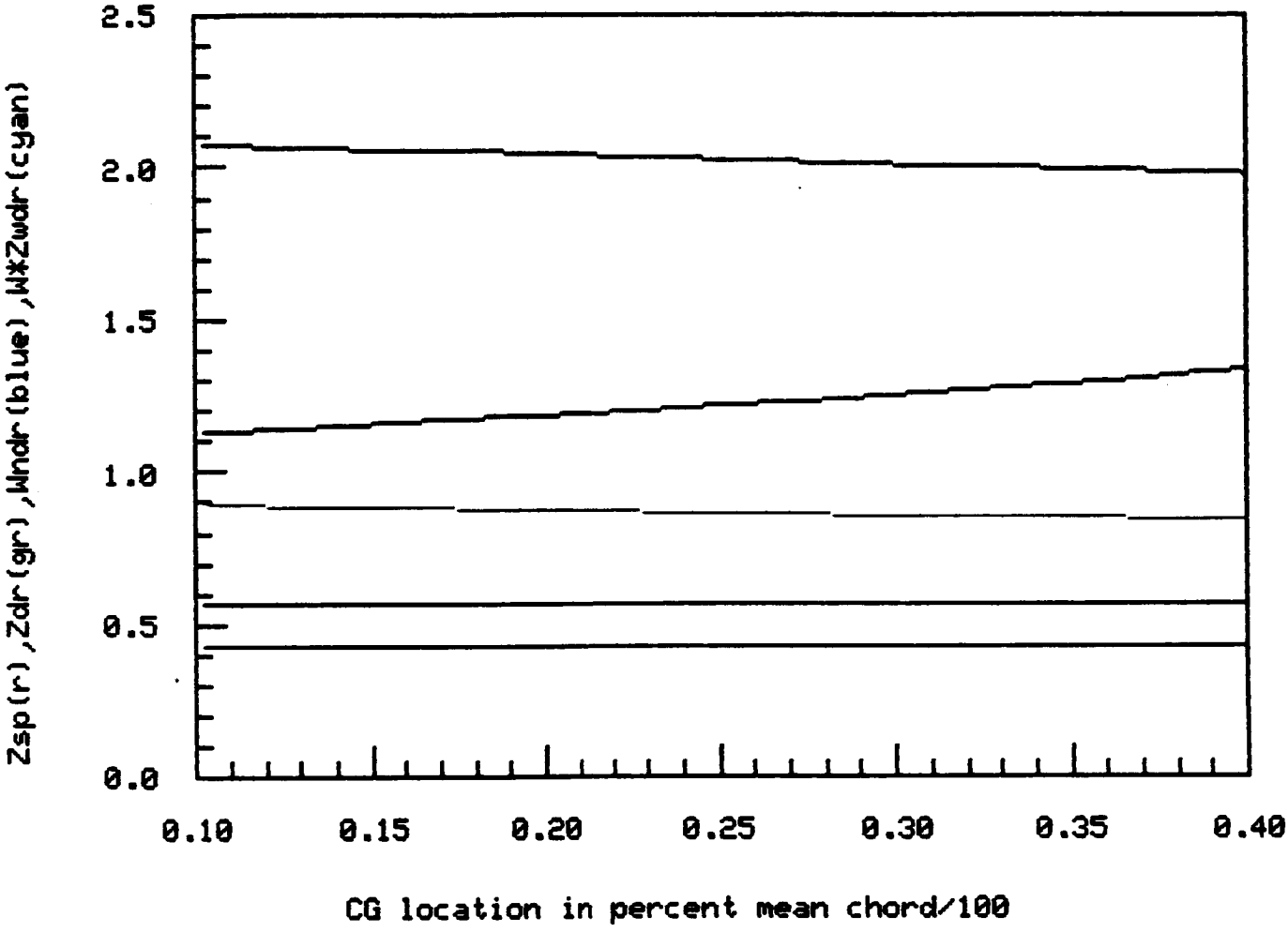

Fig. 4.2; u=75 ft/s, Zp,Zsp,Zdr,Wndr,W*Zdr vs. CG LOCATION

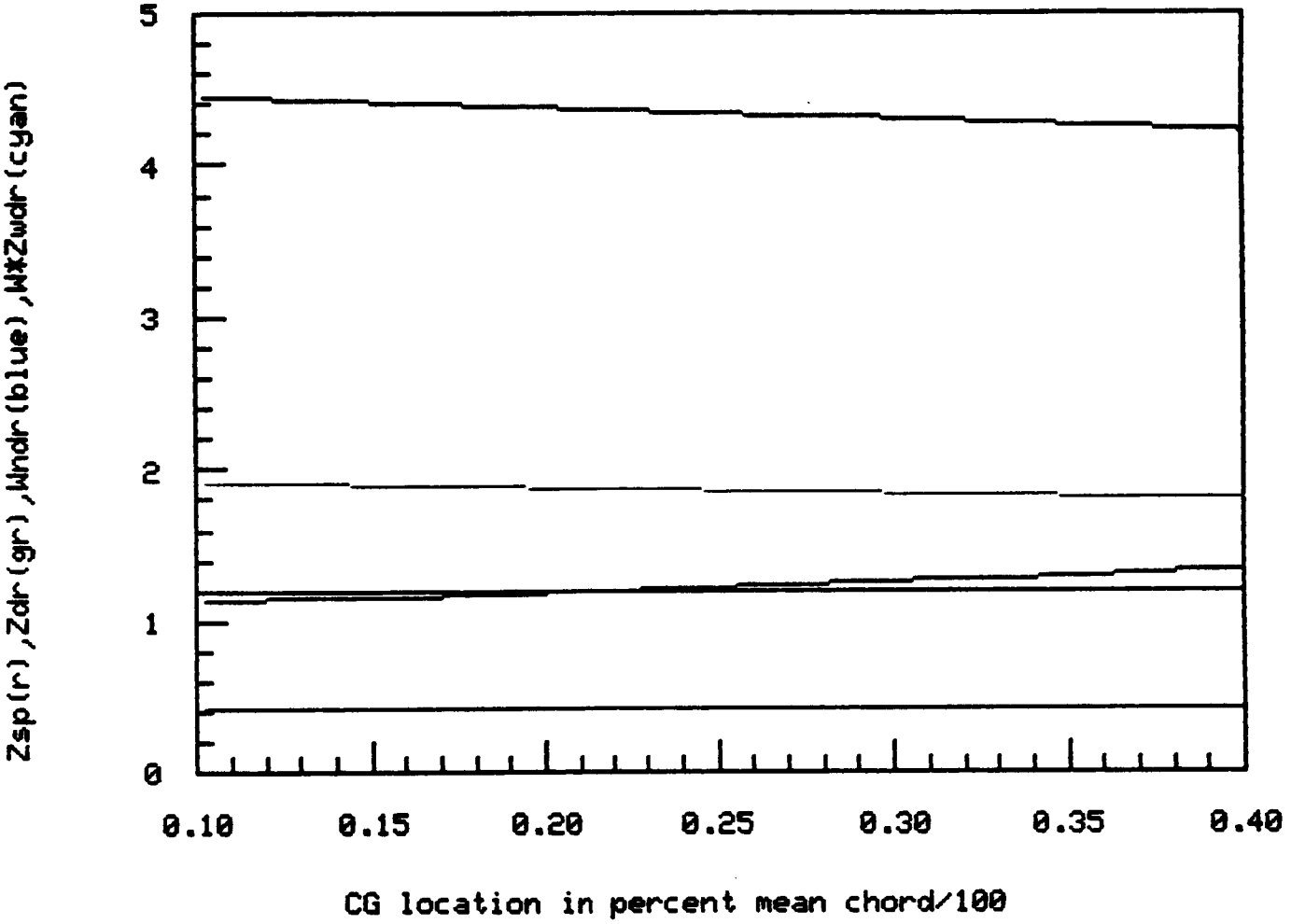

Fig. 4.3; u=115 ft/s, Zp,Zsp,Zdr,Wndr,W*Zdr vs. CG LOCATIO

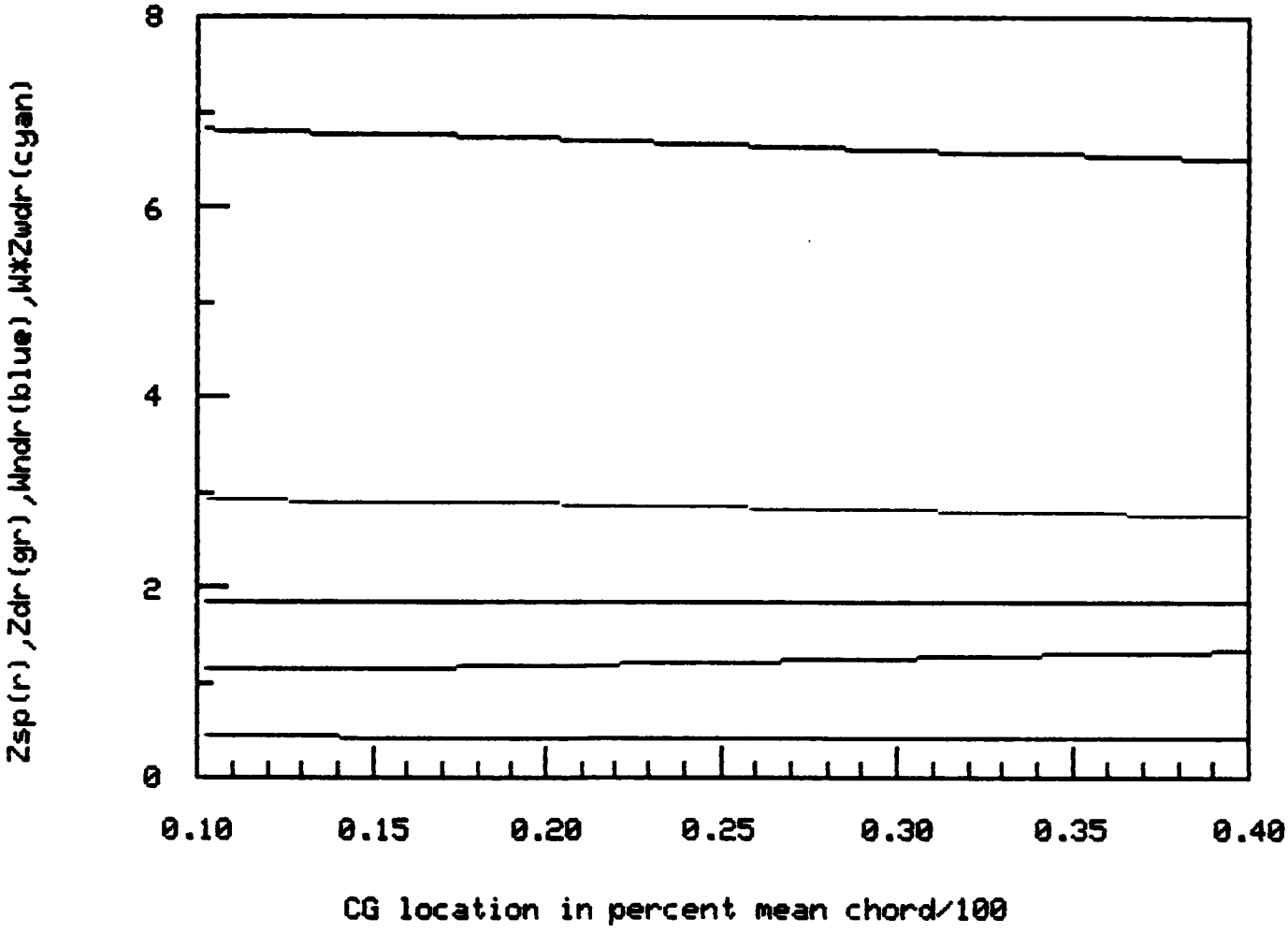

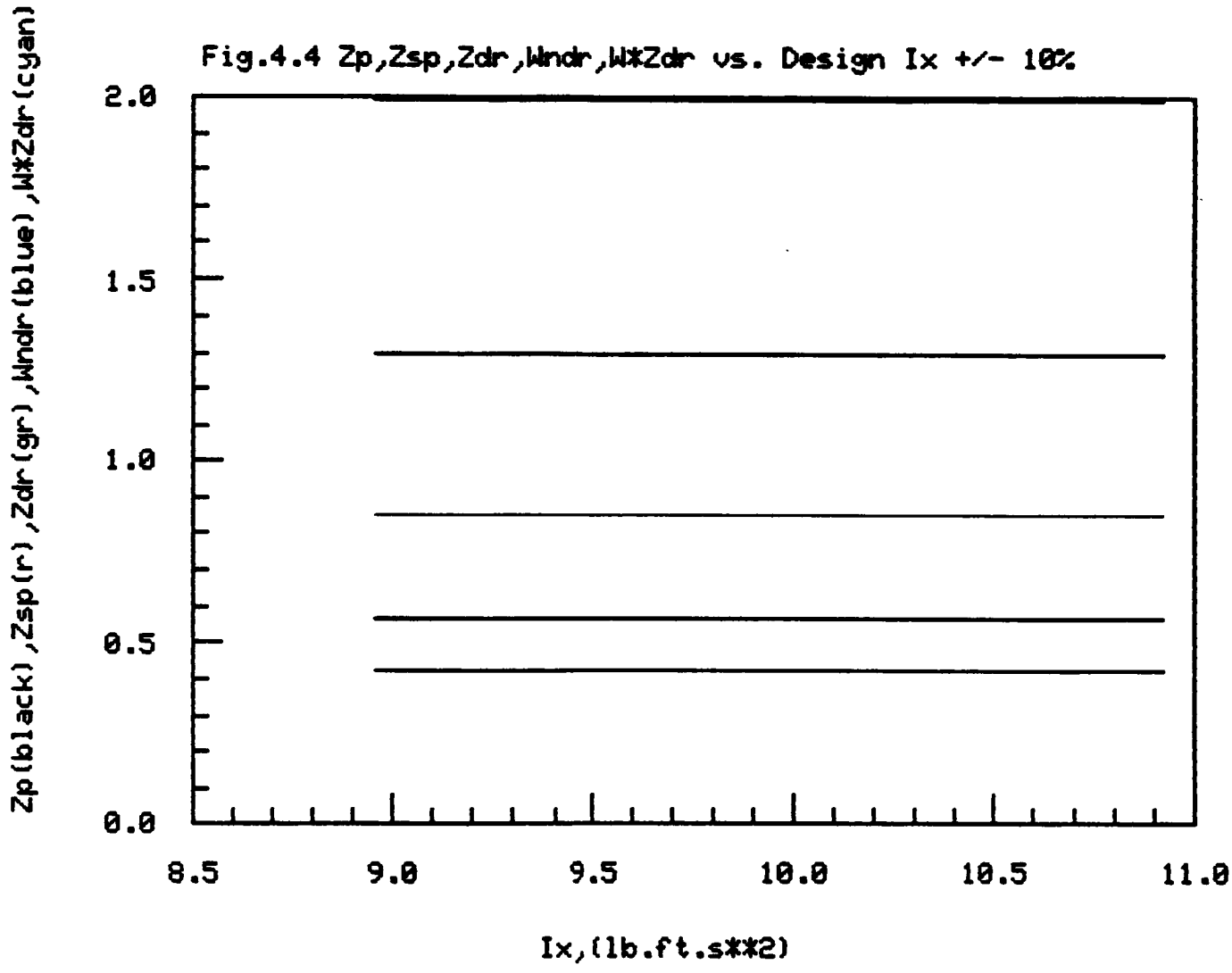
Fig.4.4 Zp,Zsp,Zdr,Wndr,W*Zdr vs. Design Ix +/- 10%
Zp(black),Zsp(r),Zdr(gr),Wndr(blue),W*Zdr(cyan)
2.0
1.5
1.0
0.5
0.0
8.5
9.0
9.5
10.0
10.5
11.0
Ix,(lb.ft.s**2)

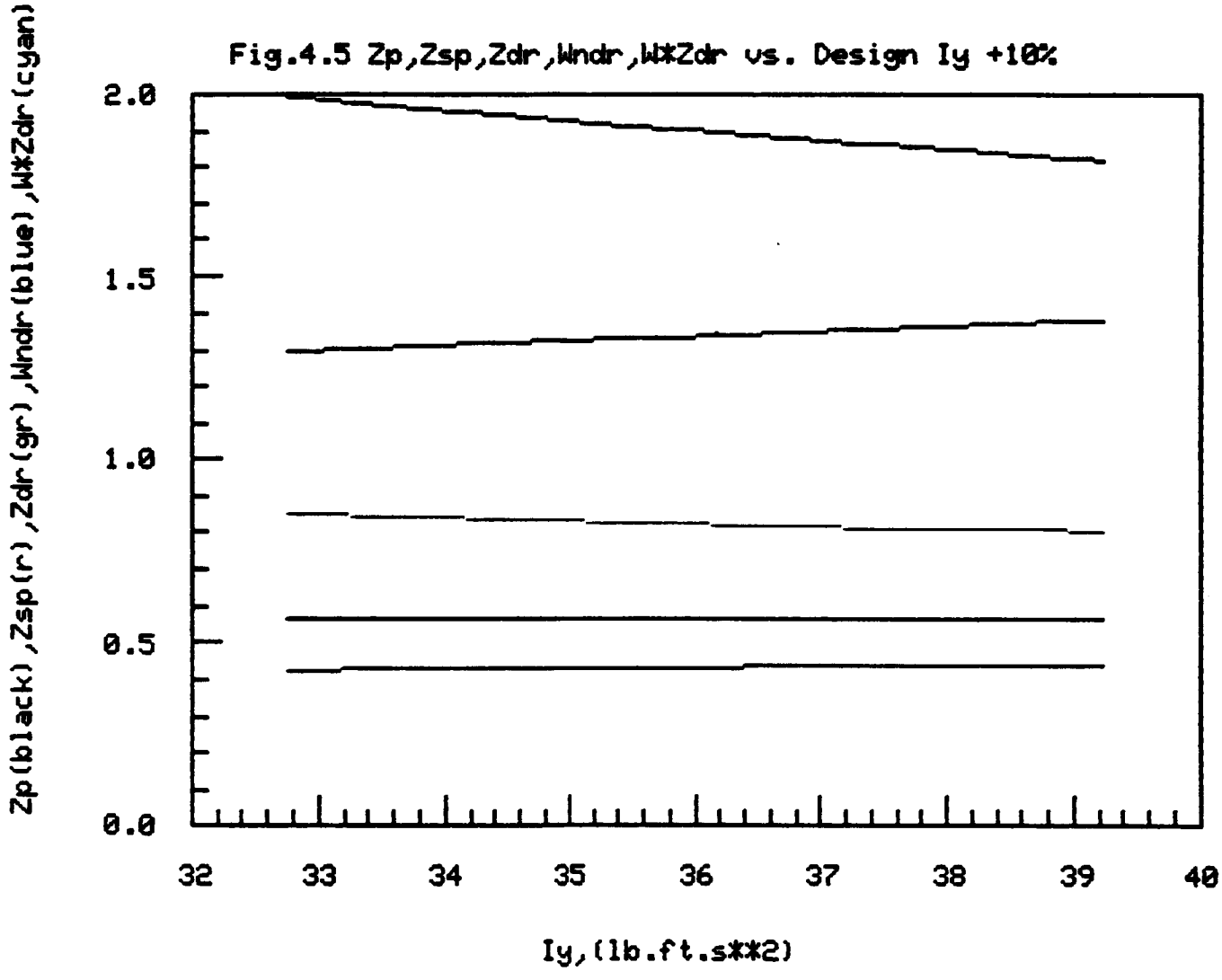
Fig.4.5 Zp,Zsp,Zdr,Wndr,W*Zdr vs. Design Iy +10%
Zp(black),Zsp(r),Zdr(gr),Wndr(blue),W*Zdr(cyan)
2.0
1.5
1.0
0.5
0.0
32
33
34
35
36
37
38
39
40
Iy,(lb.ft.s**2)

CHAPTER V
STABILITY AND CONTROL

5.1 Control Surface Location and Sizing

The stability and control of the SPiRiT presented a unique as well as important challenge. The effect of the test specimen in front of the aircraft on the longitudinal stability was quite pronounced and necessitated control surfaces sized in direct relation to the forces that the test specimen produced.

The control effectiveness of the tail was of major importance in the design of this aircraft due to the forces created by the test specimen at the front of the aircraft. The first step was to determine the maximum forces generated by the test specimen and hence the maximum moment that the test specimen could create. The tail control surface could then be sized according to the moment that the test specimen creates. A symmetric tail airfoil section was chosen from which the lift curve slope of the tail could be calculated. The $C_{L\alpha}$ for this airfoil section was calculated for aspect ratios ranging from one through seven. It was decided to use the total horizontal tail surface as the control surface thus providing a tau value of 1.0 in the equation: $dC_{Lt}/d\delta_e = (C_{L\alpha t})x(\tau)$ which determines the elevator effectiveness. τ is a parameter which depends on the amount of the tail area that is also used as the elevator. By using the entire tail surface as the elevator, the elevator effectiveness could be maximized to allow for a higher tail moment that could be created while keeping the drag of the tail section as low as possible. The horizontal tail surface had to be large enough to provide a moment that would counteract the maximum nose up moment that could be created by the largest test specimen allowed. The tail size was also somewhat limited by the desire to keep the tail volume ratio no greater than 1.0. With a limit on the tail moment arm of 1.32 meters set by structural requirements and a tail volume ratio limit of 1.0 set by aerodynamic considerations, the horizontal tail could be sized to provide sufficient

control characteristics. An assumption was made that the aircraft should be able to accept a test specimen of dimensions of 5 feet by 16 inches with a maximum lift coefficient of 1.3. This value was chosen as a reasonable lift coefficient that would encompass many airfoil sections presently developed. A margin of safety of 1.1 was also desired for the moment that the tail would have to counteract. The tail size was chosen from a parametric trade study conducted by Mr. Paul Edwards. Plots of allowable tail sizes that would provide adequate control power are referenced as Figures 5.1 and 5.2 for flight velocities of 20 m/s and 40 m/s respectively. Due to the requirement that the RPV have a tail volume ratio of 1.0 or less, a plot was developed of the tail moment versus tail volume ratio as a function of aspect ratio. This plot is referenced as Figure 5.3. The tail size was determined to be 0.75 square meters in area with an aspect ratio of 4.

5.2 Stability Characteristics

The next step was to determine the stability characteristics of the aircraft with the chosen tail design. A tail moment arm was determined from structural considerations with a length as long as possible for maximum control effectiveness yet not too long as to compromise the structural integrity of the tail boom. With a fixed fuselage shape and given wing design as well as center of gravity position, the next step was to determine if the chosen tail size satisfied the stability requirements of the aircraft. The horizontal stabilizer had to meet the requirement that the aircraft pitching moment curve have a negative slope, i.e.: $dC_m/d\alpha < 0$. This is necessary for static longitudinal stability. It was also necessary to have a positive intercept in order to trim the aircraft at positive angles of attack. This necessitated a $C_{mo} > 0$. The horizontal tail size was examined as to its longitudinal stability characteristics in accordance with a worst case scenario with the largest test specimen in front of the aircraft and flying at the fastest speed

possible. This created the largest destabilizing force from the test specimen which in turn needed to be counteracted by the tail surface also taking into account the contributions from the wing and fuselage structures to the static stability of the aircraft. A plot of the $C_{m\alpha}$ of the tail versus tail volume ratio as a function of aspect ratio is referenced as Figure 5.4.

The effect of the test specimen on the static stability of the aircraft was the first value that needed to be determined. The moment arm of the test specimen was set according to aerodynamic considerations which specified that the test specimen be as far in front of the aircraft as possible to reduce both wing and fuselage contribution on the flow characteristics over the test specimen, yet still retain the ability to construct a test specimen boom that would be structurally sound. The $C_{m\alpha}$ for the test specimen was calculated from the given measurements by a simple free body diagram method shown in Calculations 5.1. The value for the $C_{m\alpha}$ of the test specimen was determined to be approximately 1.15.

The effect of the wing on the static stability was also determined for the aircraft. The sum of the moments of the wing about the center of gravity of the aircraft was determined to yield the equation $C_{m\alpha w}=(C_{L\alpha w})x(x_{cg}/c-x_{ac}/c)$. The center of gravity as well as the chord of the wing was fixed from aerodynamic considerations. $C_{L\alpha w}$ was also fixed from the given wing design. The aerodynamic center of the wing was taken as the quarter chord of the wing and this also was determined from aerodynamic as well as general layout characteristics of the aircraft. From the given values the $C_{m\alpha}$ for the wing was determined to be approximately -0.22.

The method for calculating $C_{m\alpha}$ for the fuselage presented some unique challenges due to the wing placement in relation to the fuselage. Because the wing was not mounted in the center of the fuselage but rather above the fuselage, the method developed by H. Multhopp could not be used. Instead, a method developed by R. R. Gilruth was used to calculate the static stability contribution from the fuselage.

This method was more general than the method developed by Multhopp but was more conducive to accurate results for our aircraft. The detailed calculations for our aircraft using this method can be found in Calculations 5.2. A $C_{m\alpha}$ for the fuselage was determined to be approximately -0.00037. This value was extremely small compared to the other values for $C_{m\alpha}$.

It could then be verified that the horizontal tail size provided a sufficient $C_{m\alpha}$ to give an overall $C_{m\alpha}$ for the aircraft that was less than zero. C_{mo} for each of the components was also determined to insure a positive intercept for the pitching moment curve to enable trimming of the aircraft at positive angles of attack. The total pitching moment for the aircraft was also determined at various angles of attack and the plot of this is referenced as Figure 5.6. The calculations to determine the pitching moments for the aircraft parts is located in Calculations 5.3. In addition, the effect of elevator deflection on the moment coefficient of the tail in relation to the center of gravity was examined. A plot of tail moment coefficient as a function of angle of elevator deflection at various flight angles of attack is referenced as Figure 5.7.

The movement of the center of gravity of the aircraft was also examined to determine its effect on the static stability of the aircraft. To insure that the aircraft was statically stable, the limitations on the center of gravity position had to be determined. Setting $C_{m\alpha}$ equal to zero in the pitching moment equation enabled us to solve for the stick fixed neutral point for the aircraft. This was necessary to insure that the center of gravity position did not move past this point thus creating a statically unstable aircraft. Due to the large tail surface, a stick fixed static margin of approximately 75% was calculated. This static margin is extremely large thus providing a wide range of travel for the center of gravity position. It is desired to conduct a more indepth study of how to reduce this static margin somewhat for better maneuverability characteristics at a later time.

A program was then developed to determine suitable tail areas to provide static

stability of the aircraft. The tail volume ratios as well as the aspect ratios for the tail were varied to come up with a suitable tail design. The program to determine this is found in Appendix H. The minimum value for $C_{m\alpha}$ for the tail was determined by the need to obtain a total $C_{m\alpha}$ for the aircraft that was less than zero. Therefore, the tail had to have a sufficient $C_{m\alpha}$ to counteract the $C_{m\alpha}$'s for the other structures of the aircraft.

The elevator angle for trim was then calculated by setting the pitching moment equation equal to zero and calculating the elevator deflection angle. The calculations to determine the elevator angle to trim are located in Calculations 5.4. It was desired to have a trim angle of less than 4 degrees from horizontal which was obtained. The trim angle was determined to be approximately -2 degrees.

The directional stability of the aircraft was also examined. The contribution of the wing-body structure on the directional stability of the aircraft was first examined. This was accomplished by calculating the $C_{n\beta}$ value for the wing-fuselage structure. The method used was taken from Reference 1 and can be found in Calculations 5.5. The vertical tail could then be sized to provide an effective $C_{n\beta}$ to counteract the destabilizing contribution obtained from the wing-body structure. The program to determine $C_{n\beta}$ for the vertical tail as a function of tail size and aspect ratio is referenced in Appendix I.

The contribution of the vertical tail on the aircraft's directional control characteristics was also examined. The calculations for the directional control characteristics of the aircraft are located in Calculations 5.6. A plot of $C_{n\beta}$ for the vertical tail as a function of tail volume ratio and aspect ratio is referenced as Figure 5.8. In addition, the effect of rudder deflection on the $Cn\delta r$ of the vertical tail was also looked at. A plot of the rudder control effectiveness at various rudder deflections is referenced as Figure 5.9.

5.3 Stability and Control Conclusions

The stability and control characteristics of this aircraft are very unique due to the fact that the test specimen is located in front of the main aircraft. The test specimen created the need for large longitudinal control surfaces as well as a modified longitudinal stability analysis. The general design of the aircraft with the wing positioned above the fuselage also created difficulties in the static stability analysis of the aircraft. A program was developed to calculate most of the pertinent stability values for the aircraft. This program is located in Appendix H. A summary of the proposed control surfaces and important static stability and control values are found in Tables 5.1 and 5.2 respectively.

Although the design of this aircraft presented some interesting challenges in the field of static stability and control, the design proved feasible and effective in the collection of the necessary data for the test specimen. The chosen values are not necessarily perfect values for this aircraft yet, they are chosen from an appropriate range of values to provide sufficient stability and control. In the final design, this aircraft should demonstrate excellent static stability as well as more than sufficient control over its operating range.

TABLE 5.1: FINAL CONTROL SURFACE SIZES

COMPONENT	SURFACE AREA (METERS^2)	SPAN (METERS)	ASPECT RATIO
HORIZONTAL STABILIZER	0.75	1.73	4
VERTICAL STABILIZER	0.28	0.917	3

TABLE 5.2: STABILITY CHARACTERISTICS

COMPONENT	$C_{m\alpha}$	C_{mo}
HORIZONTAL TAIL	-3.48	0.392
FUSELAGE	-0.000374	0.00
WING	-0.218	-0.152
TEST SPECIMEN	1.16	0.0869
OVERALL	-2.54	0.327
STATIC MARGIN	77.5%	

REFERENCES

[1] Nelson, Robert C., Flight Stability and Automatic Control, McGraw-Hill, Inc., 1989.

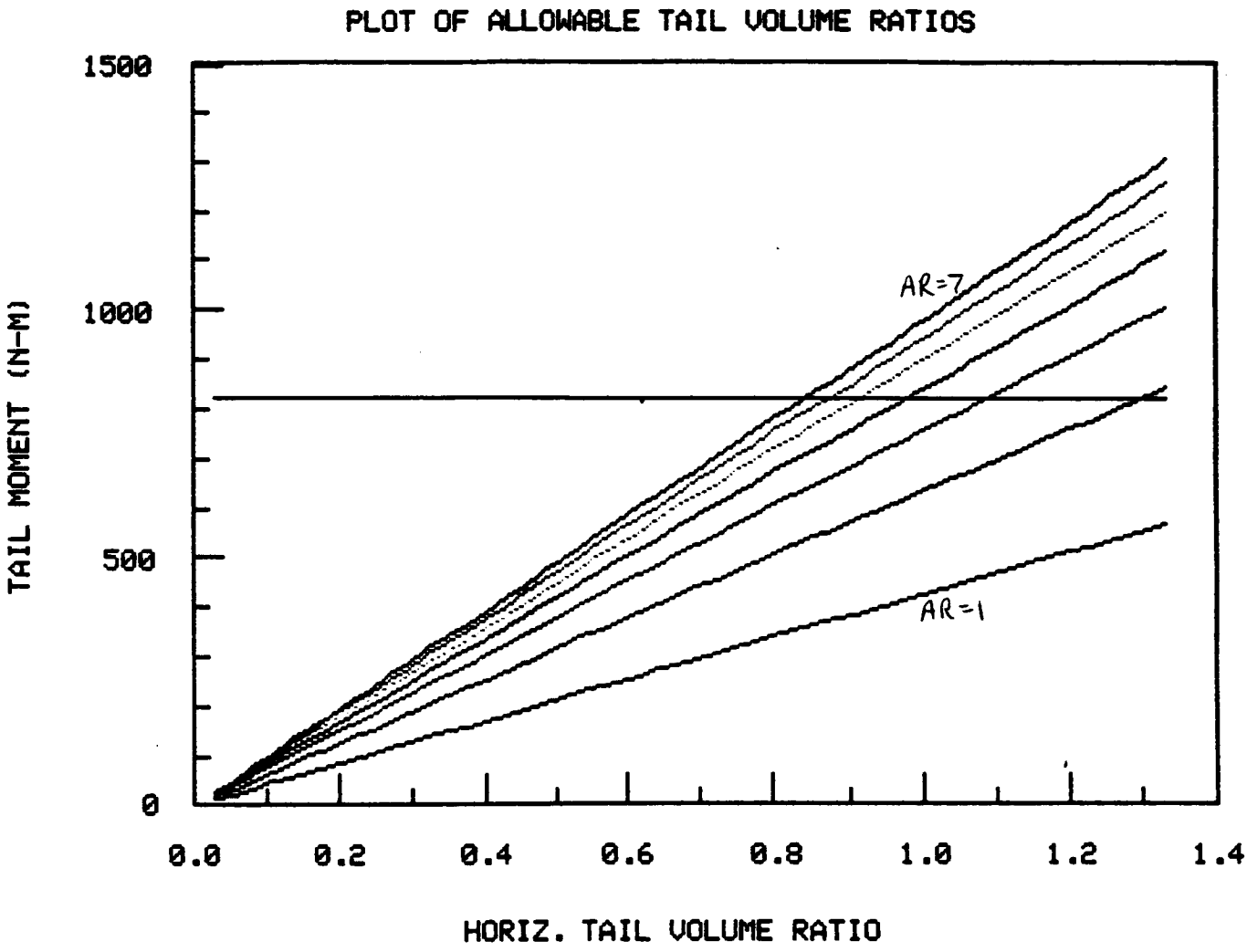
PLOT OF ALLOWABLE TAIL VOLUME RATIOS
1500
1000
500
0
TAIL MOMENT (N-M)
AR=7
AR=1
0.0
0.2
0.4
0.6
0.8
1.0
1.2
1.4
HORIZ. TAIL VOLUME RATIO

Figure 5.3

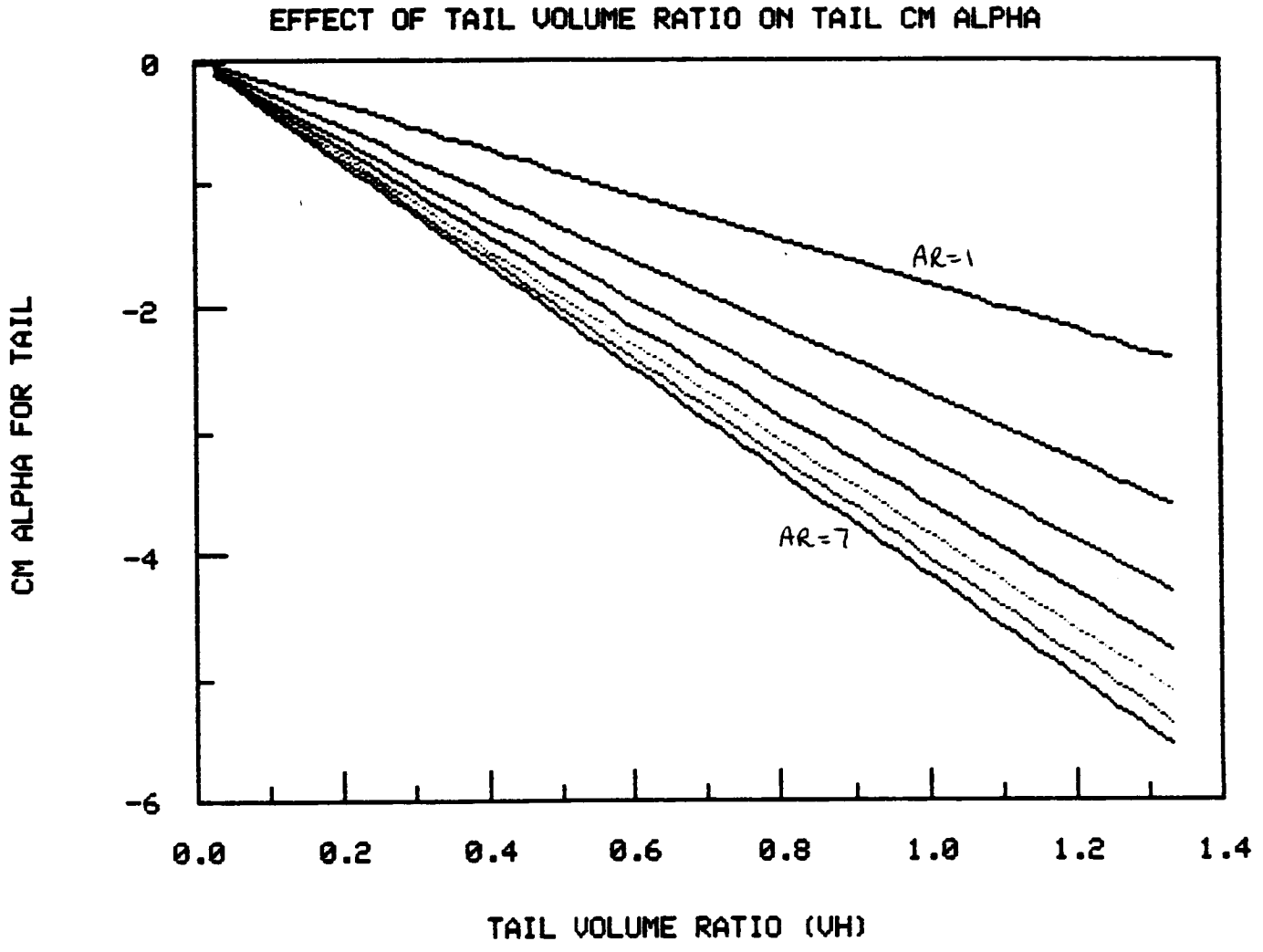
EFFECT OF TAIL VOLUME RATIO ON TAIL CM ALPHA
CM ALPHA FOR TAIL
0
-2
-4
-6
AR=1
AR=7
0.0
0.2
0.4
0.6
0.8
1.0
1.2
1.4
TAIL VOLUME RATIO (VH)

Figure 5.4

FIGURE 5.5

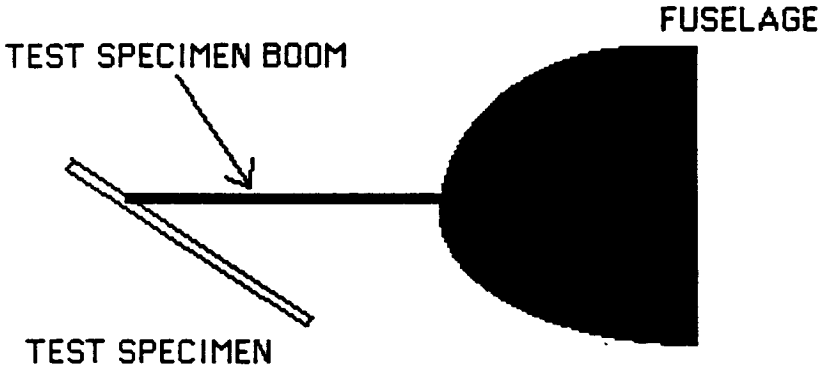

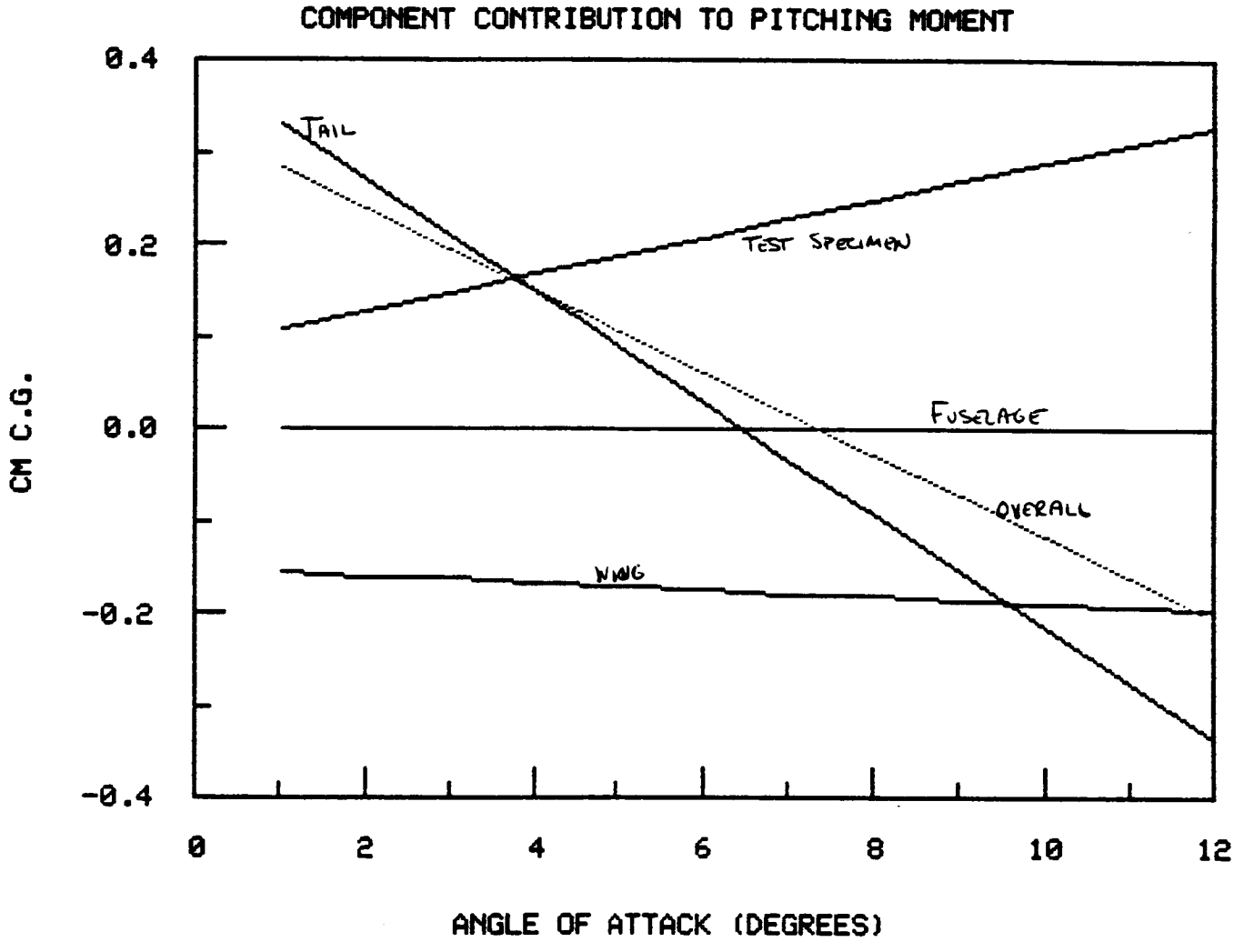
COMPONENT CONTRIBUTION TO PITCHING MOMENT
0.4
0.2
0.0
-0.2
-0.4
CM C.G.
TAIL
TEST SPECIMEN
FUSELAGE
OVERALL
WING
0
2
4
6
8
10
12
ANGLE OF ATTACK (DEGREES)

Figure 5.6

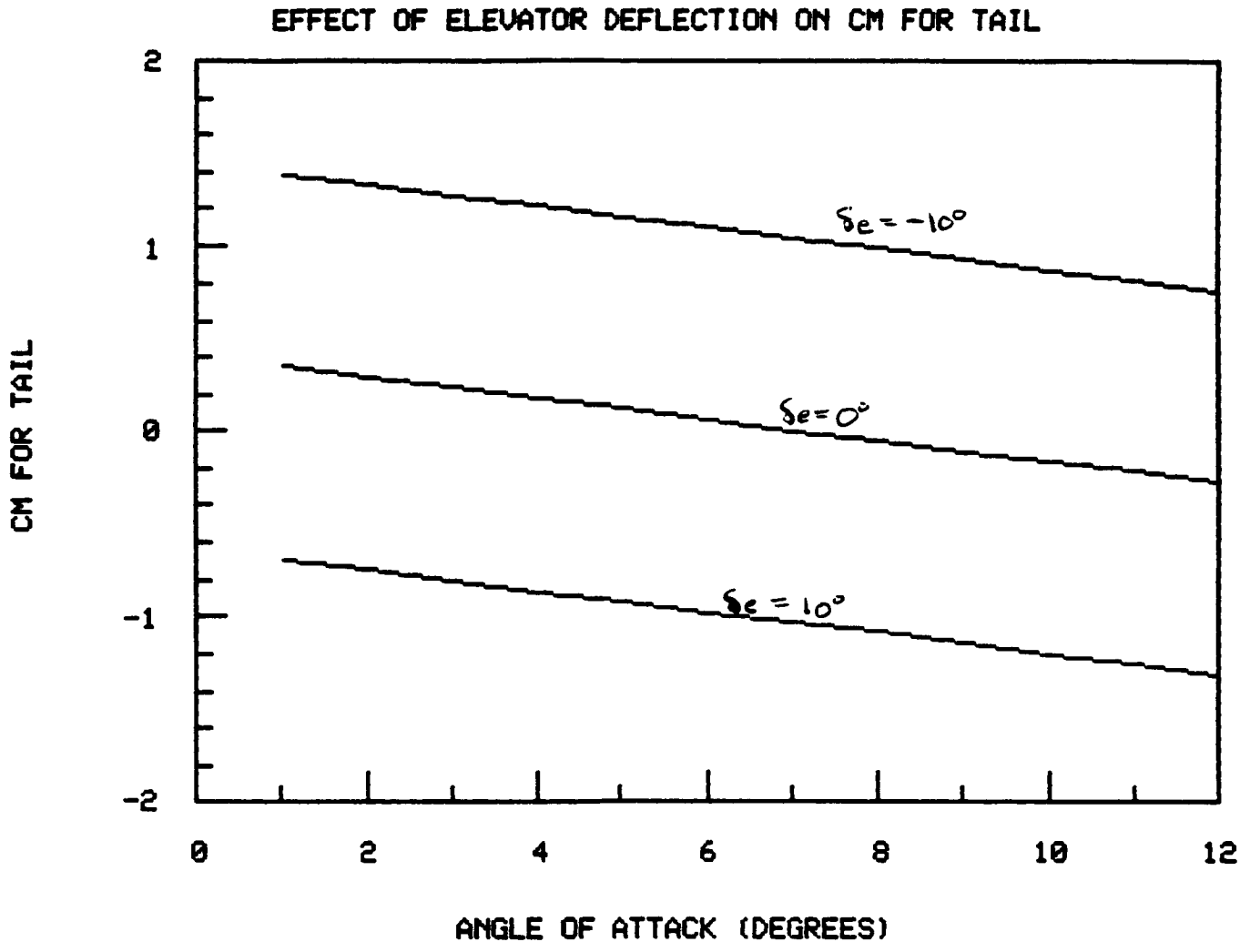
EFFECT OF ELEVATOR DEFLECTION ON CM FOR TAIL
CM FOR TAIL
2
1
0
-1
-2
0
2
4
6
8
10
12
ANGLE OF ATTACK (DEGREES)
δe = -10°
δe = 0°
δe = 10°

Figure 5.7

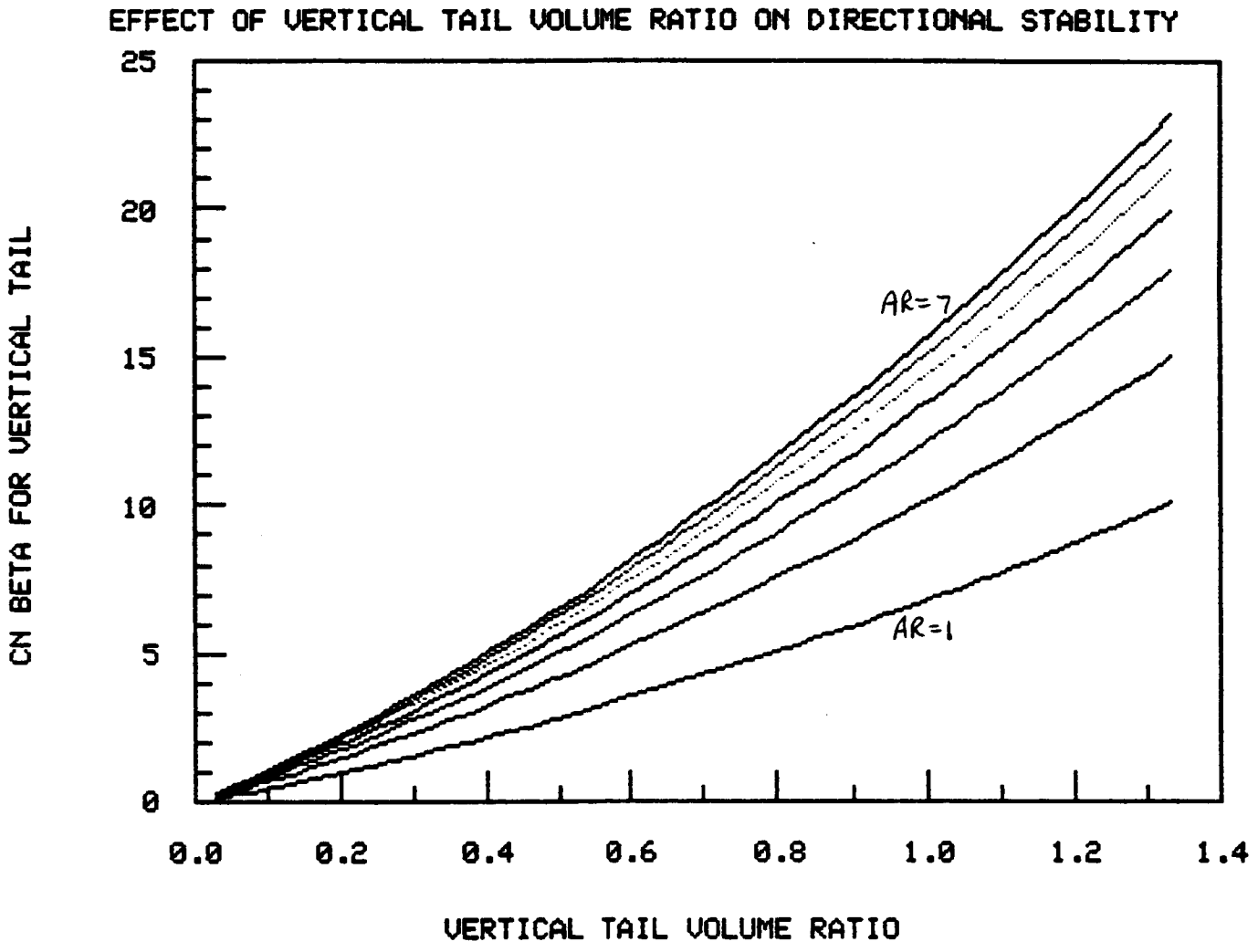
EFFECT OF VERTICAL TAIL VOLUME RATIO ON DIRECTIONAL STABILITY
CN BETA FOR VERTICAL TAIL
25
20
15
10
5
0
AR=7
AR=1
0.0
0.2
0.4
0.6
0.8
1.0
1.2
1.4
VERTICAL TAIL VOLUME RATIO

Figure 5.8

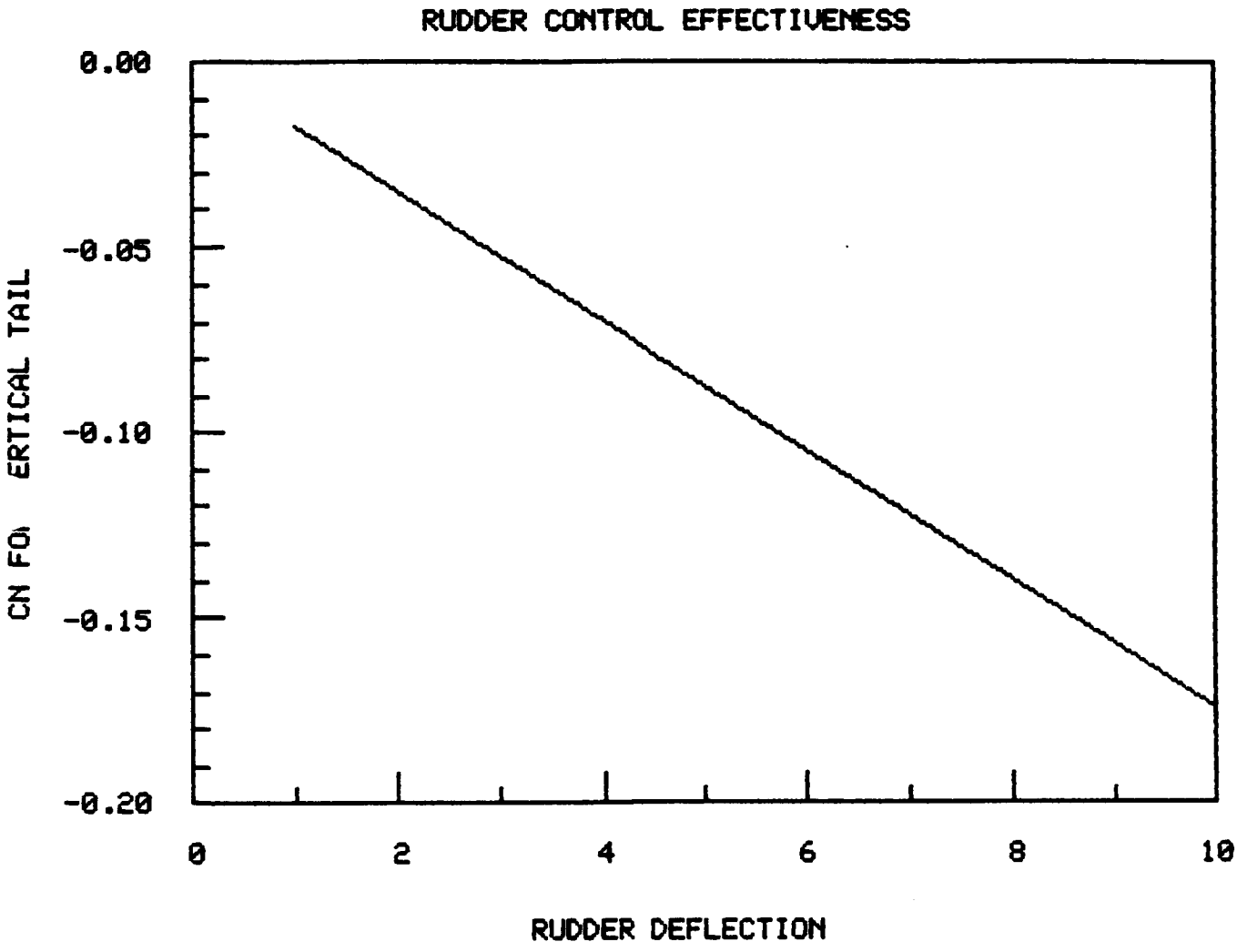
RUDDER CONTROL EFFECTIVENESS
0.00
-0.05
-0.10
-0.15
-0.20
CN FOR VERTICAL TAIL
0
2
4
6
8
10
RUDDER DEFLECTION

Figure 5.9

CALCULATION 5.1

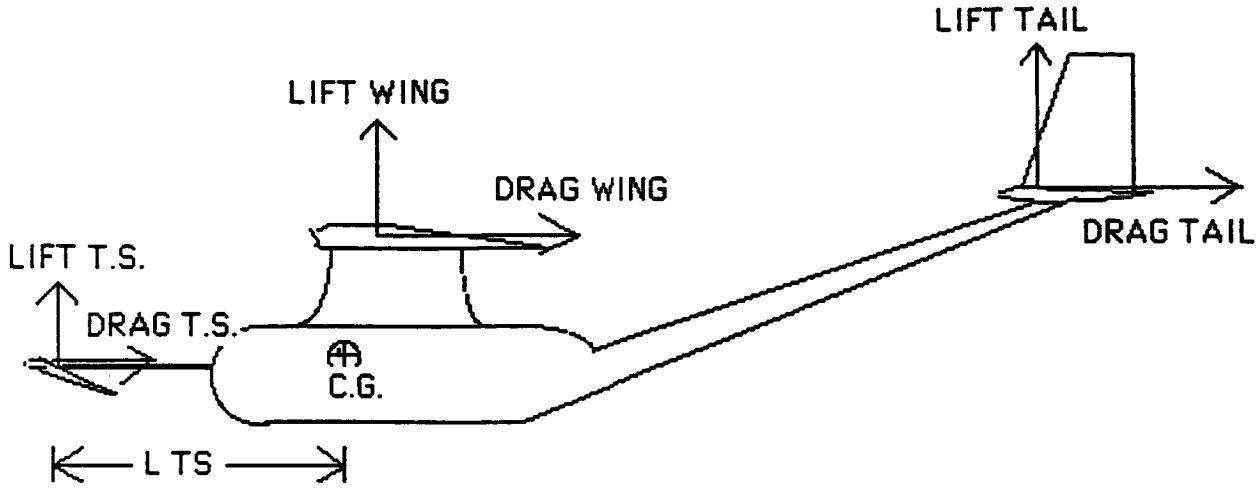

CALCULATIONS:

VHTS=(STS*LTS)/(S*C)
DEDALF=2*CLAW/(PI*AR)
CLATS=CLLAC*(1+CLLAC/(PI*E*ARTS))
CMATS=-NETA*VHTS*CLATS*(1-DEDALF)

WHERE:
S=WING AREA
C=WING CHORD
LTS=LENGTH FROM TEST SPECIMEN TO C.G.
STS=TEST SPECIMEN AREA
VHTS=TEST SPECIMEN VOLUME RATIO
DEDALF=dEPSILON/dALPHA
CLAW=CL ALPHA FOR WING
CLLAC=Cl ALPHA FOR TEST SPECIMEN
ARTS=ASPECT RATIO FOR TEST SPECIMEN
CLATS=CL ALPHA FOR TEST SPECIMEN
CMATS=Cm ALPHA FOR TEST SPECIMEN

CALCULATIONS 5.2

$(dC_m/dC_L)_{fuse} = (k_f * w_f^2 * l_f)/(S * c * a_w)$

$C_{m\alpha}$ fuselage $= (dC_m/dC_L) * \text{Alpha}_o$

Where:

k_f = wing correction factor taken from accompanying Figure 5.10

w_f = maximum width of fuselage

l_f = overall length of fuselage

S = wing area, sq. ft.

c = mean aerodynamic chord, ft.

a_w = lift curve slope of wing, per degree

$\text{Alpha}_o = dC_L/d\alpha$ from wing

CALCULATIONS 5.3

$C_{mow} = C_{macw} + C_{Low} * ((x_{cg}/c) - (x_{ac}/c))$

$C_{mof} = (C_f/(36.5 * S * c)) * \int w_f^2 * (\text{alpha}_{\ o\ \text{wing}} + i_f) dx$

$C_{mots} = \eta ts * VHts * C_{Lats} * (its - iwing)$

$C_{mot} = \eta * VH * C_{Lat} * (iwing - itail)$

$C_{mcg(component)} = C_{mo(comp.)} + C_{m\alpha(comp.)} * \alpha$

where α varies from 1 degree to 12 degrees

Where:

w = wing

f = fuselage

ts = test specimen

t = tail

ac = aerodynamic center

i = incidence angle

VH = horizontal volume ratio

C_f = fuselage correction factor read from accompanying Figure 5.11

η = neta value for component

α = angle of attack

CALCULATIONS 5.4

$dC_{Lt}/d\delta e = C_{L\alpha t} * \tau$

$C_{m\delta e} = -VH * \eta * dC_{Lt}/d\delta e$

$C_{L\delta e} = (SHT/S) * \eta * dC_{Lt}/d\delta e$

$\delta trim = -(C_{mo} * C_{L\alpha t} + C_{m\alpha} * C_{Ltrim})/(C_{m\delta e} * C_{L\alpha t} - C_{m\alpha t} * C_{L\delta e})$

Where:

$C_{L\alpha t}$ = C_L apha for tail

τ = elevator effectiveness parameter (equal to 1.0 for SPiRiT)

$dC_{Lt}/d\delta e$ = elevator effectiveness

η = neta

SHT = horizontal tail area

$\delta trim$ = elevator angle to trim (radians)

C_{Ltrim} = lift coefficient to trim

CALCULATIONS 5.5

$C_{n\beta wf} = -k_n * k_{RI} * (S_{fs}/S_w) * (l_f/b)$

Where:

k_n = empirical wing-body interference factor read from Figure 5.12

k_{RI} = empirical correction factor for fuselage Reynolds number read from Figure 5.13

S_{fs} = projected side area of the fuselage

l_f = length of the fuselage

S_w = wing area

b = span

CALCULATIONS 5.6

$dC_{Lv}/d\delta r = C_{L\alpha v} * \tau$

$C_{n\delta r} = -h * V_v * (dC_{Lv}/d\delta r)$

Where:

$C_{L\alpha v}$ = C_L alpha for vertical tail

τ = rudder control effectiveness parameter read from Figure 5.14

V_v = vertical tail volume ratio

$dC_{Lv}/d\delta r$ = rudder control effectiveness

CHAPTER VI
AIRCRAFT PERFORMANCE

6.1 Take-Off and Landing Estimates

The performance of the SPiRiT was examined to determine the RPV's general flight characteristics. One of the mission requirements was to have the RPV take-off within a circle of radius 45.72 m [150 ft]. The SPiRiT was designed to have a conventional takeoff and landing with tricycle landing gear. The landing gear would also be retractable so as to increase cruise performance of the aircraft. The ground roll distance is 12.12 m [39.75 ft] assuming a hard surface with a friction coefficient of 0.02. All performance factors were calculated assuming a takeoff weight of 13.6 kg [30 lbs] with an ambient density of 1.225 kg/m^3 [0.00237 slugs/ft^3]. A takeoff static thrust of 85.4 N. [19.2 lbf] was used for all calculations which was determined from propulsion characteristics. The transition distance was calculated to be 22.3 m [73.3 ft] assuming a takeoff velocity of 1.2 times the stall velocity and a C_L of 0.588 at takeoff. Due to the large transitional distance, the distance to clear a fifty foot obstacle is 0.994 m [3.26 ft] beyond the transitional distance. The total distance to clear a fifty foot obstacle was then determined to be 35.45 m [116.3 ft] which is well within the required take-off distance.

6.2 Range, Endurance And Rate of Climb

Rate of climb is one more performance characteristic that was examined. The rate of climb was determined for various unaccelerated flight speeds and a maximum rate of climb of 22.6 m/s [4450 ft/min] was determined at a power required value of 724 Watts. The range and endurance were two more performance characteristics that needed to be examined. The maximum range that the aircraft could fly was not of much concern due to the desire to maximize the time the aircraft was in flight. It was desired to have the RPV be able to stay in the air a fairly long time in order to obtain as many pressure readings as possible per flight. SPiRiT demonstrated very good endurance values across most of its flight envelope. It achieved a maximum endurance of greater than 105 minutes at a constant flight velocity of 11 m/s [36.1 ft/s]. The actual endurance will be slightly less due to variations in flight velocity. It was also noted that the endurance was only 7.87 minutes at a velocity of 38 m/s [125 ft/s]. It was concluded that at maximum speed the RPV would be able to have fewer tests run on it and therefore, pressure tests at the higher speeds should be well planned out so as to maximize the time available for pressure readings at these higher velocities. Overall, the SPiRiT demonstrated endurance values well within the desired values. Maximum range values were determined to be greater than 75 kilometers [46.6 mi] at a constant flight velocity of 11 m/s [36.1 ft/s]. Maximum range was not important in the design of the SPiRiT yet the RPV demonstrated excellent range anyway.

The overall performance of the SPiRiT was very good due in part to the engine chosen to provide a top end velocity of approximately 40 m/s [131 ft/s] for higher Reynolds number pressure testing. The SPiRiT is an economical test RPV that provides more than adequate performance figures over its entire flight envelope.

CHAPTER VII
LAUNCH AND RETRIEVAL

7.1 Launch

The design constraint was to launch and retrieve the RPV within a circular area of radius no greater than 45.7 m(150 ft) including a 15.2 m (50 ft) obstacle clearance altitude. Initially, several launch systems were considered, including rocket assisted take off (RATO), and pneumatic catapult rail launch (PCAT). In case a conventional landing gear take off could not satisfy launch constraints, RATO and PCAT would have been used with the disadvantage of increased weight to strengthen the structure, more and heavier supporting equipment, and possibly hazardous conditions for the launch crew.

Early on in the design, take off performance within the constraints could be guaranteed and it was decided to use a conventional launch on a retractable landing gear. 36 m (118 ft) will be required for take-off. This includes a 12.2 m (40 ft) ground roll, a 22.6 m (74 ft) transition distance, and a 1.2 m (4 ft) clearance distance. This distance was calculated using the conventional equations for the three take off segments (reference: R.C Nelson, M. Brendel; Atmospheric Flight Mechanics, unpublished notes). Take- off will be from a concrete surface. No special equipment will be needed for take off. A conventional landing gear with stearable nose wheel will be used. Landing gear retraction will be performed by a single, low power servo motor.

7.2 Retrieval

Since a conventional landing gear can be used for take off, it seemed prudent to attempt a conventional gear landing. Flight performance data show that the design can easily land within the required 91.4 m (300ft). Again using equations developed in Nelson & Brendel, a ground roll distance after touch down of 18.9 m (62ft) was calculated. This assumes zero lift upon landing and wing spoiler activation. It is estimated that the landing distance over a 50 ft obstacle at a four degree glide path will be no more than 30.5 m (100ft). Within this distance, the engine will be shut down and the speed will be low enough to retard the aircraft by hand. Landings will be made on concrete. Hard landings pose no threat to the high mounted propulsion unit or the tail surfaces. Unlike with net or balloon recoveries, the instrumentation and the test specimen will not need special protection from impact loads. It is expected that the operator can consistently make adequately soft landings. See Chapter XI section 11.2 for methods of determining take-off and landing procedures for RPVs.

CHAPTER VIII

INSTRUMENTATION

SPiRiT is designed to measure the surface pressure distribution on two dimensional and three dimensional lifting surfaces. To accomplish this mission the RPV must be able to measure the pressure field, angle of attack, and airspeed. The data taken will be stored on board the RPV in an 8-Megabyte RAM module. At the same time, however, the angle of attack, airspeed, and voltage level of the batteries will be radioed down to the systems controller to provide information on the status of the RPV. The angle of attack information will be processed and a correction signal radioed back to the RPV so that deviations from the test angle of attack may be corrected by the Automatic Flight Control System. The complete Instrumentation Package consists of: Angle of Attack sensors, Airspeed sensor, Pressure Field sensors, the Data Acquisition System, and telemetry. The total weight of the Instrumentation package is anticipated to be 0.68 kg (1.5 lbs) and occupy a volume of 368.7 cm^3 (22.5 in^3). A summary of the specifications of the Instrumentation package components is given in Table 8.1. An in depth discussion of each of the measurement components is provided below.

8.1 Measurements

AIRSPEED:

The actual airspeed will be determined from the measured dynamic pressure. The raw dynamic pressure data (in volts) will be stored in memory but the dynamic pressure data sent to the ground will be converted into appropriate pressure units and displayed by the ground based computer system. The actual dynamic pressure data will come from a pitot-static probe mounted in a wind vane on the tip of the test specimen. The wind vane will orient to the freestream direction thus always assuring that the pitot-static probe will be facing the proper direction. While this is not the most desirable place for the pitot-static probe, there is no other location on the RPV that is clear of either wing wash or prop wash.

ANGLE OF ATTACK:

The angle of attack seen by the test specimen will be determined by the use of an inclinometer operating in conjunction with a wind vane. The wind vane will provide the direction of the free stream and the inclinometer will provide the geometrical angle of attack of the test specimen relative to the local horizontal. By combining the two values, the true angle of attack can be determined. The inclinometer is mounted inside the test specimen during fabrication such that when the test specimen is at a zero angle of attack the inclinometer will output a zero voltage to the A/D. Similar when the wind vane is installed it is connected to another inclinometer that will output a voltage proportional to its rotational displacement to the A/D.

SURFACE PRESSURE FIELD:

To determine the surface pressure distribution, the static pressure must be known at all points. However, to keep the number of measurements and on board memory requirements reasonable, 118 total pressure measurements can be made. Two channels of data will be used by the angle of attack sensor and the airspeed measurement. One difficulty encountered is that the pressure field is continually changing due to the changing flow field around the RPV. Thus it becomes necessary to take the surface pressure measurements almost simultaneously. To accomplish this, the measurements must be made in parallel. Four A/D converters will be used in parallel each sampling thirty channels for a maximum of 120 channel input. Thus it will take approximately .2 seconds to acquire one complete frame of data.

One difficulty in making the pressure measurements is selecting a pressure transducer accurate enough to resolve the small pressure changes that will be encountered. Because the pressure readings will be similar from pressure tap to pressure tap a high accuracy transducer will be needed to resolve the change in pressure. The anticipated pressure range over the test velocities will be on the order of tenths of atmospheres. Typical pressure transducers have a full scale range an order of magnitude larger. Thus these transducers will not resolve the small changes in pressure. This design assumes that technology will have developed a pressure transducer with the desired accuracy, sensitivity, and stability characteristics. For a maximum of 120 pressure transducers, the estimated weight will be 3.4 kg (7.5 lb). The output lines will be passed back through the extended boom to connect to the

terminal block on the Data Acquisition System.

8.2 Data Acquisition

The Data Acquisition System (DAS) is configured to accept 120 input channels on a 1-Volt Bipolar range. The 16-Bit A/D converter will be able to resolve 1 part in 65536. This implies that the smallest voltage level that can be resolved is .0305 mV. The full scale output of a typical pressure transducer is on the order of 20 mV. This gives a .15% resolution of the full scale input range where .5% has been defined as acceptable. If the pressure transducer's output level is too low then the output must be amplified before being sampled by the data acquisition. A diagram showing the conceptual organization of the DAS system is given in figure 8.1.

The actual DAS will occupy an area of 96.8 cm^2 (15 in^2) and a volume of 368.7 cm^3 (75 in^3). The weight of the A/D component is estimated at .68 kg (1.5 lb). Powered by a rechargeable .5 A*h battery pack, the DAS can operate at +5 Volts drawing 1 Amp for up to 30 minutes of continual use. However, data will be taken for only 20 minutes of that time. The data taken will be stored on board in an 8-Meg RAM module which carries its own independent lithium battery back up to prevent accidental memory loss due to power outage. Once the mission is completed the data stored in on- board memory may be transferred to the ground based computer through an RS-232 interface port.

8.3 Automatic Flight Control System

To reduce the work load of the pilot, the Automatic Flight Control System (AFCS) will fly the RPV in a preset flight pattern during the data acquisition phase of the mission. The standard flight pattern is a figure 8 with 35.4 m (116 ft) radius turns and 1 mile long legs. The the information for the flight pattern is stored in a EPROM and can be customized by the user at the testing site.

The angle of attack of the test specimen and airspeed of the RPV is radioed down to the ground based computer. These signals are compared to the nominal values set by the systems controller and an error signal is generated proportional to the difference of the inputs. The error signal for each measurement is then radioed to the flight control which will adjust the angle at which the RPV is inclined and also change the airspeed accordingly.

Because the RPV is operated by line-of-sight, the flight controller will be able to tell if the the AFCS malfunctions. The flight controller can manually take control of the RPV if it is deemed necessary.

8.4 Telemetry Systems

The telemetry system is a standard 4-Channel frequency modulated transmitter. Such systems are available for aerodynamic applications and can be purchased off the shelf. Such a system is the REMTRON RTS-1 telemetry system. This system will take up 86.45 cm^2 (13.41 in^2) and weighs 224.4 grams (7.9 ozs). The decoder will be interface with the computer to allow the computer

and the RPV to communicate with the AFCS as needed. The angle of attack of the test specimen, airspeed, voltage of the engine battery, and the voltage of the Data Acquisition System's battery will be radioed to the ground on the four channels.

Figure 8.1

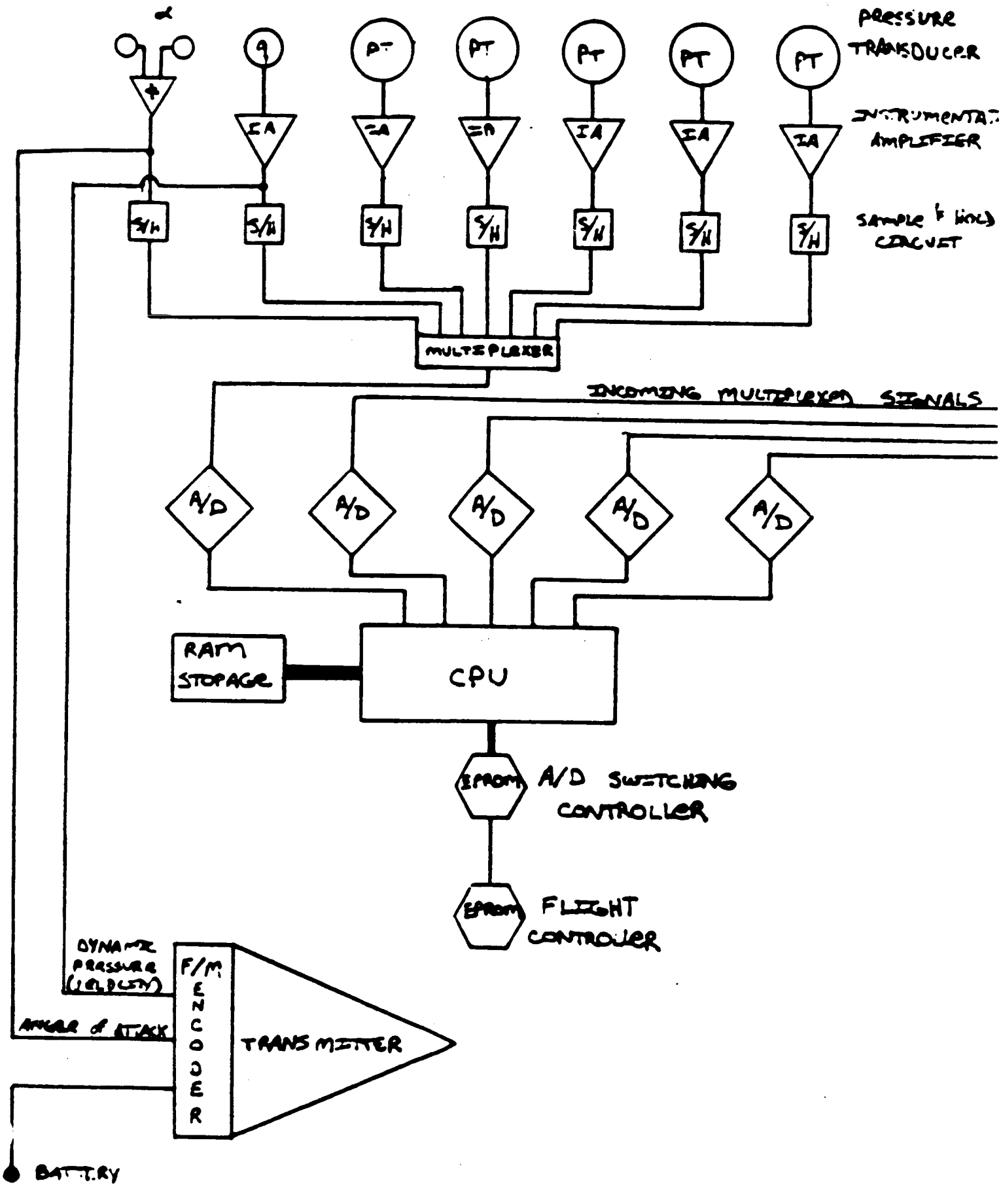
α
q
PT
PT
PT
PT
PT
PRESSURE TRANSDUCER
IA
IA
IA
IA
IA
IA
INSTRUMENTATION AMPLIFIER
S/H
S/H
S/H
S/H
S/H
S/H
S/H
SAMPLE & HOLD CIRCUIT
MULTIPLEXER
INCOMING MULTIPLEXED SIGNALS
A/D
A/D
A/D
A/D
A/D
RAM STORAGE
CPU
EPROM
A/D SWITCHING CONTROLLER
EPROM
FLIGHT CONTROLLER
DYNAMIC PRESSURE (q)
ANGLE OF ATTACK
F/M ENCODER
TRANSMITTER
BATTERY

TABLE 8.1

INSTRUMENTATION SPECIFICATIONS

WEIGHT:

Sensors	3.41 Kg (7.5 lbs)
Telemetry	224.4 grams (7.9 ozs)
Data Acquisition Package	0.68 Kg (1.5 lb)

SIZE:

Telemetry	9.5x 9.1 cm (3.75 x 3.575 in)
Data Acquisition Package	12.7 x 7.62 x 3.81 cm (5 x 3 x 1.5 in)

POWER:

Telemetry	12 Volts at 50 mA
Data Acquisition Package	+5 Volts at 1 Amp supplied by 5 A*h battery
Sensors	Powered from Data Acquisition battery

INPUT CHANNELS:

TOTAL:	120
Pressure Measurement	118
Other	2

PROCESSING:

8 Megabytes on-board RAM Storage
High Speed CMOS CPU
EEPROM Flight Pattern Storage
16-Bit A/D Converters (Total of 4 processing in parallel)

SAMPLING FEATURES:

Maximum Sample Rate	400 Hz
Minimum Frame Sample Time	.2 s

COOLING REQUIREMENTS:

2 Mini Fans
ea. 1" Diameter Blades

CHAPTER IX

STRUCTURAL DESIGN

Structures

The structure of the SPiRiT RPV can be divided into a four primary substructures, including the wing/engine structure, the main fuselage, the tail boom structure, and the test specimen/boom structure.

9.1 Wing Structure

The wing is constructed using a fiberglass spar/balsa rib configuration, as depicted in Figure 9.1. Other configurations using composites, aluminum, and pine have been considered. Although some of the results from composite materials are impressive, the weight constraint such a wing make it an unreasonable proposition. A lifting line program using a vortex filament method was used to obtain aerodynamic loading data. This data was input to two different beam bending programs, which are included in Appendices J and K, that perform analysis of various wing structural configurations. The wing structure is designed so that the maximum wingtip deflection is 2 inches, and the total wing weight is under 3 lb.

The entire wing is designed with a safety factor of 2. The V-n diagram for the aircraft can be found in Figure 9.2. The yield load factor is 4.5 which occurs at 74 ft/s at C_{Lmax}. The four concepts under consideration are shown in Figure 9.3. The results of using a

4.5 g loading at $C_{L\,max}$ for various sizes of fiberglass spars/sparcaps is shown in Figures 9.4-9.6. The weight limit of 3 lb, and the wing tip deflection limit help to pinpoint an appropriate spar thickness. In this case, the largest possible spar within the limitations is chosen in order to simplify manufacturing. A fiberglass spar .04 in. thick and a .2 in. cap is the structural element used in the wing. The secondary structural elements include balsa ribs, balsa leading and trailing edges, and plastic sheeting for the wing skin. The engine is cowled in a circular nacelle made of fiberglass. The nacelle has a hatch on the top for easy access to the engine.

9.2 Main Fuselage

The main fuselage, which houses the data acquisition equipment, controls, and fuel load, is composed of a wooden frame with a thin plastic covering. The useable cross sectional area of the fuselage is 36 in^2. The stress distribution along the fuselage profile is shown in Figure 9.7. The fuselage has a circular cross section and is composed of eight longerons with a cross sectional area of .01562 square inches. They are spaced evenly about the section, running the length of the fuselage, with the highest compressive stress being in the top longeron. While several elliptical cross sections were considered, they would complicate the construction process thus the circular cross section was chosen for its simplicity. The program used for the section geometry is found in the attached Appendix L.

The structural problem areas of the fuselage are where the tail boom connects to the main fuselage and the test specimen. Figure 9.8 shows the areas of stress concentrations where the tail boom joins the main fuselage. In this area the cross section tapers sharply. The corners where these concentrations exist are filleted to avoid this problem. Figure 9.9 shows the effect of the filleting process by modeling the taper as a sinusoidal curve. The maximum bending moment of the fuselage increases linearly as the test specimen is deflected through its range of angle of attacks. This variation is shown in Figure 9.10.

9.3 Test Specimen Boom

The boom to support the test specimen in front of the RPV is designed for strength, minimal vibration, and minimal aerodynamic interference. The specimen boom is an aluminum alloy circular cross section that is supported in the bulkhead of the main fuselage. It extends 20 inches beyond the nose of the RPV, which is enough to get the test specimen out of excessive aerodynamic interference caused by the wing or the fuselage. A summary of the boom characteristics, vibration data, and loading can be found in Tables 9.1 and 9.2. The boom is modeled as a simple beam of circular cross section which experiences a maximum bending moment of 440 N-m at the root.

9.4 Substructure Integration

An approximate weight breakdown of the aircraft can be found in table 3. The fuselage containing the data acquisition equipment, fuel and controls is separate from the wing structure. The wing/engine structure is above the fuselage, and is supported by heavy wire attached to the bulkheads in both the main fuselage and the engine/wing substructure. The wing and engine are separate from the lower substructure in order to minimize aerodynamic interference and vibrational affects that might invalidate the data acquisition process. The fact that the wing and engine can be unbolted from the rest of the structure, and the test specimen can be detached makes the SPiRiT easy to transport and maintain.

FIGURE 9.1.

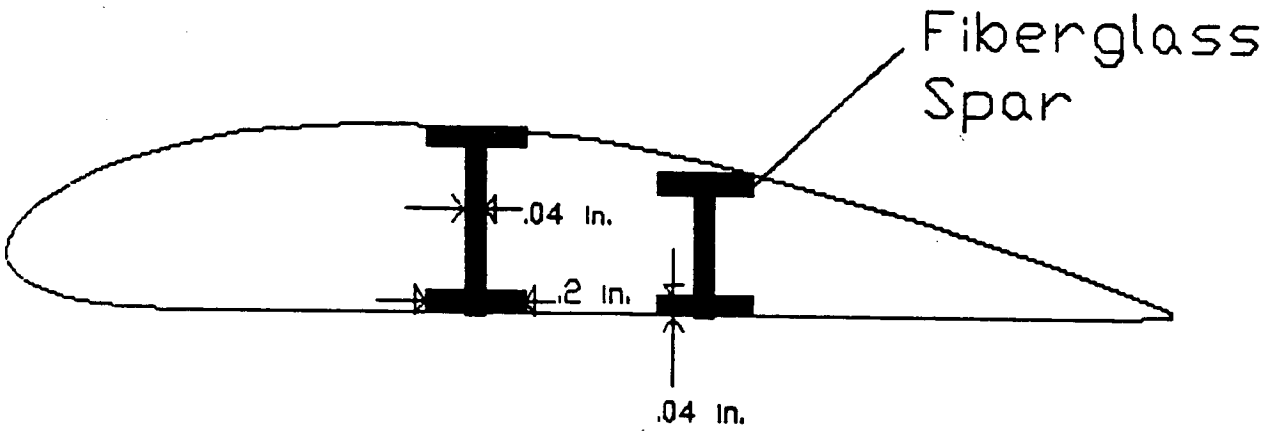

Flight Envelope

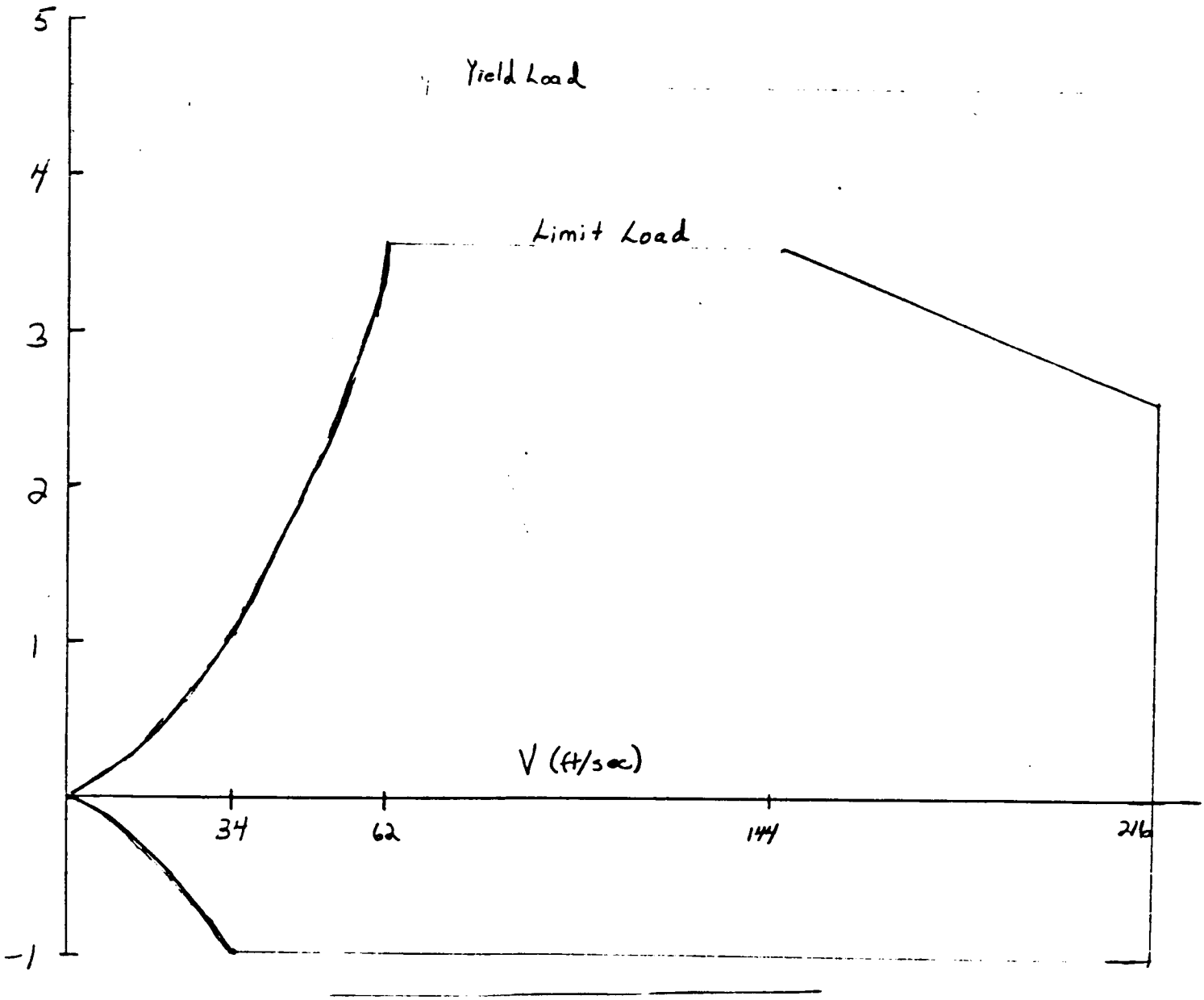

Figure 9.2

FIGURE 9.3

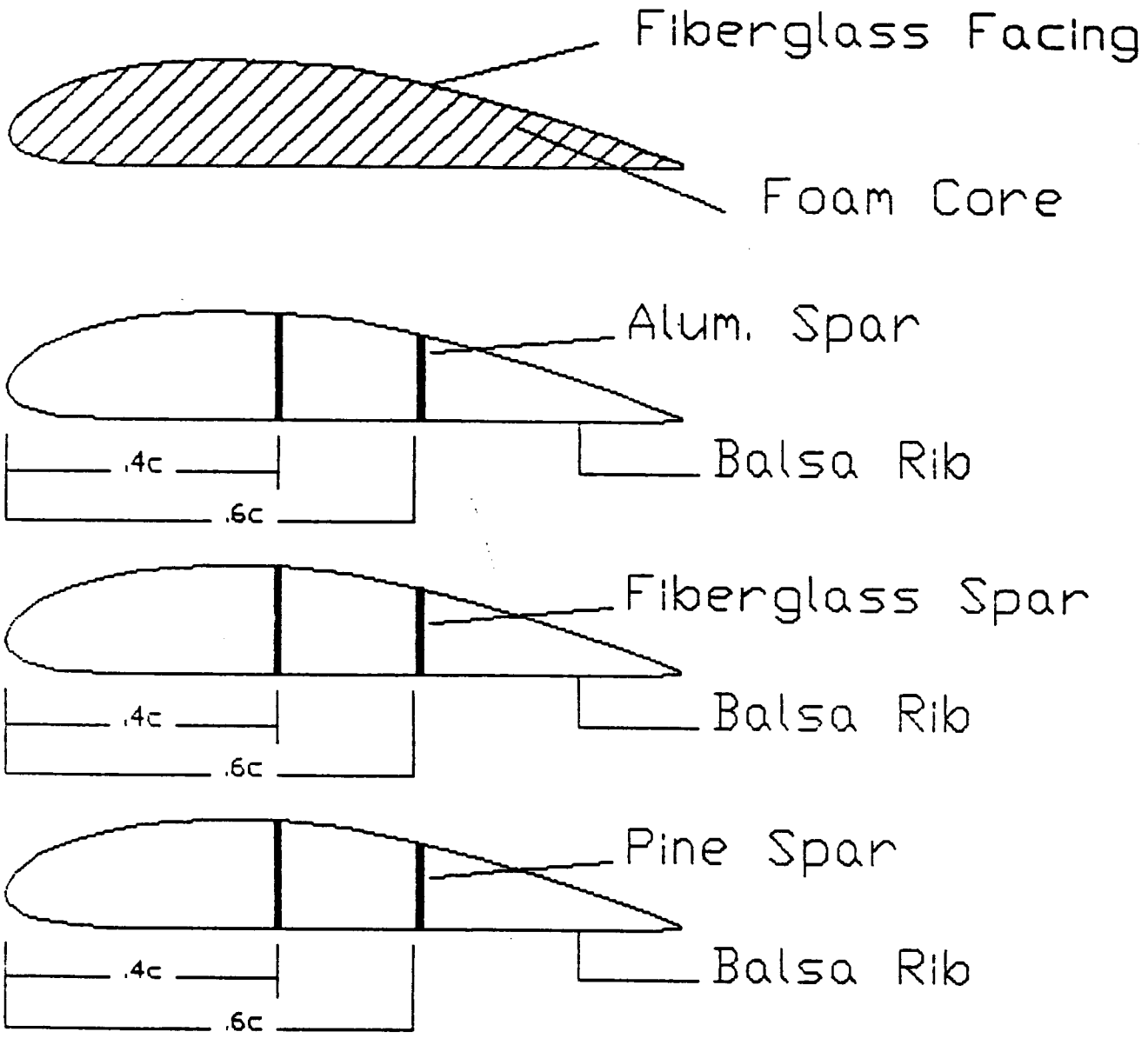
Fiberglass Facing
Foam Core
Alum. Spar
Balsa Rib
.4c
.6c
Fiberglass Spar
Balsa Rib
.4c
.6c
Pine Spar
Balsa Rib
.4c
.6c

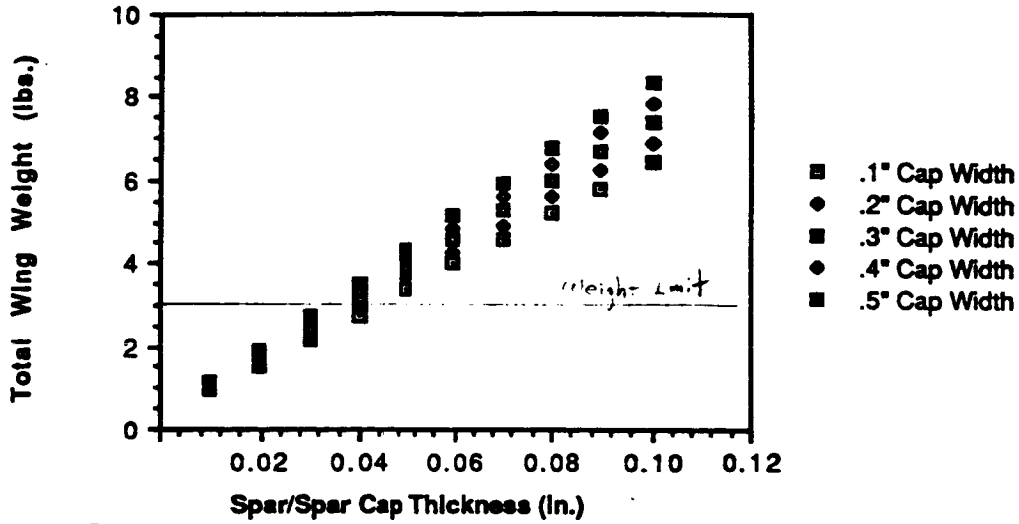

Figure 9.4 - Total Wing Weight for various Fiberglass Spar Thicknesses and Spar Cap Widths.

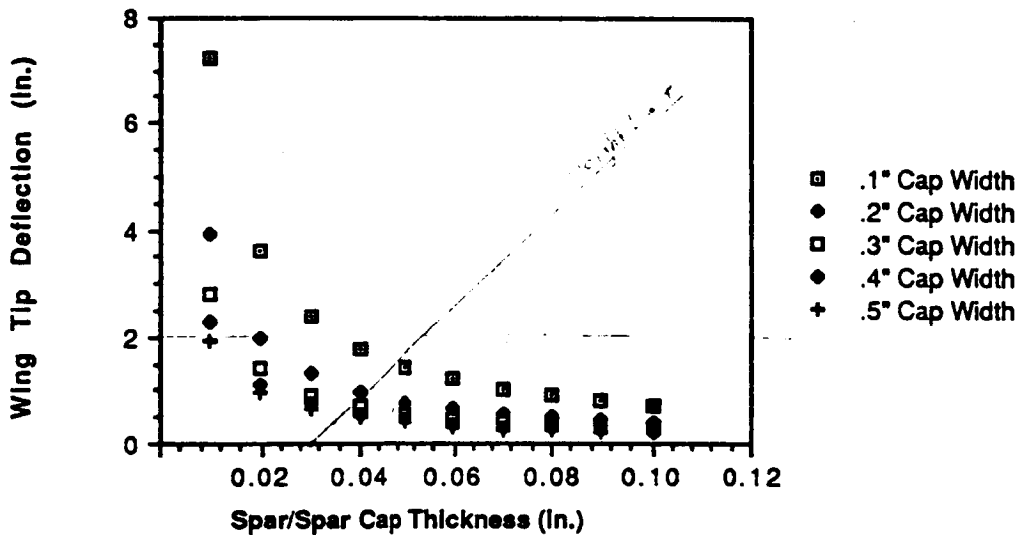

Figure 9.5 - Wing Tip Deflection for various Fiberglass Spar Thicknesses and Spar Cap Widths.

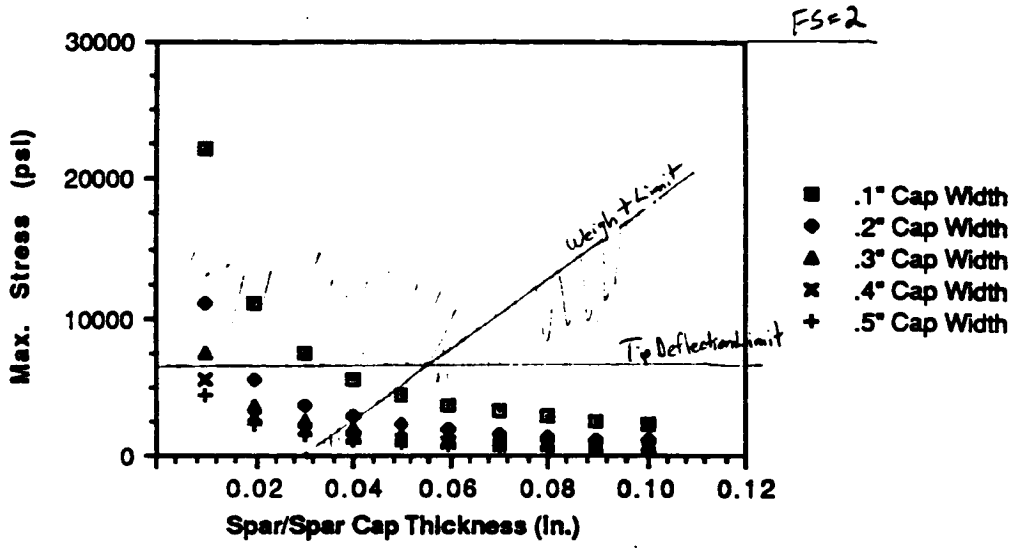

Figure 9.6 - Maximum stress occurring in the wing for various Fiberglass Spar Thicknesses and Spar Cap Widths.

Figure 9.7

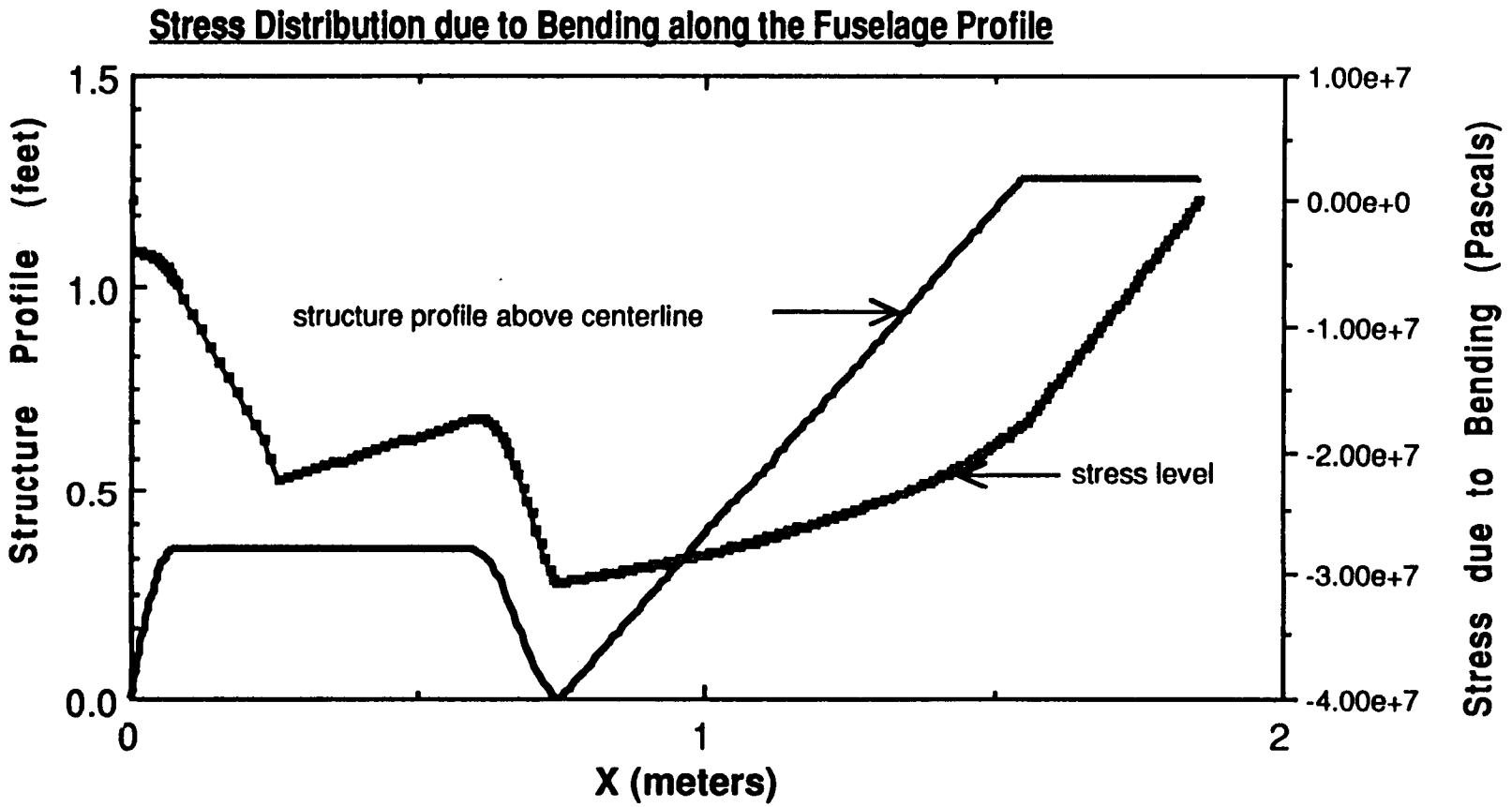
Stress Distribution due to Bending along the Fuselage Profile
Structure Profile (feet)
1.5
1.0
0.5
0.0
0
1
2
X (meters)
structure profile above centerline
stress level
1.00e+7
0.00e+0
-1.00e+7
-2.00e+7
-3.00e+7
-4.00e+7
Stress due to Bending (Pascals)

Figure 9.8

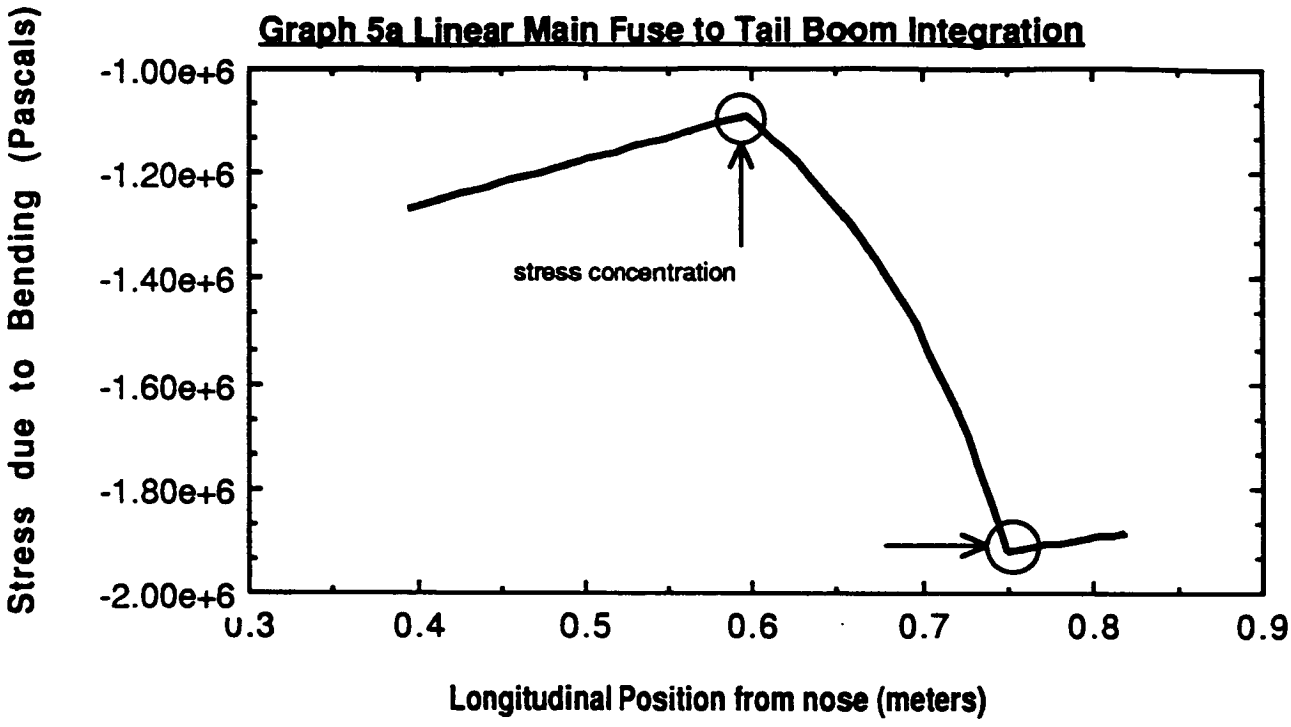

Figure 9.9

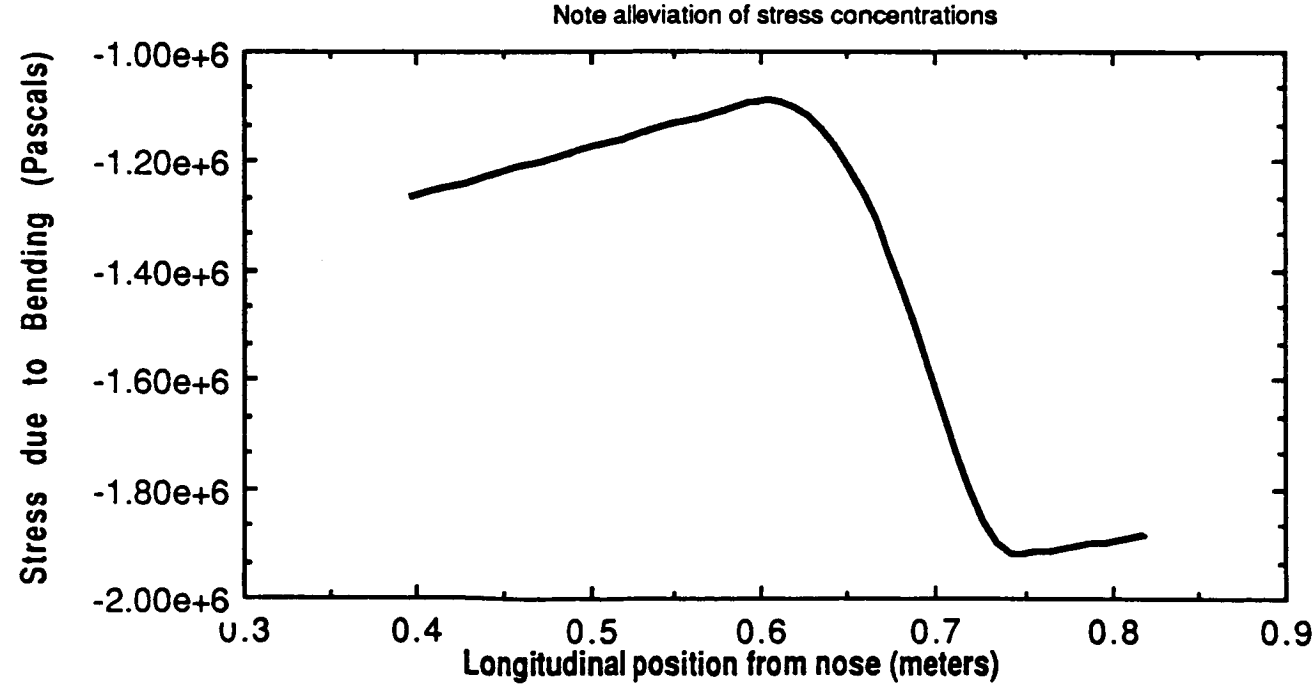

Figure 9.10

Graph 1. Relationship of Fuselage Maximum Bending Moment to Specimen Angle of Attack

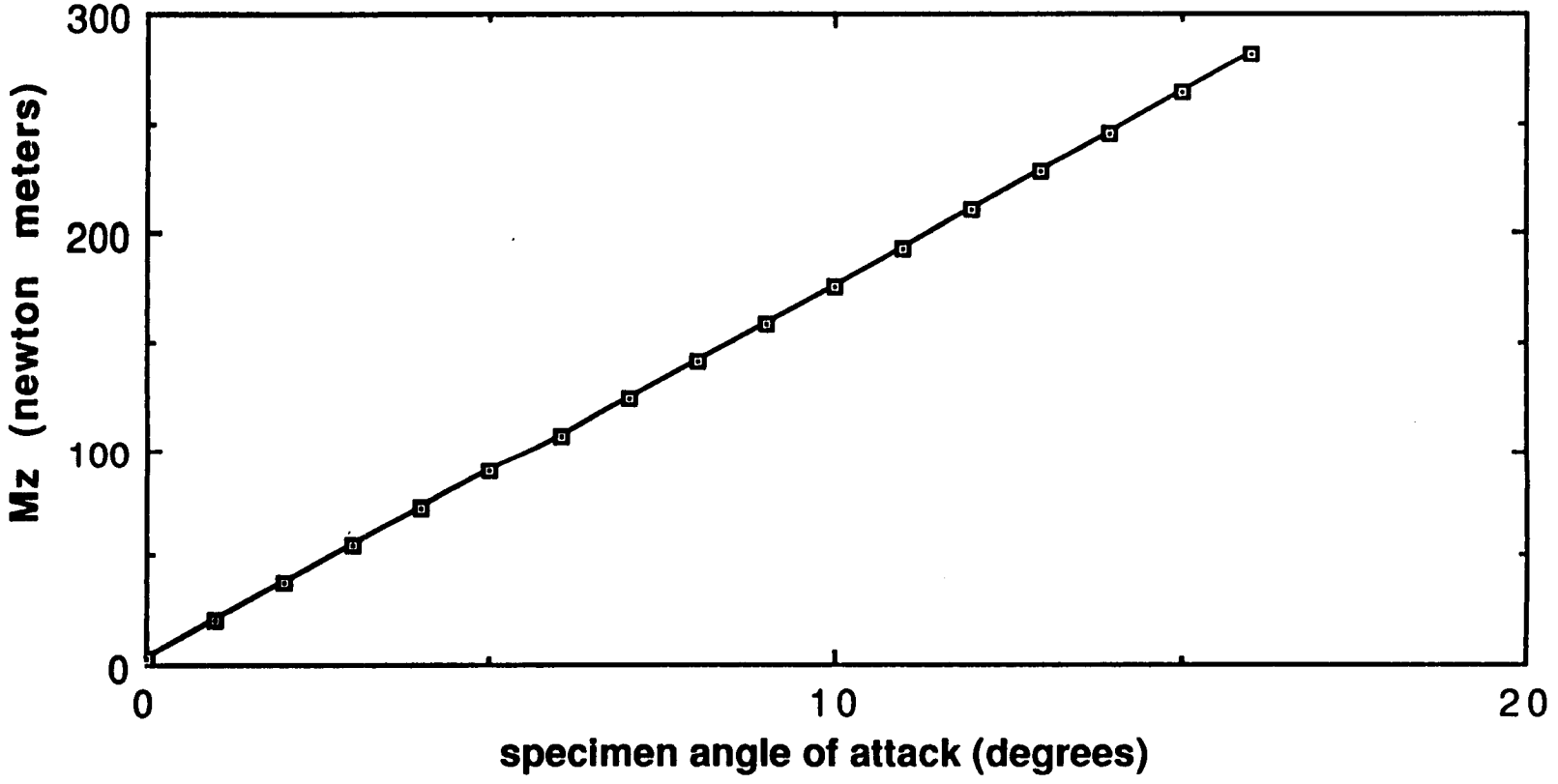

Table 9.1

	A	B	C	D	E	F	G	H	I	J	K	L
1	Cross section		Angle of Attack	Specimen S	Cd	Cl	D(max)	L(max)	Mr	Mcg	Stress at root	Stress at root
2	outer radius=	0.025		m^2						ND+ NU-	top N/m^2	bottom
3	inner radius=	0.0225	-0.3490659	0.24384	0.1645615	-1.3764375	43.6979503	-365.50165	-222.08876	279.878041	5159852.57	-5394117.7
4	XC area=	0.00037306	0.6981317	0.24384	0.658246	2.75287508	174.791801	731.003294	439.658911	-523.77767	-10915135	9978074.62
5	internal area=	0.00159043	-0.3490659	0.154838	0.08375	-1.8715	14.1218062	-315.56968	-190.92843	237.990458	4498740.13	-4574447.3
6	average radius	0.02375	0.6981317	0.154838	0.335	3.743	56.487225	631.139352	373.429463	-457.3867	-9024360.8	8721532.31
7			-0.3490659	0.12387072	0.14602	-0.58602	19.6973992	-79.051293	-48.389773	62.117986	1096976.05	-1202574
8			0.6981317	0.12387072	0.584094	1.17205	78.7914852	158.103936	97.7676998	-111.0432	-2534230.2	2111828.36
9			-0.3490659	0.0309677	0.1735925	-1.26719	5.85420314	-42.734494	-25.992533	32.8386581	601908.633	-633293.07
10			0.6981317	0.0309677	0.69437125	2.5343	23.4168547	85.4662905	51.5980165	-61.075213	-1288774.1	1163236.16
11												
12		Material										
13												
14		Magnesium	Boom Weight	PS	Vibration freq	(rad/sec)						
15	density (Kg/m	1790	0.33923467		one	two						
16	alloy type	HK31A										
17	YS (Pa)=	199955000		18.3190589								
18					1150.5	11335.4						
19		Aluminum										
20	density (Kg/m	2740	0.51927542									
21	alloy type	7079-T6										
22	YS (Pa)=	468860000		42.9550346								
23					1176.209	11588.97						
24		Titanium										
25	density (Kg/m	4428.8	0.83933102									
26	alloy type	6%Al, 4%V										
27	YS (Pa)=	999775000		91.5952943								
28					1147.52	11306.3						

Table 9.2

TEST SPECIMEN BOOM STRUCTURE DESIGN CONCEPT SUMMARY

Objectives:

Provide a structural base for the test specimen which is as free from aerodynamic and vibrational interference as possible.

To accomodate the measurement to data acquisition interface.

Description:

A thin walled, circular, closed cross section beam supported by a fuselage bulkhead.

Geometry:

Outer radius	0.025 meters	0.984 inches
Inner radius	0.0225 meters	0.886 inches
Section Area	0.000373 m^2	0.578 in^2
Internal Area	0.00159 m^2	2.464 in^2
Thickness	0.0025 meters	0.098425 inches

Loading Environment:

Maximum Stress at the root=-10,915,135.0 N/m^2

Maximum Shear Force=731.0 N

Maximum Bending Moment=439.66 N*m

Candidate Materials:	Boom Weight	Safety	Vibrational Freq.(rad/sec)	
Magnesium HK31A	0.748 lbs	18.3	1150.5	11335.4
Aluminum 7079-T6	1.145 lbs	43.0	1176.209	11588.97
Titanium (6%Al, 4%V)	1.8507 lbs	91.6	1147.52	11306.3

Table 9.3

	A	B	C	D	E
1	Payload wt=	1.5		Total weight=	30
2					
3					
4					
5		Percent of total			
6	Structure	48.58%			14.575
7	Power plant	29.44%			8.83333333
8	Fixed equip	10.31%			3.09166667
9	Test specimen	6.67%			2
10					
11	Empty weight	95.00%			28.5
12	Payload weight	5.00%			1.5
13					
14		Structure			
15		----------	----------	----------	
16		Wing	13.25%	3.975	
17		Empenage	4.42%	1.325	
18		Fuse	22.08%	6.625	
19		Nacelle	1.47%	0.44166667	
20		Gear	7.36%	2.20833333	14.575
21					
22		Fuselage			
23		----------	----------	----------	
24		Platform	0.91%	0.27383331	
25		Tail boom	7.36%	2.20833333	
26		main fuse	12.27%	3.68055556	
27		Test spec. boom	1.54%	0.46227778	6.62499998

CHAPTER X

MANUFACTURING REQUIREMENTS

10.1 System Safety Considerations

-Routine checks of aircraft alignment, weight, and balance

-Test sets run on calibration of airborne electronics

-Weather conditions (e.g. corrections for navigational errors due to wind conditions)

-Consideration of radio frequency to prevent interference with people who may be operating on the same frequency

-Parachute for the aircraft in case it's forced to abort its flight

-Capability to glide to a safe landing in case of engine failure

-Accurate computation of take - off and landing distances (e.g. consideration of groud conditions, thrust, drag, proper correlation of results with theoretical predictions)

-Consideration of programmed flight for line of sight missions

-Research groups which seek to improve aircraft performance, capabilities, and systems (e.g. instrumentation)

If the component parts comprising the RPV are defective this may result in a component part failure leading to an aircraft crash. Hence Component tests and considerations should be addressed (in the manufacturing process) to provide safety. Some of these considerations include,

(1)Service Conditions:

a) Temperature Data
b) Environmental Conditions
c) Service Stresses

(2)Presence of color or texture changes

(3)Distinguishing surface features:

a) Gross Plasticity
b) Cracks
c) Surface Defects

(4)Hardness Measurements

(5)Mechanical Tests:

a) Tensile
b) Impact
c) Fracture Toughness

(6)Corrosion Tests

(7)Stress Analysis

In determining whether or not this mission is worth undertaking, a Risk versus Benefit table has been made by Spirit's managers which addresses six Risks and Benefits they feel are important considerations in terms of societal safety, and the success of their company. The rating given to each item varies from 1 - 10 (1 = a low rating and thus not likely to occur).

Mission Risk Of:		Mission Benefits:	
Property Damage	5	Societal Need	7
Litigation Costs	7	Profits	9
Claims Settlements	7	Provides Job	8
Sales Declining	5	Expansion of Technology	8
Loss of Life	2	Public Welfare	5
Personal Injury	3	Economic Contributions (taxes benefit society)	5
	29		42

* As can be seen the Benefits do outweigh the Risks even if we add or subtract a few points from either side!

10.2 Production Plans and Cost Estimate

The design and manufacture of remotely piloted vehicles is a special project which "Spirit Corporation" has undertaken with University aid. Spirit has been under intense economic pressure from increased foreign competition and slumping markets at home. What Spirit needed was engineering assistance on the selection of advanced manufacturing technology at their plant. A list of tasks to be performed by both the plant and the universities was made. This approach taken by Spirit is known as the family unit approach. Each

unit consists of a grouping of people and processes into a specific area dedicated to the production of a family of parts or products.

University Projects Include:

--Development of programs tailored to plant needs
--Computer integrated design and manufacture
--Selection of best options for automated material handling
--Analysis and Inventory of materials used
--Manufacturing and Automation Research
--Productivity Enhancement

* Five universities will be used to accomplish the tasks listed above.

Plant Position	Responsibility
Project Director	-Advertising -Review work standards -Develop plant layout
Area Managers	-Identifies needs of consultants and engineering staff
Division Consultants	-Directs divisions activities
Manufacturing Engineers	-Oversee machine operation -Build respective products from automated (machine) part

University		Plant Site
Project Coordinator	outside consultants	Project Director
Faculty Consultants		Area Managers
Graduate Assistants		Division Consultants
Co-op Students		Manufacturing Engineers
Technical Facilities		

Plant Site = 250,000 ft^2 consisting of 3 areas (83,333 ft^2 each)

Each area consists of 3 divisions (27,778 ft^2 each)

The work force includes:

-18 Manufacturing Engineers
-09 Division Consultants
-03 Area Managers
-01 Project Director
-02 Outside Consultants

Area 1

Division 1	Construction/Assembly of	Fuselage
Division 2	"	Landing Gear
Division 3	"	Instrumentation

Area 2

Division 4	Construction/Assembly of	Wings
Division 5	"	Empennage
Division 6	"	Test Specimen

Area 3

Division 7	Construction/Assembly of	Control Surfaces
Division 8	"	Propeller
Division 9	"	Small Parts (nuts and bolts)

The product parts will be designed for automated manufacturing to be hand assembled (each division constructing/organizing its individual product). Each area will have the use of one machine for the production of its parts and a fourth machine will be used for the processing of the final product. The total number of parts required to build one plane is approximately 15,000 (i.e. 5000 parts per machine). Spirit's machines will be engaged in manufacturing/production eight hours a day five days a week. Each machine will output 63 parts per hour to be assembled by its area workers. At this rate Spirit's construction rate will be two planes per month. The three manufacturing machines will perform the following production operations:

--Machining: Process in which the shape of the part is changed by removing excess material with a cutting tool

--Plastic Molding: High - Volume manufacturing process used to make plastic parts to final shape and size

*The materials of which the plane is constructed include wood, plastic, and aluminum, fiberglass and foam.

The machine stations will be continuously monitored to ensure the quality of parts for assembly. For example, the pressure of each machine stroke is recorded and the data is sent to a computer which documents the operation of the entire machine. Deviation from the normal at any station will be quickly detected. A machine operator will be required to perform certain additional functions some of

(1) Dealing with equipment breakdowns

(2) Performing irregular cycles, such as tool changing at periodic

(3) Program editing or data input

(4) Emergency stop conditions

The plant procedure for operation is therefore:

DESIGN--->MANUFACTURE--->ASSEMBLY--->SHIPPING

A schematic of one area of the plant layout can be seen in

The last stage before shipping involves processing to buyer specifications. This procedure involves:

--Spray Coating

--Drilling, Polishing, and similar operations

Advantages of machine spray coating/polishing include:

--Consistency of Finish (better quality)

--Reduced Coating Material Usage

--Greater Productivity

COST ESTIMATE

Start - Up Costs:

- 4 Manufacturing Machines $100,000
- University Grants (total) $25,000

*Spirit is looking to other industries to help fund University research thus sharing the costs and the benefits.

Monthly Costs:

- Labor (33 workers)	$55,000
- Rent	$5,000
- Insurance	$1,000
- Electricity/Phone	$1,000
- Materials Cost (wholesale)	$30,000
	$92,000

*By selling the planes for $100,000 each (and manufacturing 2 a month) Spirit will take a 17,000 loss the first month due to start - up costs. This loss will quickly be made up the second month with a net profit of :

$200,000 - $92,000 - $17,000 = $91,000

Each successive month after the second will yield a net profit of :

$200,000 - $92,000 = $108,000

FIGURE 1.1

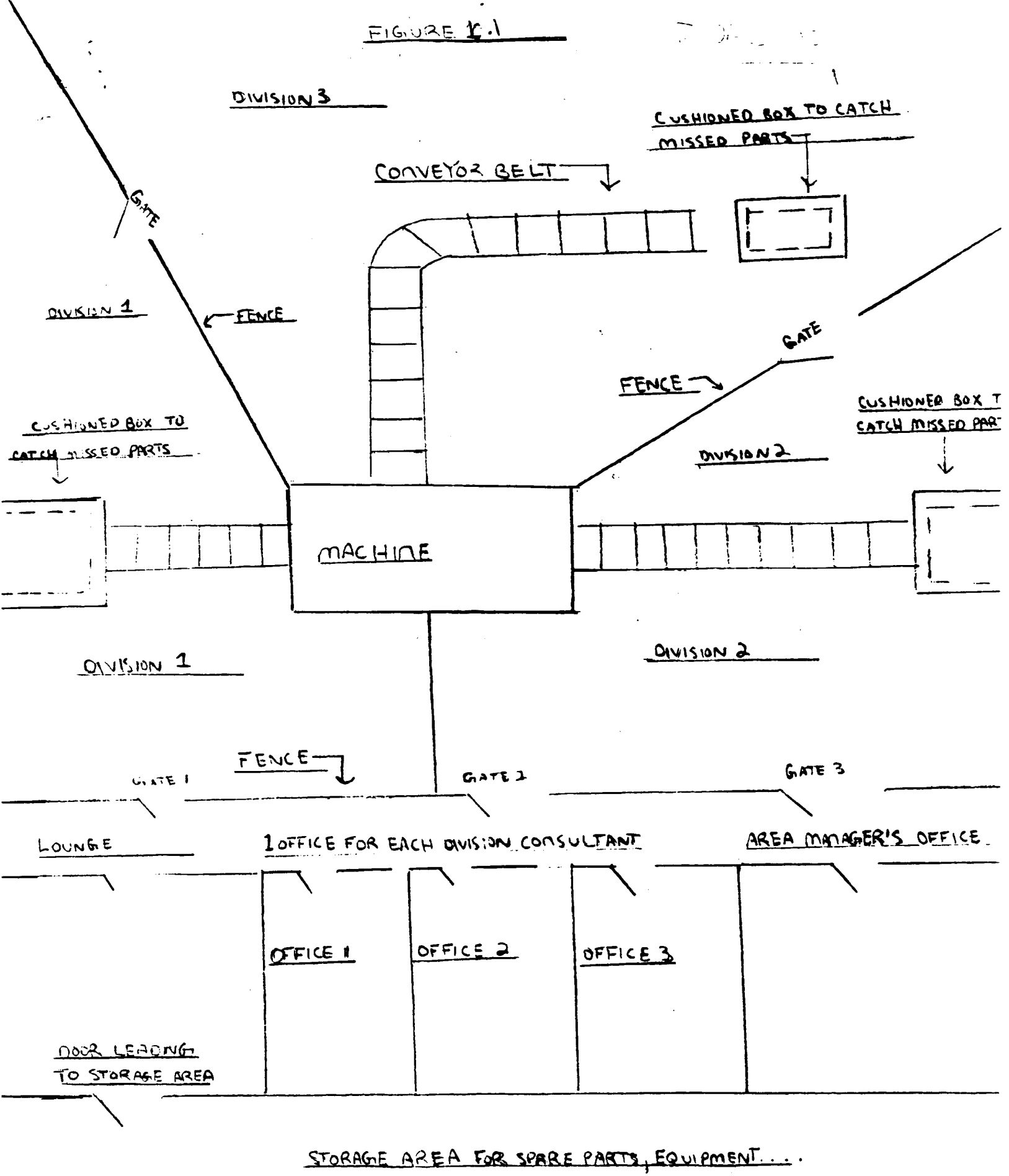
DIVISION 3
CUSHIONED BOX TO CATCH MISSED PARTS
CONVEYOR BELT
GATE
DIVISION 1
FENCE
GATE
FENCE
CUSHIONED BOX TO CATCH MISSED PARTS
CUSHIONED BOX TO CATCH MISSED PARTS
DIVISION 2
MACHINE
DIVISION 1
DIVISION 2
FENCE
GATE 1
GATE 2
GATE 3
LOUNGE
1 OFFICE FOR EACH DIVISION CONSULTANT
AREA MANAGER'S OFFICE
OFFICE 1
OFFICE 2
OFFICE 3
DOOR LEADING TO STORAGE AREA
STORAGE AREA FOR SPARE PARTS, EQUIPMENT...

CHAPTER XI
TECHNOLOGY DEMONSTRATOR

11.1 Special considerations

The following should be considered when comparing the SPiRiT design with the scaled demonstrator ("STD") and its flight performance: The scaled technology demonstrator was built to verify the validity of the flying test bed concept only. It is not an exact manufacturing prototype of the SPiRiT, but only a vehicle to demonstrate the technology of RPVs as aerodynamic test beds. The purpose of the STD is then to determine if it is possible and practical to operate a stable platform for subscale airfoil testing in flight through a wide Reynolds number range. The stability of the RPV and the feasibility of mounting the specimen in undisturbed flow while taking three dimensional pressure measurements in flight are to be investigated durind test flights with the STD.

The demonstrator is an approximately 50% scale model of the original SPiRiT design using the same wing airfoil section. The tail control surfaces are flat plates. No aileron is used and the gear is not retractable. Large scale radio control (R/C) design methods, instead of the scaled down SPiRiT design, is used throughout the structural, systems and flight control layout. However, the overall configuration of the airframe, powerplant arrangement and test section location is identical with that of the SPiRiT design. Note that it was not a goal to test manufacturing techniques, data acquisition systems, powerplants and propellers, and other subsystems in the process of building and testing the STD.

Special considerations should therefore be given mostly to in flight performance and stability of the STD. Manufacturing techniques, structural integrity and subsystems architecture and integration may be examined on a ground test rig ("iron bird"). Flight tests will show if a design like the SPiRiT can be operated by a small crew with little supporting equipment. Initial flight testing is discussed in section 11.3.

11.2 Flight Test Plan

Before any STD flight tests, all aircraft systems must be thoroughly checked on the ground. First, the CG location must be verified by balancing the STD on its wings. Second, the neutral position of the control surfaces must be set manually and compared with a neutral no-trim setting on the radio control transmitter. It is desirable to achieve a neutral control surface position without any transmitter trim input in order to have maximum deflection and trim capability before the first flight. Heat generation from the battery and the servos must be monitored carefully during ground operations without cooling airflow from the propeller. Engine power should be checked from idle to full power to investigate vibration, and the rigidity of the tail surfaces when exposed to the propeller slipstream. This also shows any control surface flutter.

Initial ground roll trials should determine the power setting required to move the STD at a speed that is comfortable for the operator. At that speed the STD should not be accelerating. Taxi trials should be done on a hard, level surface so that undesirable tendencies can be observed easily. Inaccurate steering on the ground, for instance, may be due only to the uneven surface, and ground roll behavior would then not be investigated reliably. High speed

taxi trials can be made up to estimated take-off speeds. If the STD is controllable throughout this speed range, initial stability and control tests can be made slightly above stall speed. First, however, take-off speeds and power settings must be determined accurately: Half-up elevator is applied throughout the take-off roll until the plane lifts off the ground. This speed is multiplied by no more than 1.2 to give a safe maneuvering speed and power setting near the ground.

First, longitudinal stability and elevator effectiveness can be checked near this speed. The STD is taxied at take-off speed with neutral elevator and then half elevator deflection is applied. The plane will clearly show if it has a tendency to over rotate or if it will immediately pitch to the attitude achieved during the initial ground roll, when the elevator was set to 50% from the start. Over rotation is unsafe and dynamic stability (especially CG location) should be checked before the next attempt. Slow pitch response is not unsafe. This is usually due to an excessive forward CG. At this point, the operator must be familiar and comfortable with the characteristics investigated so far.

If all tests to this point show safe characteristics, a normal take-off may be made. Since this will be the first take-off to higher altitudes, the take-off profile should be flown at the operator's discretion, regardless of theoretical take-off predictions. In other words, the pilot should take off only when and how he considers it to be safe. After a few flights, actual take-off data may be compared with predicted performance and the pilot can then try to fly near the predicted performance.

Once at altitude, stability characteristics must be checked first. The plane is best flown close to the operator at approximately treetop level, so that all

attitude and roll changes can be observed visually. Throughout the entire flight speed range, the following should be recorded:

a) The Bank Angle for Neutral Roll Stability

At this point, a turn is self sustained without any control surface input. If this bank angle is determined accurately, only a step input (actually a ramp function like input because of equipment lag) is required to sustain a turn, thereby saving a considerable amount of control energy. However, without any aileron control, such a neutral point may not even be achievable.

b) Spiral and Directional Stability

This is best done on a gusty day, but the operator should determine if these characteristics are safe for steady, level flight. Since only a rudder is used, full rudder deflection may cause an excessive crab angle in steep turns. This crab angle may put a limit on bank angles and safe useful rudder travel.

c) Phugoid Damping and Pitch Control

Both has been checked during taxi and take-off trials but now longitudinal stability and control can be examined throughout the entire speed range. Note, however, that no other stability characteristics change as much with dynamic pressure as longitudinal damping. Gradual step elevator inputs will show if elevator effectiveness is adequate. The phugoid time constant can be measured.

Slow Speed and Landing Performance

Again, this should be done at the operator's discretion. It is recommended that speeds below $1.2^{*}V_{to}$ are not used for stability flight tests. Slow speed maneuverability should be examined during approach and landing

only. Landing speeds are not very critical because the demonstrator has a very strong shock absorbing gear. Also, damage to the propeller, engine or tail surfaces is not likely.

The demonstrator will be flown with a test specimen at all times. Stability and control criteria for both, the design and the demonstrator, always included the effect of a test specimen. Handling characteristics without a specimen have not been investigated fully and flight without it is not recommended.

Part of the test program must be a post flight check of the aircraft structure, systems, and powerplant. The group leaders responsible for these areas should perform these checks. These areas should be checked especially for effects of vibration, heat and possibly excessive loads or attitudes encountered during the first flight. Ideally, the entire flight, including taxi trials, should be recorded on film. Personal impressions of the entire team and of the test pilot should be discussed immediately following the first flight. Overall responsibility for the flight test program rests with the design group leader but the operator will be responsible for the safety of the team and the demonstrator.

11.3 Flight Test Results

The RPV's maiden flight was intended to give information on the handling characteristics of the RPV. The RPV had a smooth and well controlled take off and then climbed to an altitude of approximately fifteen feet. When executing a left turn, however, the RPV may have encountered a downdraft inducing a sharp nose down moment and subsequent dive. The pilot was able to pull out of this dive in control but the RPV then porpoised into the ground.

One of the first theories formulated explaining why the RPV crashed so suddenly after take off was suggested by Dr. Batill. According to Dr. Batill the RPV might have flown into a wind shear induce by the warm air rising off the pavement coupled with the cooler air surrounding the parking lot. The RPV was apparently slightly underpowered and thus could not fully recover from the initial loss of lift. This theory, however, does not account for the RPV's recovery after the initial dive nor does it address the reasons behind the final dive.

Another possible theory is that the RPV was designed to fly with the mock test specimen on, but the RPV was flown without it. This may have altered the location of the center of gravity, changing the static and dynamic stability enough to lose control

A third theory that is prevalent with the designers is that the crash was a result of pilot error and design flaw. The control surfaces may have been oversized thus giving too much control power. Thus when the pilot corrected for the initial dive he probably over corrected for the disturbance. Had the pilot continued straight over the grassy field and accustomed himself to the handling characteristics of the RPV, the crash may not have happened.

Appendix A

```
]LIST

   0  GOTO 130
170  PRINT  CHR$ (4)"PR#1": PRINT  CHR$ (27) CHR$ (15): PRINT  CHR$ (27) CHR$
     (9)'132N": LIST : PRINT  CHR$ (4)"PR#3"
120  END
130  DIM A(20,20),C(20),B(20),THET(20),F(20)
140  DIM X(20)
150  REM  DATA INPUT SECTION FOLLOWS
160  HOME : PRINT "LIFTING LINE PROGRAM": PRINT : PRINT
170  INPUT "SPAN (FT) = ";SPAN
180  INPUT "TAPER RATIO =";TU
190  INPUT "SECTION LIFT CURVE SLOPE (PER RAD) = ";MO
200  INPUT "ROOT CHORD (FT) = ";CS
210  INPUT "ANGLE OF ATTACK OF ROOT SECTION (DEG) = ";ALPHA
220  INPUT "NUMBER OF FOURIER COEFFICIENTS, N= ";N
230  INPUT "NUMBER OF SPANWISE LOCATIONS FOR WHICH SECTION DATA IS DESIRE
     D, M=";MM
240  INPUT "DOES THE WING HAVE GEOMETRIC TWIST (Y/N ?)";DUM$
250  IF DUM$ = "Y" GOTO 280
260  IF DUM$ = "N" GOTO 300
270  GOTO 240
280 RALPR = 0
290  PRINT : INPUT "ANGLE OF ATTACK OF THE TIP RELATIVE TO THE ROOT (DEG)
      = ";TALPT
300 PI = 3.14159
310 DTR = PI / 180.
   1  REM  CONVERT ANGLES TO RADIANS
320 ALPHA = DTR * ALPHA:RALPR = RALPR * DTR:TALPT = TALPT * DTR
340 SS =  SPAN * CS / 2.) * (1. + TU)
350 AR =  SPAN ^ 2) / SS
355 AFA = CS * SPAN * (1. + TU) / 2.
360 DIL" = PI / (2. * N)
370 CNO = MO + CS / (4. * SPAN)
380  FOR J = 1 TO N
390  FOR I = 1 TO N
400 THET I) = I * DILTH
410 B(I) = ALPHA *  SIN (THET(I))
420 YI =  SPAN / 2.) *  COS (THET(I))
430  IF DUM$ = "N" GOTO 470
440 A2ALP = RALPR + ((2. * YI) / SPAN) * (TALPT - RALPR)
450 A2ALPHA = ALPHA + A2ALP
460 B(I) = A2ALPHA *  SIN (THET(I))
470 CI = CS * (1. - (YI / (.5 * SPAN)) * (1. - TU))
480 F(I) = B(I)
490 A(I,J  = ((CS / CI) *  SIN (THET(I)) + (2. * J - 1) * CNO) *  SIN ((2
     * J - 1) * THET(I))
500  NEXT I: NEXT J
510  GOSUB 1250
520  PRINT : PRINT : PRINT "FOURIER COEFFICIENTS"
530  FOR I = 1 TO N: PRINT I,X(I): NEXT I
540  PRINT : PRINT
550  PRINT "HIT ANY KEY TO CONTINUE OUTPUT"
     POKE  - 16368,0: WAIT  - 16384,128
570  PRINT : PRINT
580  REM  SECTION DATA OUTPUT
590  DIM Y(20),CC(20),CL(20),CDI(20)
600  FOR I = 1 TO MM
610 DILTH = PI / (2. * MM)
620 YI = I * DILTH
```

APPENDIX A

```
650 F1 = 0.:F2 = 0.
660  FOR J = 1 TO N
670 F3 = F1:F4 = F2
680 F1 = F3 + X(J) *  SIN ((2 * J - 1) * T3TH)
690 F2 = F4 + (2 * J - 1) * X(J) *  SIN ((2 * J - 1) * T3TH)
700  NEXT J
710 CL(I) = (MO * CS / CC(I)) * F1
720 CDI(I) = (MO * CS) ^ 2 / (4. * SPAN * CC(I)) * F1 * F2 /  SIN (T3TH)
730  NEXT I
740 M = MM
750  REM
760  REM  THIS SECTION REARRANGES THE DATA FORM ROOT TO TIP
770  REM
780 MS = M + 1
790 J = 0
800  FOR I = MM TO 1 STEP  - 1
810 J = J + 1:A(J,1) = CC(I):A(J,2) = CL(I):A(J,3) = CD(I):A(J,4) = Y(I):
     NEXT I
820  FOR I = 1 TO MM
830 Y(I) = A(I,4):CC(I) = A(I,1):CL(I) = A(I,2):CD(I) = A(I,3): NEXT I
840 Y(MS) = SPAN / 2.:CC(MS) = CS * TU:CL(MS) = 0.:CD(MS) = 0.
850 Z1 = 1000
860 Z2 = 100000
870  FOR K = 1 TO MS
880 Y(K) =  INT (Z1 * Y(K) + .5) / Z1
890 CC(K) =  INT (Z1 * CC(K) + .5) / Z1
900 CL(K) =  INT (Z1 * CL(K) + .5) / Z1
910 CD(K) =  INT (Z2 * CD(K) + .5) / Z2
920  NEXT K
930  PRINT "I          Y(I)(FT)      CHORD(I)(FT)      CL(I)            C
     D(I)"
940  PRINT
950  FOR I = 1 TO MS
960  PRINT I;: POKE 36,10: PRINT Y(I);: POKE 36,25: PRINT CC(I);: POKE 36
     ,40: PRINT CL(I);: POKE 36,60: PRINT CD(I)
970  NEXT I
980 FS = 0.
990  FOR I = 1 TO N
1000 FS = FS + (2 * I - 1) * X(I) ^ 2: NEXT I
1010 W1CD = ((MO * CS) ^ 2 * PI) / (16. * SS) * FS
1020 W2CL = ((MO * CS * PI * SPAN) / (4. * SS)) * X(1)
1030  PRINT : PRINT "TOTAL WING LIFT COEFFICIENT, CL= ";W2CL
1040  PRINT : PRINT "TOTAL WING INDUCED DRAG COEFFICIENT, CDI =";W1CD
1050 F6 = 0.
1060  FOR I = 2 TO N
1070 F6 = F6 + (2 * I - 1) * (X(I) / X(1)) ^ 2: NEXT I
1080 EPS = 1. / (1. + F6)
1090  PRINT : PRINT "WING EFFICIENCY(EPSILON) = ";EPS
1092  PRINT : INPUT "DO YOU WISH TO PRINT THESE RESULTS (Y/N)?";DUM$
1094  IF DUM$ = "Y" GOTO 1098
1096  IF DUM$ = "N" GOTO 1100
1097  GOTO 1092
1098  GOSUB 1900
1100  INPUT "DO YOU WISH TO SAVE THE RESULTS FOR FUTURE ANALYSIS OR PLOTT
     ING ? (Y/N)";DUM$
1110  IF DUM$ = "N" THEN  PRINT "BYE BYE"
1120  IF DUM$ = "N" THEN  END
1130  IF DUM$ = "Y" GOTO 1150
1140  GOTO 1100
1150  INPUT "INPUT THE DATA FILE NAME        ";PL$
1160 P1$ = PL$ + ".LL"
1170 D$ =  CHR$ (4): REM  CTRL-D
1180  PRINT D$;"OPEN";P1$: PRINT D$;"WRITE";P1$
1190  PRINT ALPHA: PRINT MS: PRINT AEA
```

```
1220  PRINT D$;"CLOSE";P1$
1230  PRINT "THE SEQUENTIAL DATA FILE "P1$" HAS BEEN CREATED"
1240  END
1250  REM     SUBROUTINE SOLVES THE MATRIX EQUATION
1260  REM     [A] {X} = {F}
1270  REM    BY MEANS OF GAUSS ELIMINATION WITH PARTIAL PIVOTING
  30  REM          [A] = MATRIX OF COEFFICIENTS (STORED IN ROWS)
1290  REM          {X} = SOLUTION
1300  REM          {F} = RIGHT HAND SIDE
1310  REM           N  = ORDER OF THE MATRIX
1320  FOR L = 2 TO N
1330 LM1 = L - 1
1340 AMAX =  ABS (A(LM1,LM1))
1350 JMAX = LM1
1360  FOR J = L TO N
1370 TEMP =  ABS (A(J,LM1))
1380  IF TEMP <  = AMAX GOTO 1410
1390 AMAX = TEMP
1400 JMAX = J
1410  NEXT J
1420  IF AMAX <  = .000000001 GOTO 1710
1430  IF JMAX = LM1 GOTO 1520
1440 PTEM = F(LM1)
1450 F(LM1) = F(JMAX)
1460 F(JMAX) = PTEM
1470  FOR K = LM1 TO N
1480 PTEM = A(LM1,K)
1490 A(LM1,K) = A(JMAX,K)
1500 A(JMAX,K) = PTEM
1510  NEXT K
1520  FOR J = L TO N
  30 Q = A(J,LM1) / A(LM1,LM1)
  40  FOR K = L TO N
1550 A(J,K) = A(J,K) - Q * A(LM1,K)
1560  NEXT K
1570 F(J) = F(J) - Q * F(LM1)
1580  NEXT J
1590  NEXT L
1600 X(N) = F(N) / A(N,N)
1610  FOR M = 2 TO N
1620 J = N - M + 1
1630 JP1 = J + 1
1640 S = 0.
1650  FOR K = JP1 TO N
1660 S = S + A(J,K) * X(K)
1670  NEXT K
1680 X(J) = (F(J) - S) / A(J,J)
1690  NEXT M
1700  GOTO 1720
1710 N = 999999
1720  RETURN
1900  REM  THIS SECTION PRINTS RESULTS
1910  PRINT  CHR$ (4)"PR#1"
1920  PRINT "************ LIFTING LINE ANALYSIS ***********************":
      PRINT
1930  PRINT "WING SPAN = ";SPAN;" FT"
1940  PRINT "WING TAPER RATIO =";TU
   5  PRINT "SECTION LIFT CURVE SLOPE =";MO;" PER RAD"
  30  PRINT "ROOT CHORD =";CS;" FT"
1953 ALPHA = ALPHA / DTR:TALPT = TALPT / DTR
1955  PRINT "ANGLE OF ATTACK OF ROOT SECTION =";ALPHA;" DEG"
1969  PRINT "ANGLE OF ATTACK OF TIP RELATIVE TO THE ROOT =";TALPT;" DEG"
1983 ALPHA = ALPHA * DTR:TALPT = TALPT * DTR
1990  PRINT : PRINT
2000  PRINT "I          Y(I)FT          CHORD(I)FT          C'L(I)
```

APPENDIX A

APPENDIX A

```
2010  PRINT
2020  FOR I = 1 TO MS
2030  PRINT I;: POKE 36,10: PRINT Y(I);: POKE 36,25: PRINT CC(I);: POKE 3
      6,40: PRINT CL(I);: POKE 36,60: PRINT CD(I)
2040  NEXT I
2050  PRINT : PRINT : PRINT
2075  PRINT : PRINT "TOTAL WING AREA = ";AEA;" FT^2"
2080  PRINT : PRINT "TOTAL WING LIFT COEFFICIENT, CL= ";W2CL
2070  PRINT : PRINT "TOTAL WING INDUCED DRAG COEFFICIENT, CDI =";W1CD
2080  PRINT : PRINT "WING EFFICIENCY(EPSILON) = ";EPS
2090  PRINT  CHR$ (4)"PR#3"
2100  RETURN
```

APPENDIX B

********** LIFTING LINE ANALYSIS **********

WING SPAN = 15.2 FT
WING TAPER RATIO =1
SECTION LIFT CURVE SLOPE =5.3 PER RAD
ROOT CHORD =1.52 FT
ANGLE OF ATTACK OF ROOT SECTION =-5 DEG
ANGLE OF ATTACK OF TIP RELATIVE TO THE ROOT =Ø DEG

I	Y(I)FT	CHORD(I)FT	CL(I)	CD(I)
1	Ø	1.52	-.421	3.33E-Ø3
2	2.349	1.52	-.416	3.63E-Ø3
3	4.467	1.52	-.4	4.74E-Ø3
4	6.149	1.52	-.357	7.11E-Ø3
5	7.228	1.52	-.246	.Ø1ØØ5
6	7.6	1.52	Ø	Ø

TOTAL WING AREA = 23.1Ø4 FT^2

TOTAL WING LIFT COEFFICIENT, CL= -.3818Ø1258

TOTAL WING INDUCED DRAG COEFFICIENT, CDI =5.Ø9896348E-Ø3

WING EFFICIENCY(EPSILON) = .91ØØØ4ØØ5

********** LIFTING LINE ANALYSIS **********

WING SPAN = 15.2 FT
WING TAPER RATIO =1
SECTION LIFT CURVE SLOPE =5.3 PER RAD
ROOT CHORD =1.52 FT
ANGLE OF ATTACK OF ROOT SECTION =5 DEG
ANGLE OF ATTACK OF TIP RELATIVE TO THE ROOT =Ø DEG

I	Y(I)FT	CHORD(I)FT	CL(I)	CD(I)
1	Ø	1.52	.421	3.33E-Ø3
2	2.349	1.52	.416	3.63E-Ø3
3	4.467	1.52	.4	4.74E-Ø3
4	6.149	1.52	.357	7.11E-Ø3
5	7.228	1.52	.246	.Ø1ØØ5
6	7.6	1.52	Ø	Ø

TOTAL WING AREA = 23.1Ø4 FT^2

TOTAL WING LIFT COEFFICIENT, CL= .3818Ø1258

TOTAL WING INDUCED DRAG COEFFICIENT, CDI =5.Ø9896348E-Ø3

WING EFFICIENCY(EPSILON) = .91ØØØ4ØØ5

APPENDIX B

********** LIFTING LINE ANALYSIS **********

WING SPAN = 15.2 FT
WING TAPER RATIO =1
SECTION LIFT CURVE SLOPE =5.3 PER RAD
ROOT CHORD =1.52 FT
ANGLE OF ATTACK OF ROOT SECTION =10 DEG
ANGLE OF ATTACK OF TIP RELATIVE TO THE ROOT =0 DEG

I	Y(I)FT	CHORD(I)FT	CL(I)	CD(I)
1	0	1.52	.841	.0133
2	2.349	1.52	.833	.01452
3	4.467	1.52	.799	.01895
4	6.149	1.52	.714	.02843
5	7.228	1.52	.491	.04021
6	7.6	1.52	0	0

TOTAL WING AREA = 23.104 FT^2

TOTAL WING LIFT COEFFICIENT, CL= .763602516

TOTAL WING INDUCED DRAG COEFFICIENT, CDI =.02039585 39

WING EFFICIENCY(EPSILON) = .910004005

********** LIFTING LINE ANALYSIS **********

WING SPAN = 15.2 FT
WING TAPER RATIO =1
SECTION LIFT CURVE SLOPE =5.3 PER RAD
ROOT CHORD =1.52 FT
ANGLE OF ATTACK OF ROOT SECTION =12 DEG
ANGLE OF ATTACK OF TIP RELATIVE TO THE ROOT =0 DEG

I	Y(I)FT	CHORD(I)FT	CL(I)	CD(I)
1	0	1.52	1.009	.01916
2	2.349	1.52	.999	.0209
3	4.467	1.52	.959	.02728
4	6.149	1.52	.857	.04094
5	7.228	1.52	.589	.0579
6	7.6	1.52	0	0

TOTAL WING AREA = 23.104 FT^2

TOTAL WING LIFT COEFFICIENT, CL= .91632302

TOTAL WING INDUCED DRAG COEFFICIENT, CDI =.02937 00296

WING EFFICIENCY(EPSILON) = .910004005

********** LIFTING LINE ANALYSIS **********

WING SPAN = 4.24 FT
WING TAPER RATIO =1
SECTION LIFT CURVE SLOPE =6.3 PER RAD
ROOT CHORD =2.118 FT
ANGLE OF ATTACK OF ROOT SECTION =-5 DEG
ANGLE OF ATTACK OF TIP RELATIVE TO THE ROOT =Ø DEG

I	Y(I)FT	CHORD(I)FT	CL(I)	CD(I)
1	Ø	2.118	-.321	.Ø1166
2	.655	2.118	-.311	.Ø1179
3	1.246	2.118	-.277	.Ø1199
4	1.715	2.118	-.216	.Ø1145
5	2.Ø16	2.118	-.123	8.34E-Ø3
6	2.12	2.118	Ø	Ø

TOTAL WING AREA = 8.98Ø32 FT^2

TOTAL WING LIFT COEFFICIENT, CL= -.2655745Ø9

TOTAL WING INDUCED DRAG COEFFICIENT, CDI =.Ø113263213

WING EFFICIENCY(EPSILON) = .99Ø135177

********** LIFTING LINE ANALYSIS **********

WING SPAN = 4.24 FT
WING TAPER RATIO =1
SECTION LIFT CURVE SLOPE =6.3 PER RAD
ROOT CHORD =2.118 FT
ANGLE OF ATTACK OF ROOT SECTION =1 DEG
ANGLE OF ATTACK OF TIP RELATIVE TO THE ROOT =Ø DEG

I	Y(I)FT	CHORD(I)FT	CL(I)	CD(I)
1	Ø	2.118	.Ø64	4.7E-Ø4
2	.655	2.118	.Ø62	4.7E-Ø4
3	1.246	2.118	.Ø55	4.8E-Ø4
4	1.715	2.118	.Ø43	4.6E-Ø4
5	2.Ø16	2.118	.Ø25	3.3E-Ø4
6	2.12	2.118	Ø	Ø

TOTAL WING AREA = 8.98Ø32 FT^2

TOTAL WING LIFT COEFFICIENT, CL= .Ø531149Ø18

TOTAL WING INDUCED DRAG COEFFICIENT, CDI =4.53Ø52853E-Ø4

WING EFFICIENCY(EPSILON) = .99Ø135177

APPENDIX C

********** LIFTING LINE ANALYSIS **********

WING SPAN = 4.24 FT
ING TAPER RATIO =1
SECTION LIFT CURVE SLOPE =6.3 PER RAD
ROOT CHORD =2.118 FT
ANGLE OF ATTACK OF ROOT SECTION =5 DEG
ANGLE OF ATTACK OF TIP RELATIVE TO THE ROOT =Ø DEG

I	Y(I)FT	CHORD(I)FT	CL(I)	CD(I)
1	Ø	2.118	.321	.Ø1166
2	.655	2.118	.311	.Ø1179
3	1.246	2.118	.277	.Ø1199
4	1.715	2.118	.216	.Ø1145
5	2.Ø16	2.118	.123	8.34E-Ø3
6	2.12	2.118	Ø	Ø

TOTAL WING AREA = 8.98Ø32 FT^2

TOTAL WING LIFT COEFFICIENT, CL= .265574Ø9

TOTAL WING INDUCED DRAG COEFFICIENT, CDI =.Ø113263213

ING EFFICIENCY(EPSILON) = .99Ø135177
********** LIFTING LINE ANALYSIS **********

WING SPAN = 4.24 FT
WING TAPER RATIO =1
SECTION LIFT CURVE SLOPE =6.3 PER RAD
ROOT CHORD =2.118 FT
ANGLE OF ATTACK OF ROOT SECTION =1Ø DEG
ANGLE OF ATTACK OF TIP RELATIVE TO THE ROOT =Ø DEG

I	Y(I)FT	CHORD(I)FT	CL(I)	CD(I)
1	Ø	2.118	.642	.Ø4662
2	.655	2.118	.621	.Ø4717
3	1.246	2.118	.554	.Ø4797
4	1.715	2.118	.433	.Ø458
5	2.Ø16	2.118	.246	.Ø3335
6	2.12	2.118	Ø	Ø

TOTAL WING AREA = 8.98Ø32 FT^2

TOTAL WING LIFT COEFFICIENT, CL= .531149Ø18

TOTAL WING INDUCED DRAG COEFFICIENT, CDI =.Ø453Ø52853

WING EFFICIENCY(EPSILON) = .99Ø135177

APPENDIX D

```
c-------------------------------------------------------------------------------
c
c
c       A program to calculate power required for the SPiRiT RPV
c
c       March 1989  Nicholas J. Simon
c
c-------------------------------------------------------------------------------
        REAL VI(400), PR(400), HP(400),hpp(21),vpp(21),hpa(400),rc(400)
        REAL M
        CHARACTER*10 PDATA
        CHARACTER*10 VDATA
        PA = 7.5
        AR=10.0
        E = .91
        PROP=.7
        PIE = 3.14
        CDO=.066
        M=13.6
        S=2.16
        ROW=1.225
        VI(1) = .1
        DO 10 J=1,400
        CL=2.0*M*9.8/(ROW*S*VI(J)**2)
        CDI = CL**2/(PIE*E*AR)
        CD = CDO +CDI
        TR = M*9.8/(CL/CD)
         PR(J) = TR*VI(J)
        ef=5.626e-2+4.76e-2*vi(j)-1.0799e-3*vi(j)**2+1.143e-5*vi(j)**3
       !-4.66e-8*vi(j)**4
        hpa(j) = PA*ef
        hp(j) = PR(J)/746.
        rc(j) = (hpa(j) - hp(j))*746.0/(m*9.8)
        IF (J.EQ.400) THEN
        GO TO 22
         ENDIF
         VI(J+1) = VI(J) + .1
 22      CONTINUE
 10      CONTINUE

        write(9,2)
        J=0
        DO 15 I = 1,20
        WRITE(9,3) HP(J), VI(J), RC(J)
        hpp(i)=hp(j)
        vpp(i)=vi(j)
        J=J+20
 15     CONTINUE
c       open(unit=41, file=PDATA, Status='new')
c       write(41,1)hpp
c       CLOSE(UNIT=41)
c       open(unit=42, file=VDATA, Status='new')
c       write(42,1)vpp
c       CLOSE(UNIT=42)
```

APPENDIX D

```
1       format(' ',1f5.2)
2       format(' ','power required',9x,'velocity  (m/s)','Rate of climb
       !(m/s)')
3       format(' ',1f5.2,14x,1f5.2,14x,1f5.2)
        pause
        STOP
        END
```

APPENDIX E

```
c-------------------------------------------------------------------------------
c       A program to calculate the power available, endurance, and range of the SPiRiT
c       RPV.
c               March 1989  By Nicholas J. Simon
c
c
c-------------------------------------------------------------------------------
        REAL VI(400), HP(400),epp(21),vpp(21),lost(400),range(400)
        REAL M
        CHARACTER*10 filnm
        CHARACTER*13 A1,A2,A3,A4
        character*(*) t
        parameter (t=9)
        write(9,*)'Enter Power available'
        read(9,*)PA
        w1=11.33*9.8
        w0=13.6*9.8
        AR=10.0
        E = .91
        PROP=.7
        PIE = 3.14
        CDO=.066
        M=13.6
        S=2.16
        ROW=1.225
        VI(1) = .1
        DO 10 J=1,400
        CL=2.0*M*9.8/(ROW*S*VI(J)**2)
        CDI = CL**2/(PIE*E*AR)
        CD = CDO +CDI
c
c-------------------------------------------------------------------------------
c                           endurance calculations
c-------------------------------------------------------------------------------
c
        ef=5.626e-2+4.76e-2*vi(j)-1.0799e-3*vi(j)**2+1.143e-5*vi(j)**3
       !-4.66e-8*vi(j)**4
        hp(j) = PA*ef
        sfc=(1./2.1102**.21396)*PA*1.64e-6
        lost(j) = ef/sfc*cl**1.5/cd*(2.0*row*s)**.5*(W1**-.5-W0**-.5)
        range(j)=ef/sfc*cl/cd*log(w0/w1)
           IF (J.EQ.400) THEN
         GO TO 22
         ENDIF
         VI(J+1) = VI(J) + .1
 22      CONTINUE
 10      CONTINUE

         A1='power output'
         A2='velocity'
         A3='endurance (s)'
```

APPENDIX E

```
          A4='range (km)'
          write(9,2) A1,A2,A3,A4
           J=0
          DO 15 I = 1,20
          WRITE(9,3) HP(J), VI(J),lost(j)/60.,range(j)/1000.
          epp(i)=lost(j)
           vpp(i)=vi(j)
          J=J+20
 15       CONTINUE
         write(9,*) 'Enter name for the output file'
         read(9,1) filnm
         open(unit=41, file=filnm, Status='new')
         do 501 i=1,21
         write(41,*) t,vpp(i),t,epp(i)
 501     continue
         CLOSE(UNIT=41)
 1       format(a10)
 2       format(' ',a12,7x,a8,7x,a13,7x,a10)
 3       format(' ',1f5.2,12x,1f5.2,12x,1f7.2,12x,1f7.2)
         pause
         STOP
         END
```

Appendix F

```
C
C     This program determines the location of the center of gravity
C     given the component location as measured from any arbitraray
C     reference line (most forward point).  Component weight, X and
C     Y distance from the datum line are entered in a data file.
C     Incremental CG shift with a change in component location is
C     only computed along the X axis.
C     M. Weninger; Notre Dame Spring '89.

C        -- All units in ft, lb, s.
C        -- x axis:  originating at datum line; positive along
C                    longitudinal axis.
C        -- y axis:  originating at datum line; positive vertically
C                    up along yaw axis.


C
      CHARACTER*15 TEIL
      DIMENSION TEIL(30),WYXI(30,3)
      REAL MXCG
      WRITE(1,*)'IWR='
      READ(1,*) IWR
      OPEN (UNIT=55,FILE='ATD.DATA',STATUS='UNKNOWN')
      READ(55,*) LIM
      READ(55,*) XLT
      NUMBER=1
C
C     reference values*****
      XWT=0.0
      YWT=0.0
      WT=0.0
      XIW=0.0
      YIW=0.0

C     read data file, add incremental weight to WT******
      DO 10 I=1,LIM
      READ(55,*) TEIL(I),WYXI(I,1),WYXI(I,2),WYXI(I,3)
      WT=WT+WYXI(I,1)
      YWT=YWT+WYXI(I,2)*WYXI(I,1)
         XWT=XWT+WYXI(I,3)*WYXI(I,1)
   10 CONTINUE
      CLOSE (UNIT=55)
         XLT=XWT/WT
      YCG=YWT/WT
      DO 66 I=1,LIM
         XIW=XIW+WYXI(I,1)*ABS(XLT-WYXI(I,3))**2
         YIW=YIW+WYXI(I,1)*ABS(YCG-WYXI(I,2))**2
   66 CONTINUE
      WRITE(IWR,*)'

     .'
      WRITE(IWR,8) XLT
      WRITE(IWR,2) YCG
      WRITE(IWR,*)'
     .'
      WRITE(IWR,5) WT
      WRITE(IWR,*)'
     .'
      WRITE(IWR,3) YIW
      WRITE(IWR,4) XIW
      WRITE(IWR,*)'
     .'
      WRITE(IWR,7)
      WRITE(IWR,*) ' '
      DO 77 I=1,LIM
      WRITE(IWR,6) TEIL(I),WYXI(I,1),WYXI(I,2),WYXI(I,3)
   77 CONTINUE
      WRITE(IWR,*)'
     .'
      WRITE(IWR,1)
      DO 88 I=1,LIM
         DIFP=1.0
         DIFN=-1.0
         MXCG=WYXI(I,1)*DIFP/WT
         WRITE(IWR,9) TEIL(I),DIFP,MXCG
   88 CONTINUE
```

APPENDIX F

```
C      format only*********

    7 FORMAT(1X,' ',22X,'WEIGHT,lb',12X,'YcgC(ft)',12X,
     .'XcgC(ft)')
    6 FORMAT(1X,A,9X,F7.3,10X,F9.3,8X,F9.3)
    5 FORMAT(1X,'gross weight WT = ',F7.3,' pounds')
    4 FORMAT(1X,'Iyy = ',F15.3,' lb.ft.s**2')
    3 FORMAT(1X,'Ixx = ',F15.3,' lb.ft.s**2')
    8 FORMAT(1X,'Xcg =',F7.3,'feet from datum line')
    2 FORMAT(1X,'Ycg =',F7.3,'ft')
    1 FORMAT(1X,'incremental component shift by (ft)',7X,'causes XCG shi
     .ft by (ft)')
      WRITE(IWR,*)' '
    9 FORMAT(1X,A,10X,F5.3,15X,F7.3)
      STOP
      END
```

Appendix G

```
C**********************************************************
C**********************************************************
C
C     WENINGER Markus; Notre Dame, Spring '89.
C     Copy of Trade Study Program (graphs) for SPiRiT design.
C     Influence of Speed, Clav, Clat, Ix, Iy, Cg shift on
C     Longitudinal and Dutch Roll Dynamic Stability.
C
C
C     Figures of Merit as Graphed:
C        - Phugoid Damping Ratio: Zp
C        - Short Period Damping Ratio: Zsp
C        - Dutch Roll Damping Ratio: Zdr
C        - Dutch Roll Undamped Natural Frequency: Wndr
C        - Product of Zdr and Dutch Roll
C          Damped Natural Frequency     : W*Zdr
C
C**********************************************************
C**********************************************************
C
      DIMENSION Y(100,5),ZP(100),ZSP(100),ZDR(100),WNDR(100),
     .WZ(100),TAU(100),LSPIRL(100),IX(100)
      REAL M,MA,MAD,MU,MWD,MW,MQ,IX,IXI,IZ,LROLL,LSPIRL,LB,LP,LR
      REAL MASS,LT,LV,IY,NDS,KN,KRI,LF,N,NSP,NDHSP,NDH,NB,NR,NP
C
      PI=3.14159
      CBAR=1.52
      WRITE(1,*) 'IWR='
      READ(1,*) IWR
      WRITE(1,*)'U='
      READ(1,*) U
      WRITE(IWR,*) 'U=',U
      WRITE(1,*)'CDO=.0395 CLEAN    .0995 GEAR,TEST   .1295 WORST'
      cdo=.100
      READ(1,*) CDO
      WRITE(IWR,*)'CDO=',CDO
      WRITE(1,*)'DIHEDRAL IN DEGREES='
      READ(1,*) DHED
      DIHED=DHED*PI/180.
      WRITE(IWR,*)'DIHEDRAL=',DIHED,'rad.'
      WRITE(1,*)'XCG FACTOR='
      READ (1,*) CG
      WRITE(IWR,*)'XCG Factor=',CG
      XCG=CG*CBAR
      XAC=.25*CBAR
      WRITE(IWR,*)'XCG=',XCG
      LT=5.018-CG*CBAR
      WRITE(IWR,*)'LT=',LT
      ST=8.070
      SV=3.880
C
      IXI=8.934
      DO 99 I=1,100
      IXI=IXI+.0199
      IX(I)=IXI
C
      CLAVI=2.
      DO 99 I=1,100
      CLAVI=CLAVI+.05
      CLAV(I)=CLAVI
C
      VEL=35.
      DO 99 I=1,100
      VEL=VEL+.8
      U(I)=VEL
C
      CGI=.1
      DO 99 I=1,100
      CGI=CGI+.003
      CG(I)=CGI
      XCG(I)=CG(I)*CBAR
      LT(I)=5.018-CG(I)*CBAR
C***  then plot cg-factor (cg(I)) vs other params and note that
      this cg range constitutes a net LT change  since LT is
      measured from the CG.
```

APPENDIX G

```
C       DO 99 I=1,40
C       DHED=(DHED+.25)*PI/180.
C       DIHED(I)=DHED

        SC=ST+SV
        S=23.12
        RHO=.002378
        E=.74
        B=15.2
        W=23.
        MASS=W/32.2

        PI=3.14159
        G=1.4
        R=1545.
        T=520.

        CLA=4.35
        CL=W/(.5*RHO*U**2*S)
        CLO=.532
        CLAW=4.35
        CLAT=3.043
        CLAV=3.973
        LV=LT
        AR=10.
        ZWW=.353
        IY=32.68
C       IX=9.927
        IZ=IY
        TR=1.
        SA=0.
        D=.705
        LAMBDA=1.0

C       **************LONGITUDINAL STAB. DERIVATIVES***************

        CDI=CL**2/PI/E/AR
C       CDI never used, Cla in cda %ZW of plane
        G=RHO*U**2/2.
        GT=1.2*G
        GV=1.2*G
        CDA=2.*CLO*CLA/PI/E/AR
        XW=(CLO-CDA)*G*S/MASS/U
        C=SQRT(G*T*R)
        M=U/C
        CZU=-(M**2*CLO/(1.-M**2))-2.*CLO
        CLU=-(CZU+2*CLO)
        ZU=(-(CLU+2.*CLO)*S*G)/MASS/U
        ZW=(-(CLA+CDO)*S*G)/MASS/U
        VH=LT*ST/S/CBAR
        VV=LV*SV/S/B
        ATA=GT/G
        DEDA=2.*CLA/PI/AR/E
        CMAW=CLAW*(XCG-XAC)/CBAR
        CMAT=(-VH*ATA*CLAT*(1.-DEDA))
        CMAS=.1
        CMAF=-.0003738
        CMA=CMAW+CMAT+CMAF+CMAS
        MW=CMA*(G*S*CBAR/U/IY)
        CMAD=(-2.*ATA*CLAT*VH*LT/CBAR*DEDA)
        MWD=CMAD*CBAR/2./U*G*S*CBAR/U/IY
        CMG=-2.*ATA*CLAT*VH*LT/CBAR
        MG=CMG*CBAR*G*S*CBAR/IY/2./U
        MU=0.
        XU=-2.*CDO*G*S/MASS/U

C       ************LONGITUDINAL   APPROXIMATIONS****

        WNP=SQRT(-ZU*G/U)
        ZP(I)=-XU/2./WNP
C       WP=WNP*SQRT(1.-ZP(I)**2)
        N=-ZP(I)*WNP
        THALF=.693/ABS(N)
C       NDH=.11*ABS(WP/N)
```

APPENDIX G

```
C      ********** SHORT PERIOD***********

       MA=U*MW
       MAD=U*MWD
       ZA=U*ZW
       WNSP=SQRT(ZA*MG/U-MA)
       ZSP(I)=(-(MG+MAD+ZA/U)/(2.*WNSP))
       WRITE(IWR,*)'ZSP=',ZSP(I)
CCCCC  WSP=WNSP*SQRT(1.-ZSP(I)**2)
       NSP=-ZSP(I)*WNSP
       THALFS=.693/ABS(NSP)
C      NDHSP=.11*ABS(WSP/NSP)

C      LATERAL STAB DERIVATIVES AND COEFFICIENTS*********

       EPSIL=2.*CL/3.14159/AR
       TAU(I)=SC/S
       NDS=.724+3.06*(SV/S)/(1.+COS(SA))+.4*ZWW/D+.009*AR
       KN=.001
       KRI=1.
       SFS=4.8
       LF=5.1
       CNBF=-KN*KRI*SFS/S*LF/B
       ATAV=QV/Q
       ZV=.178

C      *********LATERAL COEFFICIENTS*************

       CYB=-NDS*SV/S*CLAV
       CYP=0.
       CYR=-2.*LV/B*CYB
       CNB=CNBF+VV*CLAV*NDS
       CLP=-CLA/12.*(1.+3.*LAMBDA)/(1.+LAMBDA)
       CNR=-CDO/4.-2.*ATAV*VV*LV/B*CLAV
       CLB=-.0003*DIHED
       CNP=CL/8.*(1.-DEDA)
       CLR=CL/4.-2.*LV/B**2*ZV*CYB

C     ********* LATERAL DERIVATIVES*************

       YB=Q*S*CYB/MASS
       YP=Q*S*B*CYP/2./MASS/U
       YR=Q*S*B*CYR/2./MASS/U
       LB=Q*S*B*CLB/IX(I)
       LP=Q*S*B*CLP/2./IX(I)/U*B
       LR=Q*S*B*CLR/2./IX(I)/U*B
       NB=Q*S*B*CNB/IZ
       NP=Q*S*B**2*CNP/2./IZ/U
       NR=Q*S*B**2*CNR/2./IZ/U

C      *********  LATERAL APPROXIMATIONS ********

C      *******  SPIRAL    *********

C      LSPIRL(I)=(LB*NR-LR*NB)/LB

C      *******  ROLL      *********

       LROLL=LP
       TAU(I)=-1./LP

C      *******  DUTCH ROLL*********

       WNDR(I)=SQRT((YB*NR-NB*YR+U*NB)/U)
       ZDR(I)=-((YB+U*NR)/U)/2./WNDR(I)
       WZ(I)=WNDR(I)*ZDR(I)

       Y(I,1)=ZP(I)
       Y(I,2)=ZSP(I)
       Y(I,3)=ZDR(I)
       Y(I,4)=WNDR(I)
       Y(I,5)=WZ(I)

C      write(1,*)'       U          Zp          Zsp          Zdr          Wndr
C          W*Zdr       LSPIRL(I)          TAU(I)
C      WRITE(IWR,*)U(I),ZP(I),ZSP(I),Zdr(I),WNDR(I),WZ(I),(I),TAU(I)
```

APPENDIX G

```
 79 CONTINUE

    CALL TPLOT (-011, IX, Y, 100, 100, 5)
    CALL TLABEL('Ix                                    ', ' Zp(black), Zsp(r),
   . Zdr(gr), Wndr(blue), W*Zdr(cyan)')
    CALL TITLE ('Design Ix +/_ 10% vs.  Zp, Zsp, Zdr, Wndr, W*Zdr')

    STOP
    END
```

APPENDIX H

```
      PROGRAM DESIGN
C     ********************************
C     *                              *
C     *  PAUL H. EDWARDS             *
C     *  AERO 441: AEROSPACE DESIGN  *
C     *  GROUP D                     *
C     *  STATIC STABILITY PROGRAM    *
C     *                              *
C     ********************************
      REAL IWING,ITAIL,LF,LT,KF,LFF,LC,NETA,NETAC,IF,MFL
      DIMENSION ALPHA(12),CMCGW(12),CMCGF(12),CMCGC(12),CMCGT(12),DX(20)
     &,CMOFP(20),CMCGO(12),X(12),Y(12,5),DEGREE(12),CM(12,3),CN(10),RUDA
     &NG(10),RUDRAD(10)
      WRITE (1,*) 'INPUT IWR INTEGER'
      READ (1,*) IWR
      WRITE (1,*) 'IF PRIME PLOT IS DESIRED INPUT: 1, IF TEXTRONIKS PLOT
     & IS DESIRED, INPUT ANY INTEGER OTHER THAN 1'
      READ (1,*) M
      WRITE (1,*) 'INPUT: 1 FOR COMPONENT CONTRIBUTION PLOT, INPUT: 2 FO
     &R ELEVATOR DEFLECTION PLOT, INPUT:3 FOR RUDDER CONTROL PLOT '
      READ (1,*) N

      PI=3.1415927
      SHT=0.834
      SVT=0.280
      AR=10.0
      ART=5.0
      C=0.46
      B=4.64
      S=B**2/AR
      LT=1.321
      ALPHOW=-0.122173
C     **DF=DIAMETER (DIAGONAL) OF FUSELAGE
      DF=0.2156
C     **DTS=DIAMETER OF THE TAIL BOOM (6")
      DTS=0.1524
      VTAIL=49.3
      VWING=44.0
      ITAIL=-1.5*2.0*PI/360.0
      IWING=0.0523599
      NETA=VTAIL**2/VWING**2
      E=0.91
      VH=(LT*SHT)/(S*C)
C     **CLLAW=CL ALPHA OF WING CROSS SECTION
      CLLAW=5.72
C     **CLAW=CL ALPHA OF THE WING
      CLAW=CLLAW/(1+CLLAW/(PI*E*AR))

C     **TAIL CONTRIBUTION TO CM ALPHA**
C     **DEDALF=dE/dANG
      DEDALF=2*CLAW/(PI*AR)
      CLLAT=6.0876766
      CLAT=CLLAT/(1+CLLAT/(PI*E*ART))
C     **FR=FINENESS RATIO
      LF=1.55
      FR=LF/DF
      CMOT=NETA*VH*CLAT*(IWING-ITAIL)
      CMAT=-NETA*VH*CLAT*(1-DEDALF)

C     **TEST SPECIMEN CONTRIBUTION TO CM ALPHA**
      RHO=1.2250
      ICANRD=0.0
      RLTS=0.295929
      LC=-0.295929
      SC=((16*2.54)/100.)*((5*12*2.54)/100.)
      VHC=(LC*SC)/(S*C)
      VHCR=(RLTS*SC)/(S*C)
      CLLAC=2*PI
      ARC=3.75
      CLAC=CLLAC*(1+CLLAC/(PI*E*ARC))
      NETAC=0.9
      CMAC=-NETAC*VHC*CLAC*(1-DEDALF)
      CMOC=NETAC*VHC*CLAC*(ICANRD-IWING)
      CLC=CLAC*20.0*2.0*PI/360.0
      VELL=20.0
      VELH=44.0
```

APPENDIX H

```
      GMCL=CLC*0.5*RHO*(VELL**2)*SC*RLTS
      GMCH=CLC*0.5*RHO*(VELH**2)*SC*RLTS
C
C     **WING CONTRIBUTION TO CM ALPHA**
C       WRITE (1,*) 'INPUT VALUE FOR X CG (IN METERS)'
C       READ (1,*) XCG
        XCG=0.229
C       WRITE (1,*) 'INPUT VALUE FOR X AC (IN METERS)'
C       READ (1,*) XAC
        XAC=0.25
        CMACW=-0.12
        CLOW=0.7
        CMAW=CLAW*(XCG/C-(XAC/C))
        CMOW=CMACW+CLOW*((XCG/C)-(XAC/C))
C
C     **FUSELAGE CONTRIBUTION TO CM ALPHA**
        AW=CLAW*2*PI/360.0
        WRITE (1,*) 'INPUT EMPIRICAL FACTOR (KF)'
        READ (1,*) AKF
        KF=AKF/57.3
        LFF=LF*3.2808
        DFF=DF*3.2808
        CF=C*3.28080
C       WRITE (1,*) 'INPUT WING SURFACE AREA IN SQUARE FEET'
C       READ (1,*) SF
        SF=23.12
        DCMDCL=KF*DFF**2*LFF/(SF*CF*AW)
        CMAF=DCMDCL*ALPHOW
C       WRITE (1,*) 'INPUT TOTAL FUSELAGE LENGTH'
C       READ (1,*) TFL
        TFL=1.55
C       WRITE (1,*) 'INPUT MAIN FUSELAGE LENGTH'
C       READ (1,*) MFL
        MFL=0.5452
C       WRITE (1,*) 'INPUT MAXIMUM FUSELAGE DIAMETER'
C       READ (1,*) WFI
        WFI=0.2156
C       WRITE (1,*) 'INPUT TAIL BOOM DIAMETER'
C       READ (1,*) TBD
        TBD=0.1524
C       WRITE (1,*) 'INPUT THE WING ZERO-LIFT ANGLE RELATIVE TO FUSELAGE R
C      %EFERENCE LINE'
C       READ (1,*) ALFOW
        ALFOW=-0.0698132
C       WRITE (1,*) 'INPUT THE FUSELAGE INCIDENCE ANGLE FOR THE TAIL BOOM'
C       READ (1,*) TBIA
        TBIA=0.1332243
C       WRITE (1,*) 'INPUT THE CORRECTION FACTOR FOR BODY FINENESS RATIO'
C       READ (1,*) CF
        CF=0.9
        CX=TFL/20.0
        RMFL=MFL/20.0
        CMOFS=0.0
        DO 10 J=1,20
           DX(J)=CX*REAL(J)
           IF (DX(J) .LE. RMFL) THEN
              IF=0.0
              WF=WFI
           ELSE
              IF=TBIA
              WF=TBD
           END IF
           CMOFP(J)=(CF/(36.5*S*C))*WF**2*(ALFOW+IF)*DX(J)
           CMOFS=CMOFP(J)*CMOFS
10      CONTINUE
        CMOF=CMOFS
C
C     **TOTAL PITCHING MOMENT FOR AIRPLANE**
        DO 20 I=1,12
           ALPHA(I)=REAL(I)*2.0*PI/360.0
           DEGREE(I)=REAL(I)
           CMCGW(I)=CMOW+CMAW*ALPHA(I)
           CMCGF(I)=CMOF+CMAF*ALPHA(I)
           CMCGC(I)=CMOC+CMAC*ALPHA(I)
           CMCGT(I)=CMOT+CMAT*ALPHA(I)
           CMCGO(I)=CMCGW(I)+CMCGF(I)+CMCGC(I)+CMCGT(I)
```

APPENDIX H

```
153)  20     CONTINUE
154)         CMO=CMOW+CMOF+CMOC+CMOT
155)
156)  C    **TOTAL CM ALPHA FOR AIRPLANE**
157)         CMAOA=CMAT+CMAW+CMAF+CMAC
158)
159)  C    **EFFECT OF ELEVATOR DEFLECTION ON CM FOR TAIL**
160)         CMDE=-VH*NETA*CLAT
161)         DO 40 J=1,3
162)            IF (J .EQ. 1) THEN
163)               DEDEG=-10.0
164)               DERAD=DEDEG*2.0*PI/360.0
165)            ELSE IF (J .EQ. 2) THEN
166)               DEDEG=0.0
167)               DERAD=0.0
168)            ELSE IF (J .EQ. 3) THEN
169)               DEDEG=10.0
170)               DERAD=DEDEG*2.0*PI/360.0
171)            END IF
172)            DO 30 I=1,12
173)               CM(I,J)=CMO+CMAOA*ALPHA(I)+CMDE*DERAD
174)  30        CONTINUE
175)  40    CONTINUE
176)
177)         IF (N .EQ. 1) THEN
178)  C    **PLOT FOR CM CG VERSUS ANGLE OF ATTACK**
179)            DO 60 I=1,5
180)               DO 50 K=1,12
181)                  X(K)=DEGREE(K)
182)                  IF (I .EQ. 1) THEN
183)                     Y(K,I)=CMCGW(K)
184)                  ELSE IF (I .EQ. 2) THEN
185)                     Y(K,I)=CMCGC(K)
186)                  ELSE IF (I .EQ. 3) THEN
187)                     Y(K,I)=CMCGF(K)
188)                  ELSE IF (I .EQ. 4) THEN
189)                     Y(K,I)=CMCGT(K)
190)                  ELSE
191)                     Y(K,I)=CMCGO(K)
192)                  END IF
193)  50           CONTINUE
194)  60        CONTINUE
195)            IF (M .EQ. 1) THEN
196)               CALL PLOT(2,X,Y,12,12,5)
197)            ELSE
198)               CALL TPLOT(-011,X,Y,12,12,5)
199)               CALL TLABEL('ANGLE OF ATTACK (DEGREES)','CM C.G.')
200)               CALL TITLE('COMPONENT CONTRIBUTION TO PITCHING MOMENT')
201)            END IF
202)         ELSE IF (N .EQ. 2) THEN
203)            IF (M .EQ. 1) THEN
204)               CALL PLOT(2,DEGREE,CM,12,12,3)
205)            ELSE
206)               CALL TPLOT(-011,DEGREE,CM,12,12,3)
207)               CALL TLABEL('ANGLE OF ATTACK (DEGREES)','CM FOR TAIL')
208)               CALL TITLE('EFFECT OF ELEVATOR DEFLECTION ON CM FOR TAIL')
209)            END IF
210)         END IF
211)
212)  C    **TRIM CONTROL EFFECTIVENESS**
213)         TAU=1.0
214)  C    **DCLTDE=dCL TAIL/ d DELTA ELEVATOR
215)         DCLTDE=CLAT*TAU
216)         CMDET=-VH*NETA*DCLTDE
217)         CLTRIM=0.8
218)         CLDET=(SHT/S)*NETA*DCLTDE
219)         TRIMAN=-(CMOT*CLAT+CMAOA*CLTRIM)/(CMDET*CLAT-CMAT*CLDET)
220)         TRIMDE=TRIMAN*360.0/(2.0*PI)
221)
222)  C    **STATIC MARGINS**
223)         CLATP=0.0
224)         F=0.0
225)         XNPP=XAC/C+VH*NETA*(CLATP/CLAW)*(1-DEDALF)
226)         XNP=XNPP+(1-F)*VH*NETA*(CLAT/CLAW)*(1-DEDALF)
227)  C    **SFXSM=STICK FIXED STATIC MARGIN
228)         SFXSM=XNP-(XCG/C)
```

APPENDIX H

```
C     **SFRSM=STICK FREE STATIC MARGIN
        SFRSM=XNPP-(XCG/C)

C     **STATIC DIRECTIONAL STABILITY**
        RKN=0.002
        RKL=1.3
        SFS=0.4299651
        CNBWF=-RKN*RKL*SFS*TFL/(S*B)
        CLAV=3.043
        SV=0.28
        VV=(LT*SV)/(S*C)
        ANGQC=0.0
        ZW=0.381
        D=WFI/2.0
        CNBV=VV*CLAV*(0.724+3.06*(SV/S)/(1+ANGQC)+0.4*ZW/D+0.009*AR)
        CNBETA=CNBWF+CNBV

C     **DIRECTIONAL CONTROL CHARACTERISTICS**
C     **DCLVDR=dCLv/dDELTA RUDDER
        TAUV=0.50
        DCLVDR=CLAT*TAUV
        CNDR=-NETA*VV*DCLVDR
        QW=0.5*RHO*VWING**2
        QV=0.5*RHO*VTAIL**2
        DO 70 K=1,10
           RUDANG(K)=REAL(K)
           RUDRAD(K)=RUDANG(K)*2.0*PI/360.0
           CN(K)=CNDR*RUDRAD(K)
70      CONTINUE
        IF (N .EQ. 3) THEN
           IF (M .EQ. 1) THEN
              CALL PLOT(2,RUDANG,CN,10,10,1)
           ELSE IF (M .EQ. 2) THEN
              CALL TPLOT(-011,RUDANG,CN,10,10,1)
              CALL TLABEL('RUDDER DEFLECTION','CN FOR VERTICAL TAIL')
              CALL TITLE('RUDDER CONTROL EFFECTIVENESS')
           END IF
        END IF

        WRITE (IWR,*) 'VH FOR TAIL IS: ',VH
        WRITE (IWR,*) 'VH FOR TEST SPECIMEN IS: ',VHCR
        WRITE (IWR,*) 'CM ALPHA TAIL IS: ',CMAT
        WRITE (IWR,*) 'CM 0 FOR TAIL IS: ',CMOT
        WRITE (IWR,*) 'CM ALPHA WING IS: ',CMAW
        WRITE (IWR,*) 'CM 0 FOR WING IS: ',CMOW
        WRITE (IWR,*) 'CM ALPHA FUSELAGE IS: ',CMAF
        WRITE (IWR,*) 'CM 0 FOR FUSELAGE IS: ',CMOF
        WRITE (IWR,*) 'CM ALPHA TEST SPECIMEN IS: ',CMAC
        WRITE (IWR,*) 'CM 0 FOR TEST SPECIMEN IS: ',CMOC
        WRITE (IWR,*) 'CM ALPHA OVERALL IS: ',CMAOA
        WRITE (IWR,*) 'CM 0 OVERALL IS: ',CMO
        WRITE (IWR,*) 'ELEVATOR ANGLE FOR TRIM: ',TRIMDE
        WRITE (IWR,*) 'CN BETA IS EQUAL TO: ',CNBETA
        WRITE (IWR,*) 'STICK FIXED STATIC MARGIN IS: ',SFXSM
        WRITE (IWR,*) 'STICK FREE STATIC MARGIN IS: ',SFRSM
        WRITE (IWR,*) 'MOMENT ABOUT TEST SPECIMEN:  20 M/S',GMCL
        WRITE (IWR,*) 'MOMENT ABOUT TEST SPECIMEN:  44 M/S',GMCH
        STOP
        END
```

APPENDIX H

```
VH FOR TAIL IS:          1.11244
VH FOR TEST SPECIMEN IS:      0.185068
CM ALPHA TAIL IS:        -4.15330
CM 0 FOR TAIL IS:         0.468297
CM ALPHA WING IS:        -0.217594
CM 0 FOR WING IS:        -0.151957
CM ALPHA FUSELAGE IS:    -3.737927E-04
   0 FOR FUSELAGE IS:     0.000000E+00
   ALPHA TEST SPECIMEN IS:       1.15622
CM 0 FOR TEST SPECIMEN IS:     8.691178E-02
CM ALPHA OVERALL IS:        -3.21504
CM 0 OVERALL IS:          0.403252
ELEVATOR ANGLE FOR TRIM:       -1.94927
CN BETA IS EQUAL TO:          2.98392
STICK FIXED STATIC MARGIN IS:      0.917031
STICK FREE STATIC MARGIN IS:     4.565215E-02
MOMENT ABOUT TEST SPECIMEN:  20 M/S       156.208
MOMENT ABOUT TEST SPECIMEN:  44 M/S       756.049
```

-970

APPENDIX I

```
      PROGRAM TAIL
C     ***********************************
C     *                                 *
C     *  PAUL H. EDWARDS                *
C     *  AERO 441:  AEROSPACE DESIGN    *
C     *  GROUP D                        *
C     *  INDIVIDUAL TRADE STUDY         *
C     *  TAIL SURFACE SIZING PROGRAM    *
C     *                                 *
C     ***********************************
      DIMENSION SHT(50),SVT(50),ART(7),CLAT(7),VH(50),CMOT(50,7),CNBV(50
     &,7),CMAT(50,7),X(50),Y(50,7),VV(50),CLT(7),FTH(50,7),FTL(50,7),DTL
     &(50,7),DTH(50,7)
      REAL LT,NETA,IWING,ITAIL
      WRITE (1,*) 'INPUT IWR INTEGER'
      READ (1,*) IWR
      WRITE (1,*) 'INPUT: 1 IF PRIME PLOT IS DESIRED, OTHERWISE INPUT: 2
     & FOR TEKTRONIXS PLOT'
      READ (1,*) M
      WRITE (1,*) 'INPUT: 1 FOR HORIZONTAL TAIL SIZE PLOT, INPUT: 2 FOR
     &VERTICAL TAIL SIZE PLOT, INPUT: 3 FOR LOW SPEED CONTROL PLOT, INPU
     &T: 4 FOR HIGH SPEED CONTROL PLOT'
      READ (1,*) N
      LT=1.32
      C=0.46
      S=2.15296
      E=0.91
      AR=10.0
      ZW=0.381
      D=0.2156/2.0
      PI=3.1415927
      CLLAW=5.72
      CLAW=CLLAW/(1+CLLAW/(PI*E*AR))
      CLLAT=6.0876
      VTAIL=49.3
      VWING=44.0
      NETA=VTAIL**2/VWING**2
      RHO=1.2250
      VELL=20.0
      VELH=44.0
      DEDALF=2*CLAW/(PI*AR)
      IWING=-3.0*2.0*PI/360.0
      ITAIL=0.0
      DO 20 K=1,7
         ART(K)=REAL(K)
         CLAT(K)=CLLAT/(1+CLLAT/(PI*ART(K)))
         CLT(K)=CLAT(K)*10.0*2.0*PI/360.0
         DO 10 I=1,50
            SHT(I)=REAL(I)/50.0
            SVT(I)=REAL(I)/50.0
            VH(I)=(LT*SHT(I))/(S*C)
            VV(I)=(LT*SVT(I))/(S*C)
            CMOT(I,K)=NETA*VH(I)*CLAT(K)*(IWING-ITAIL)
            CMAT(I,K)=-NETA*VH(I)*CLAT(K)*(1-DEDALF)
            CNBV(I,K)=VV(I)*CLAT(K)*(0.724+3.06*SVT(I)/S+0.4*ZW/D+0.0
     &09*AR)
            DTL(I,K)=CLT(K)*0.5*RHO*(VELL**2)*SHT(I)
            DTH(I,K)=CLT(K)*0.5*RHO*(VELH**2)*SHT(I)
            FTL(I,K)=DTL(I,K)*LT
            FTH(I,K)=DTH(I,K)*LT
10       CONTINUE
20    CONTINUE
      DO 40 J=1,7
         DO 30 L=1,50
            X(L)=VH(L)
            Y(L,J)=CMAT(L,J)
30       CONTINUE
40    CONTINUE
      IF (N .EQ. 1) THEN
         IF (M .EQ. 1) THEN
            CALL PLOT(2,X,Y,50,50,7)
         ELSE
            CALL TPLOT(-011,X,Y,50,50,7)
            CALL TLABEL('TAIL VOLUME RATIO (VH)','CM ALPHA FOR TAIL')
            CALL TITLE('EFFECT OF TAIL VOLUME RATIO ON TAIL CM ALPHA')
         END IF
```

APPENDIX I

```
      ELSE IF (N .EQ. 2) THEN
          IF (M .EQ. 1) THEN
              CALL PLOT(2, VV, CNBV, 50, 50, 7)
          ELSE
              CALL TPLOT(-011, VV, CNBV, 50, 50, 7)
              CALL TLABEL('VERTICAL TAIL VOLUME RATIO', 'CN BETA FOR VERTIC
     &AL TAIL')
              CALL TITLE('EFFECT OF VERTICAL TAIL VOLUME RATIO ON DIRECTIO
     &NAL STABILITY')
          END IF
      ELSE IF (N .EQ. 3) THEN
          IF (M .EQ. 1) THEN
              CALL PLOT(2, SHT, FTL, 50, 50, 7)
          ELSE
              CALL TPLOT(-011, SHT, FTL, 50, 50, 7)
              CALL TLABEL('HORIZONTAL TAIL AREA (M^2)', 'TAIL MOMENT (N.)')
              CALL TITLE('MAXIMUM TAIL MOMENT CREATED VS. TAIL AREA: VELOC
     &ITY = 20 M/S')
          END IF
      ELSE IF (N .EQ. 4) THEN
          IF (M .EQ. 1) THEN
              CALL PLOT(2, SHT, FTH, 50, 50, 7)
          ELSE
              CALL TPLOT(-011, SHT, FTH, 50, 50, 7)
              CALL TLABEL('HORIZONTAL TAIL AREA (M^2)', 'TAIL MOMENT (N.)')
              CALL TITLE('MAXIMUM TAIL MOMENT CREATED VS. TAIL AREA: VELOC
     &ITY = 44 M/S')
          END IF
      END IF
      STOP
      END
```

Appendix J

```
C     ****   This is the structural analysis program for the
C     ****     sandwich concept.

      PROGRAM SIZE

      REAL*4 X(25,3)
      REAL*4 CARE(25)
      REAL*4 CCEN(25,2)
      REAL*4 FACC(25,2,2)
      REAL*4 FACL(25,2)
      REAL*4 IYY,IZZ,IYZ
      REAL*4 SD(100),FD(100),DEFL(100),Q(100),FDPHI(100),ROT(100)
      REAL*4 YPOS(100),VY(100),VZ(100),MX(100),MY(100),MZ(100)
      CHARACTER*4 ASTRG
      CHARACTER*10 FILENM

      WRITE (*,*) 'DO YOU WANT PRINTER SUMMARY ? (1=YES,2=to file)'
      READ (*,*) IPT
      IF (IPT.EQ.1) FILENM='LPT1:'
      IF (IPT.EQ.2) THEN
         WRITE(*,*) '       INPUT FILENAME TO SAVE TO'
         READ (*,'(A10)') FILENM
      ENDIF
      WRITE (*,*) 'DO YOU WANT DETAILS TO SCREEN ? (1=YES)'
      READ (*,*) ISC
      IF (IPT .NE. 0) THEN
      OPEN (3,FILE=FILENM,STATUS='NEW')
      WRITE (3,*) '      FACE       CORE                    MAX          TIP'
      WRITE (3,*) '   THICK(IN.)  LEN(IN.)    WT.(LB)  STRESS(PSI)    DEFLE
     &CTION(IN.)'
      WRITE (3,*) '-----------------------------------------------------
     &----------'
      ENDIF
      OPEN (2,FILE='MAXLOAD',STATUS='OLD')
       READ (2,199) SPAN
       READ (2,199) CHRD
  199  FORMAT (F8.3)
       READ (2,*) MS
      DO 11 IX=1,MS
   11  READ (2,200) YPOS(IX),VY(IX),VZ(IX),MX(IX),MY(IX),MZ(IX)
  200 FORMAT (1X,F8.3,F8.3,F8.3,F8.3,F8.3,F8.3)
      CLOSE (2)

      OPEN (2,FILE='AIRFOIL',STATUS='OLD')
      READ (2,*) N
      READ (2,*) CHORD
      DO 10 I=1,N
      READ (2,101) X(I,1),X(I,2),X(I,3)
      X(I,1)=X(I,1)*CHRD/CHORD
      X(I,2)=X(I,2)*CHRD/CHORD
      X(I,3)=X(I,3)*CHRD/CHORD
      FORMAT (F6.2,3X,F6.2,3X,F6.2)
   10 CONTINUE
      CLOSE (2)

      OPEN (2,FILE='MATPROP',STATUS='OLD')
      READ (2,199) EFAC
      READ (2,199) ECOR
      READ (2,199) FACDEN
```

```
      READ (2,199) SMAXFC
      READ (2,199) SMAXCO
      READ (2,199) GFAC
      READ (2,199) GCOR
      CLOSE (2)

      CONTINUE
      WRITE (*,*) 'INPUT DO YOU WANT A RANGE OF THICKNESSES 1=YES'
      READ (*,*) IRA

      IF (IRA.NE.1) THEN
      WRITE (*,*) 'INPUT THE THICKNESS OF THE FACING MATERIAL'
      READ (*,*) THICK
      ELSE
      WRITE (*,*) 'INPUT THE LOWEST THICKNESS'
      READ (*,*) TLO
      WRITE (*,*) 'INPUT THE HIGHEST THICKNESS'
      READ (*,*) THI
      WRITE (*,*) 'INPUT THE INCREMENT'
      READ (*,*) TINC
      NT=(THI-TLO)/TINC
      ENDIF

      WRITE (*,*) 'INPUT THE AMOUNT OF SPAN (FT.) FILLED WITH CORE'
      READ (*,*) CSPAN
      CSPAN=CSPAN*12.
      DO 99 IIT=0,NT+1
      IF (IRA .EQ. 1) THEN
         THICK=TLO+IIT*TINC
      ENDIF
C     CALCULATE INNER AREA AND PERIMETER
      PERIM=0.0
      AREA=0.0
      DO 20 I=1,N-1
         DX=X(I+1,1)-X(I,1)
         CARE(I)=.5*DX*(X(I,2)-X(I,3)+X(I+1,2)-X(I+1,3))
         AREA=AREA+CARE(I)

         IF (X(I,2) .LT. X(I+1,2)) THEN
            IL2=I
            IH2=I+1
         ELSE
            IL2=I+1
            IH2=I
         ENDIF
         IF (X(I,3) .GT. X(I+1,3)) THEN
            IL3=I
         ELSE
            IL3=I+1
         ENDIF

         AA=DX*(X(IL2,2)-X(IL3,3))
            IF (AA .LT. 0.0 ) WRITE (*,*) 'AA NEG AT I=',I
         ABLOB=AA
         CCEN(I,1)=AA*(X(I+1,1)+X(I,1))/2.
         CCEN(I,2)=AA*(X(IL2,2)+X(IL3,3))/2.
         AA=.5*DX*(X(IH2,2)-X(IL2,2))
         ABLOB=ABLOB+AA
         IF (IL2 .EQ. I) THEN
            XX=DX*2./3.+X(I,1)
         ELSE
            XX=DX/3.+X(I,1)
         ENDIF
            YY=(X(IH2,2)-X(IL2,2))/3.+X(IL2,2)
```

APPENDIX J

```
      AA=.5*DX*(X(IL3,3)-X(IH3,3))
      ABLOB=ABLOB+AA
      IF (IL3 .EQ. I) THEN
         XX=DX*2./3.+X(I,1)
      ELSE
         XX=DX/3.+X(I,1)
      ENDIF
         YY=(X(IH3,3)-X(IL3,3))/3.+X(IL3,3)
      CCEN(I,1)=CCEN(I,1)+AA*XX
      CCEN(I,2)=CCEN(I,2)+AA*YY
      CCEN(I,1)=CCEN(I,1)/ABLOB
      CCEN(I,2)=CCEN(I,2)/ABLOB

      FACL(I,1)=((X(I+1,1)-X(I,1))**2+(X(I+1,2)-X(I,2))**2)**.5
      FACL(I,2)=((X(I+1,1)-X(I,1))**2+(X(I+1,3)-X(I,3))**2)**.5
      PERIM=PERIM+FACL(I,1)+FACL(I,2)
      FACC(I,1,1)=(X(I+1,1)+X(I,1))/2.
      FACC(I,1,2)=(X(I+1,2)+X(I,2))/2.
      FACC(I,2,1)=FACC(I,1,1)
      FACC(I,2,2)=(X(I+1,3)+X(I,3))/2.
20    CONTINUE

      FACA=PERIM*THICK
      CVOL=AREA*CSPAN
      CWT=CVOL*CORDEN
      FACVOL=FACA*SPAN
      FWT=FACVOL*FACDEN
      TWT=CWT+FWT

      IF (ISC .EQ. 1) THEN
      WRITE (*,*) 'INNER AREA =',AREA
      WRITE (*,*) '       VOL  =',CVOL
      WRITE (*,*) 'CORE WEIGHT =',CWT
      WRITE (*,*)
      WRITE (*,*) 'PERIMETER = ',PERIM
      WRITE (*,*)
      WRITE (*,*) 'FACING AREA = ',FACA
      WRITE (*,*) '         VOL = ',FACVOL
      WRITE (*,*) 'FACING WEIGHT =',FWT
      WRITE (*,*) 'TOTAL WEIGHT = ',TWT
      ENDIF
C FIND MODULUS WEIGHTED SECTION PROPERTIES
      EREF=EFAC
      ASTAR=0.0
C  ASTAR
      DO 30 I=1,N-1
         ASTAR=ASTAR+(FACL(I,1)+FACL(I,2))*THICK
         ASTAR=ASTAR+ECOR/EREF*CARE(I)
30    CONTINUE

C  YSTAR
      YSTAR=0.0
      DO 40 I=1,N-1
         YSTAR=YSTAR+FACC(I,1,2)*FACL(I,1)*THICK
     &             +FACC(I,2,2)*FACL(I,2)*THICK
         YSTAR=YSTAR+ECOR/EREF*CCEN(I,2)*CARE(I)
      CONTINUE
      YSTAR=YSTAR/ASTAR


C  ZSTAR
      ZSTAR=0.0
      DO 50 I=1,N-1
```

APPENDIX J

```
         ZSTAR=ZSTAR+ECOR/EREF*CCEN(I,1)*CARE(I)
   50    CONTINUE
         ZSTAR=ZSTAR/ASTAR
```

APPENDIX J

```
C     /YSTAR
         IYY=0.0
         DO 60 I=1,N-1
            IYY=IYY+(FACC(I,1,1)-ZSTAR)**2*FACL(I,1)*THICK
        &          +(FACC(I,2,1)-ZSTAR)**2*FACL(I,2)*THICK
            IYY=IYY+ECOR/EREF*(CCEN(I,1)-ZSTAR)**2*CARE(I)
   60    CONTINUE


C     IZZSTAR
         IZZ=0.0
         DO 70 I=1,N-1
            IZZ=IZZ+(FACC(I,1,2)-YSTAR)**2*FACL(I,1)*THICK
        &          +(FACC(I,2,2)-YSTAR)**2*FACL(I,2)*THICK
            IZZ=IZZ+ECOR/EREF*(CCEN(I,2)-YSTAR)**2*CARE(I)
   70    CONTINUE



C     IYZSTAR
         IYZ=0.0
         DO 80 I=1,N-1
            IYZ=IYZ+(FACC(I,1,2)-YSTAR)*(FACC(I,1,1)-ZSTAR)*FACL(I,1)
        &                                                  *THICK
        &          +(FACC(I,2,2)-YSTAR)*(FACC(I,2,1)-ZSTAR)*FACL(I,2)
        &                                                  *THICK
            IYZ=IYZ+ECOR/EREF*(CCEN(I,2)-YSTAR)*(CCEN(I,1)-ZSTAR)*CARE(I)
   80    CONTINUE

         IF (ISC .EQ. 1) THEN
         WRITE (*,*) 'ASTAR =',ASTAR
         WRITE (*,*) 'YSTAR= ',YSTAR
         WRITE (*,*) 'ZSTAR= ',ZSTAR
         WRITE (*,*) 'IYYSTAR= ',IYY
         WRITE (*,*) 'IZZSTAR= ',IZZ
         WRITE (*,*) 'IYZSTAR= ',IYZ
         WRITE (*,*) '       PRESS RETURN TO CONTINUE'
         READ (*,'(A2)') ASTRG
         ENDIF




C NOW ANALYZE THE INTERNAL STRESS DISTRIBUTION

C     REDUCE THE STRESS EQN. TO SIGMA = E(Bz-Ay)
C       FIND A AND B

         AMZ=MZ(1)
         AMY=MY(1)
         A=(AMZ*IYY+AMY*IYZ)/(IYY*IZZ-IYZ**2)/EREF
         B=(AMY*IZZ+AMZ*IYZ)/(IYY*IZZ-IYZ**2)/EREF
```

APPENDIX J

```
      E=EFAC
      IF (ISC.EQ.1) THEN
      WRITE (*,*) 'THESE ARE THE STRESSES (PSI) IN THE IDEAL'
      WRITE (*,*) 'AREAS OF THE FACING'
      WRITE (*,*)  'TOP OF AIRFOIL   BOTTOM OF AIRFOIL'
      ENDIF
      SIGMAX=0.0
      DO 90 I=1,N-1
         YTOP=FACC(I,1,2)-YSTAR
         YBOT=FACC(I,2,2)-YSTAR
         ZTOP=FACC(I,1,1)-ZSTAR
         ZBOT=FACC(I,2,1)-ZSTAR
         SIGTOP=E*(B*ZTOP-A*YTOP)
         SIGBOT=E*(B*ZBOT-A*YBOT)
      IF (ABS(SIGTOP) .GT. ABS(SIGMAX)) SIGMAX=SIGTOP
      IF (ABS(SIGBOT) .GT. ABS(SIGMAX)) SIGMAX=SIGBOT
      IF (ISC .EQ. 1)  WRITE (*,*) SIGTOP,'                ',SIGBOT
   90 CONTINUE
      IF (ISC.EQ.1) THEN
      WRITE (*,*) '        PRESS RETURN TO CONTINUE            MAX SIGMA='
     &             ,SIGMAX
      READ (*,'(A2)') ASTRG
      ENDIF

      SIGMAX=ABS(SIGMAX)

C NOW ANALYZE THE INNER CORE STRESSES
      E=ECOR
      SCORMX=0.0
      IF (ISC.EQ.1) THEN
      WRITE (*,*) 'THESE ARE THE STRESSES (PSI) IN THE IDEAL'
      WRITE (*,*) 'AREAS OF THE INNER CORE'
      ENDIF
      DO 91 I=1,N-1
         Y=CCEN(I,2)-YSTAR
         Z=CCEN(I,1)-ZSTAR
         SIGMA=E*(B*Z-A*Y)
         IF (ABS(SIGMA) .GT. ABS(SCORMX)) SCORMX=SIGMA
         IF (ISC.EQ.1) WRITE (*,*) SIGMA
   91 CONTINUE
      IF (ISC.EQ.1) THEN
      WRITE (*,*) '        PRESS RETURN TO CONTINUE            MAX SIGMA='
     &             ,SCORMX
      READ (*,'(A2)') ASTRG
      ENDIF

C NOW FIND THE TIP DEFLECTION
C   FIRST GET THE SECOND DERIVATIVE
C
      DO 92 I=1,MS
   92    SD(I)=(MZ(I)*IYY+MY(I)*IYZ)/(IYY*IZZ-IYZ**2)/EREF
      FD(1)=0.0
      DO 93 I=2,MS
         DX=YPOS(I)-YPOS(I-1)
   93    FD(I)=FD(I-1)+SD(I-1)*DX
      DEFL(1)=0.0
      IF (ISC.EQ.1) THEN
      WRITE (*,*) 'BENDING IN Y DIRECTION (IN.)'
      WRITE (*,*) 1,DEFL(1)
      ENDIF
      DO 94 I=2,MS
         DX=YPOS(I)-YPOS(I-1)
         DEFL(I)=DEFL(I-1)+FD(I-1)*DX
```

```
      WRITE (*,*) '        PRESS RETURN TO CONTINUE'
      READ (*,'(A2)') ASTRG
      ENDIF
```

APPENDIX J

```
C NOW DO A TORSION ANALYSIS
C
      DO 95 I=1,MS
   95    Q(I)=MX(I)/2./AREA

      DO 96 I=1,MS
   96    FDPHI(I)=Q(I)*PERIM/2./AREA/GFAC/THICK

      ROT(0)=0.0

      IF (ISC.EQ.1) THEN
      WRITE (*,*) '                TWIST (DEG.)'
      WRITE (*,*) 0,0.0
      ENDIF
      DO 97 I=2,MS
         DX=YPOS(I)-YPOS(I-1)
         ROT(I)=ROT(I-1)+FDPHI(I-1)*DX
   97    IF (ISC.EQ.1) WRITE (*,*) I,ROT(I)*180.0/3.14159265
      IF (ISC.EQ.1) THEN
      WRITE (*,*) '        PRESS RETURN FOR NEW PARAMETERS'
      READ (*,'(A2)') ASTRG
      ENDIF

      IF (IPT.NE.0) WRITE (3,599) THICK,CSPAN,TWT,SIGMAX,DEFL(MS)

  599 FORMAT (5X,F5.3,5X,F5.1,5X,F6.3,5X,F7.0,10X,F7.5)
      CONTINUE

      GOTO 3
      END
```

Appendix K -

```
c*   ***   This is the structural analysis program for the three
c*******     spar concepts

      PROGRAM SIZE



      REAL*4 X(25,3)
      REAL*4 CARE(25)
      REAL*4 CCEN(25,2)
      REAL*4 FACC(6,2)
      REAL*4 FACL(6)
      REAL*4 CAPAR(6)
      INTEGER NS(2)
      REAL*4 IYY,IZZ,IYZ
      REAL*4 SD(100),FD(100),DEFL(100),Q(100),FDPHI(100),ROT(100)
      REAL*4 YPOS(100),VY(100),VZ(100),MX(100),MY(100),MZ(100)
      CHARACTER*4 ASTRG
      CHARACTER*10 FILENM

      WRITE (*,*) 'DO YOU WANT PRINTER SUMMARY ? (1=YES,2=to file)'
      READ (*,*) IPT
      IF (IPT.EQ.1) FILENM='LPT1:'
      IF (IPT.EQ.2) THEN
         WRITE(*,*) '       INPUT FILENAME TO SAVE TO'
         READ (*,'(A10)') FILENM
      ENDIF
      WRITE (*,*) 'DO YOU WANT DETAILS TO SCREEN ? (1=YES)'
      READ (*,*) ISC
      IF (IPT .NE. 0) THEN
      OPEN (3,FILE=FILENM,STATUS='NEW')
      WRITE (3,*) '  SPAR/CAP                    MAX          TIP
     & CAP'
      WRITE (3,*) '  THICK(IN.)    WT.(LB)  STRESS(PSI)    DEFL(IN.)      W
     &IDTH(IN.)'
      WRITE (3,*) '-----------------------------------------------------
     &----------'
      ENDIF
      OPEN (2,FILE='MAXLOAD',STATUS='OLD')
       READ (2,199) SPAN
       READ (2,199) CHRD
198    FORMAT (I5)
199    FORMAT (F8.3)
       READ (2,*) MS
      DO 11 IX=1,MS
 11    READ (2,200) YPOS(IX),VY(IX),VZ(IX),MX(IX),MY(IX),MZ(IX)
200   FORMAT (1X,F8.3,F8.3,F8.3,F8.3,F8.3,F8.3)
      CLOSE (2)

      OPEN (2,FILE='AIRFOIL',STATUS='OLD')
      READ (2,*) N
      READ (2,*) CHORD
      DO 10 I=1,N
      READ (2,101) X(I,1),X(I,2),X(I,3)
      X(I,1)=X(I,1)*CHRD/CHORD
      X(I,2)=X(I,2)*CHRD/CHORD
      X(I,3)=X(I,3)*CHRD/CHORD
101   FORMAT (F6.2,3X,F6.2,3X,F6.2)
```

APPENDIX K

```
      OPEN (2,FILE='MATPROP2',STATUS='OLD')
      READ (2,199) EFAC
      READ (2,199) ECOR
      READ (2,199) FACDEN
      READ (2,199) CORDEN
      READ (2,199) SMAXFC
      READ (2,199) SMAXCO
      READ (2,199) GFAC
      READ (2,199) GCOR
      READ (2,199) RIBTHI
      READ (2,198) NS(1)
      READ (2,198) NS(2)
      CLOSE (2)

  3   CONTINUE
      WRITE (*,*) 'INPUT DO YOU WANT A RANGE OF THICKNESSES 1=YES'
      READ (*,*) IRA

      IF (IRA.NE.1) THEN
      WRITE (*,*) 'INPUT THE THICKNESS OF THE SPAR MATERIAL'
      READ (*,*) THICK
      CAPTHK=THICK
      ELSE
      WRITE (*,*) 'INPUT THE LOWEST THICKNESS'
      READ (*,*) TLO
      WRITE (*,*) 'INPUT THE HIGHEST THICKNESS'
      READ (*,*) THI
      WRITE (*,*) 'INPUT THE INCREMENT'
      READ (*,*) TINC
      NT=(THI-TLO)/TINC
      ENDIF

      WRITE (*,*) 'INPUT THE NUMBER OF RIBS'
      READ (*,*) CSPAN
      CSPAN=CSPAN*RIBTHI
      WRITE (*,*) 'INPUT THE WIDTH OF THE CAP OF THE SPAR'
      READ (*,*) CAPWDT

      DO 99 IIT=0,NT+1
      IF (IRA .EQ. 1) THEN
         THICK=TLO+IIT*TINC
         CAPTHK=THICK
      ENDIF



C     CALCULATE INNER AREA AND PERIMETER

      PERIM=0.0
      AREA=0.0
      DO 20 I=1,N-1
         DX=X(I+1,1)-X(I,1)
         CARE(I)=.5*DX*(X(I,2)-X(I,3)+X(I+1,2)-X(I+1,3))
         AREA=AREA+CARE(I)

         IF (X(I,2) .LT. X(I+1,2)) THEN
            IL2=I
            IH2=I+1
         ELSE
            IL2=I+1
            IH2=I
         ENDIF
         IF (X(I,3) .GT. X(I+1,3)) THEN
```

APPENDIX K

```
      ELSE
         IL3=I+1
      ENDIF

      AA=DX*(X(IL2,2)-X(IL3,3))
         IF (AA .LT. 0.0 ) WRITE (*,*) 'AA NEG AT I=',I
      ABLOB=AA
      CCEN(I,1)=AA*(X(I+1,1)+X(I,1))/2.
      CCEN(I,2)=AA*(X(IL2,2)+X(IL3,3))/2.
      AA=.5*DX*(X(IH2,2)-X(IL2,2))
      ABLOB=ABLOB+AA
      IF (IL2 .EQ. I) THEN
         XX=DX*2./3.+X(I,1)
      ELSE
         XX=DX/3.+X(I,1)
      ENDIF
         YY=(X(IH2,2)-X(IL2,2))/3.+X(IL2,2)
      CCEN(I,1)=CCEN(I,1)+AA*XX
      CCEN(I,2)=CCEN(I,2)+AA*YY

      AA=.5*DX*(X(IL3,3)-X(IH3,3))
      ABLOB=ABLOB+AA
      IF (IL3 .EQ. I) THEN
         XX=DX*2./3.+X(I,1)
      ELSE
         XX=DX/3.+X(I,1)
      ENDIF
         YY=(X(IH3,3)-X(IL3,3))/3.+X(IL3,3)
      CCEN(I,1)=CCEN(I,1)+AA*XX
      CCEN(I,2)=CCEN(I,2)+AA*YY
      CCEN(I,1)=CCEN(I,1)/ABLOB
      CCEN(I,2)=CCEN(I,2)/ABLOB

      PERIM=PERIM
     &           +((X(I+1,1)-X(I,1))**2+(X(I+1,2)-X(I,2))**2)**.5
     &           +((X(I+1,1)-X(I,1))**2+(X(I+1,3)-X(I,3))**2)**.5

20    CONTINUE
      FACL(1)=CAPWDT
      FACL(2)=(X(NS(1),2)-X(NS(1),3))
      FACL(3)=CAPWDT
      FACL(4)=CAPWDT
      FACL(5)=(X(NS(2),2)-X(NS(2),3))
      FACL(6)=CAPWDT
      CAPAR(1)=FACL(1)*CAPTHK
      CAPAR(2)=FACL(2)*THICK
      CAPAR(3)=FACL(3)*CAPTHK
      CAPAR(4)=FACL(4)*CAPTHK
      CAPAR(5)=FACL(5)*THICK
      CAPAR(6)=FACL(6)*CAPTHK
      TOTSP=0.0
      DO 16 I=1,6
16       TOTSP=TOTSP+CAPAR(I)

      YCEN1=(X(NS(1),2)+X(NS(1),3))/2.
      YCEN2=(X(NS(2),2)+X(NS(2),3))/2.
      FACC(1,1)=X(NS(1),1)
      FACC(1,2)=X(NS(1),2)
      FACC(2,1)=X(NS(1),1)
      FACC(2,2)=X(NS(1),3)
      FACC(3,1)=X(NS(1),1)
      FACC(3,2)=X(NS(2),2)
      FACC(4,1)=X(NS(2),1)
      FACC(4,2)=X(NS(2),3)
      FACC(5,1)=X(NS(2),1)
```

```
      FACC(6,2)=X(NS(2),3)
```

APPENDIX K

```
      FACA=TOTSP
      CVOL=AREA*CSPAN
      CWT=CVOL*CORDEN
      FACVOL=TOTSP*SPAN
      FWT=FACVOL*FACDEN
      TWT=CWT+FWT

      IF (ISC .EQ. 1) THEN
      WRITE (*,*) 'INNER AREA =',AREA
      WRITE (*,*) '       VOL  =',CVOL
      WRITE (*,*) 'CORE WEIGHT =',CWT
      WRITE (*,*)
      WRITE (*,*) 'PERIMETER = ',PERIM
      WRITE (*,*)
      WRITE (*,*) 'SPAR AREA = ',FACA
      WRITE (*,*) '       VOL = ',FACVOL
      WRITE (*,*) 'SPAR WEIGHT =',FWT
      WRITE (*,*) 'TOTAL WEIGHT = ',TWT
      ENDIF
C FIND MODULUS WEIGHTED SECTION PROPERTIES
      EREF=EFAC
      ASTAR=0.0
C  ASTAR
      DO 30 I=1,6
         ASTAR=ASTAR+CAPAR(I)
   30 CONTINUE

C  YSTAR
      YSTAR=0.0
      DO 40 I=1,6
         YSTAR=YSTAR+CAPAR(I)*FACC(I,2)
   40 CONTINUE
      YSTAR=YSTAR/ASTAR


C  ZSTAR
      ZSTAR=0.0
      DO 50 I=1,6
         ZSTAR=ZSTAR+CAPAR(I)*FACC(I,1)
   50 CONTINUE
      ZSTAR=ZSTAR/ASTAR



C  IYYSTAR
      IYY=0.0
      DO 60 I=1,6
         IYY=IYY+(FACC(I,1)-ZSTAR)**2*CAPAR(I)
   60 CONTINUE


C  IZZSTAR
      IZZ=0.0
      DO 70 I=1,6
```

APPENDIX K

```
C  IYZSTAR
      IYZ=0.0
      DO 80 I=1,6
         IYZ=IYZ+(FACC(I,2)-YSTAR)*(FACC(I,1)-ZSTAR)*CAPAR(I)
   80 CONTINUE

      IF (ISC .EQ. 1) THEN
      WRITE (*,*) 'ASTAR =',ASTAR
      WRITE (*,*) 'YSTAR= ',YSTAR
      WRITE (*,*) 'ZSTAR= ',ZSTAR
      WRITE (*,*) 'IYYSTAR= ',IYY
      WRITE (*,*) 'IZZSTAR= ',IZZ
      WRITE (*,*) 'IYZSTAR= ',IYZ
      WRITE (*,*) '       PRESS RETURN TO CONTINUE'
      READ (*,'(A2)') ASTRG
      ENDIF



C NOW ANALYZE THE INTERNAL STRESS DISTRIBUTION

C     REDUCE THE STRESS EQN. TO SIGMA = E(Bz-Ay)
C       FIND A AND B

      AMZ=MZ(1)
      AMY=MY(1)
      A=(AMZ*IYY+AMY*IYZ)/(IYY*IZZ-IYZ**2)/EREF
      B=(AMY*IZZ+AMZ*IYZ)/(IYY*IZZ-IYZ**2)/EREF


C  FIRST ANALYZE THE FACING STRESSES
      E=EFAC

      IF (ISC.EQ.1) THEN
      WRITE (*,*) 'THESE ARE THE STRESSES (PSI) AT THE IDEAL'
      WRITE (*,*) 'AREAS OF THE SPARS'
      WRITE (*,*)  'TOP OF AIRFOIL   BOTTOM OF AIRFOIL'
      ENDIF
      SIGMAX=0.0
      DO 90 I=1,2
         YTOP=X(NS(I),2)-YSTAR
         YBOT=X(NS(I),3)-YSTAR
         ZTOP=X(NS(I),1)-ZSTAR
         ZBOT=X(NS(I),1)-ZSTAR
         SIGTOP=E*(B*ZTOP-A*YTOP)
         SIGBOT=E*(B*ZBOT-A*YBOT)
      IF (ABS(SIGTOP) .GT. ABS(SIGMAX)) SIGMAX=SIGTOP
      IF (ABS(SIGBOT) .GT. ABS(SIGMAX)) SIGMAX=SIGBOT
      IF (ISC .EQ. 1)  WRITE (*,*) SIGTOP,'              ',SIGBOT
   90 CONTINUE
      IF (ISC.EQ.1) THEN
      WRITE (*,*) '       PRESS RETURN TO CONTINUE            MAX SIGMA='
     &            ,SIGMAX
      READ (*,'(A2)') ASTRG
      ENDIF
```

```
      SIGMA=...(SIGMAX)

C NOW ANALYZE THE INNER CORE STRESSES
      E=ECOR
      SCORMX=0.0
      IF (ISC.EQ.1) THEN
      WRITE (*,*) 'THESE ARE THE STRESSES (PSI) IN THE IDEAL'
      WRITE (*,*) 'AREAS OF THE INNER CORE'
      ENDIF
      DO 91 I=1,N-1
         Y=CCEN(I,2)-YSTAR
         Z=CCEN(I,1)-ZSTAR
         SIGMA=E*(B*Z-A*Y)
         IF (ABS(SIGMA) .GT. ABS(SCORMX)) SCORMX=SIGMA
         IF (ISC.EQ.1) WRITE (*,*) SIGMA
   91 CONTINUE
      IF (ISC.EQ.1) THEN
      WRITE (*,*) '        PRESS RETURN TO CONTINUE              MAX SIGMA='
     &             ,SCORMX
      READ (*,'(A2)') ASTRG
      ENDIF

C NOW FIND THE TIP DEFLECTION
C   FIRST GET THE SECOND DERIVATIVE
C
      DO 92 I=1,MS
   92    SD(I)=(MZ(I)*IYY+MY(I)*IYZ)/(IYY*IZZ-IYZ**2)/EREF
      FD(1)=0.0
      DO 93 I=2,MS
         DX=YPOS(I)-YPOS(I-1)
   93    FD(I)=FD(I-1)+SD(I-1)*DX
      DEFL(1)=0.0
      IF (ISC.EQ.1) THEN
      WRITE (*,*) 'BENDING IN Y DIRECTION (IN.)'
      WRITE (*,*) 1,DEFL(1)
      ENDIF
      DO 94 I=2,MS
         DX=YPOS(I)-YPOS(I-1)
         DEFL(I)=DEFL(I-1)+FD(I-1)*DX
   94    IF (ISC.EQ.1) WRITE (*,*) I,DEFL(I)
      IF (ISC.EQ.1) THEN
      WRITE (*,*) '        PRESS RETURN TO CONTINUE'
      READ (*,'(A2)') ASTRG
      ENDIF


C NOW DO A TORSION ANALYSIS
C
      DO 95 I=1,MS
   95    Q(I)=MX(I)/2./AREA

      DO 96 I=1,MS
   96    FDPHI(I)=Q(I)*PERIM/2./AREA/GFAC/THICK

      ROT(0)=0.0

      IF (ISC.EQ.1) THEN
      WRITE (*,*) '                TWIST (DEG.)'
      WRITE (*,*) 0,0.0
      ENDIF
      DO 97 I=2,MS
         DX=YPOS(I)-YPOS(I-1)
         ROT(I)=ROT(I-1)+FDPHI(I-1)*DX
   97    IF (ISC.EQ.1) WRITE (*,*) I,ROT(I)*180.0/3.14159265
      IF (ISC.EQ.1) THEN
```

APPENDIX K

```
      READ (*,'(A2)') ASTRG
      ENDIF
```

APPENDIX K

```
      IF (IPT.NE.0) WRITE (3,599) THICK,TWT,SIGMAX,DEFL(MS),CAPWDT
      IF (IPT.EQ.0) WRITE (*,599) THICK,TWT,SIGMAX,DEFL(MS),CAPWDT
599   FORMAT (5X,F5.3,5X,F6.3,5X,F7.0,10X,F7.4,5X,F6.4)
      CONTINUE

      GOTO 3
      END
```

```
c     APPENDIX L
c
c     Trade Study Program for Aerospace Design 4/2/89
c
c     This program will calculate the Iyy, Izz, and Iyz for a
c     generalized elliptical cross section with a range of
c     eccentricity. The longeron areas are assumed to all be
c     the same, and they are positioned from zero with equal
c     angular displacements.
c
c
      real*8 iyy(50), izz(50), iyz(50)
      character*20 filnm
c
      pi=acos(-1.)
      write(9,*) 'Enter cross sectional area of longerons'
      read(9,*) al
      write(9,*) 'Enter number of longerons'
      read(9,*) nl
      write(9,*) 'Enter Y eccentricity maximum'
      read(9,*) yem
      write(9,*) 'Enter Y eccentricity step'
      read(9,*) yes
      write(9,*) 'Enter the useable section area desired'
      read(9,*) usa
c
      step=(2.*pi)/nl
      n=(yem-1)/yes
      theta=0.
      do 2 i=1,50
      iyy(i)=0.
      izz(i)=0.
      iyz(i)=0.
 2    continue
c
      do 5 i=1,n+1
      if(i .eq. 1) then
      e=yem
      else
      e=e-yes
      endif
      b=sqrt(usa/(2.*e))
      a=b*e
      do 10 j=1,nl
      if(j .eq. 1) then
      theta=0.
      else
      theta=theta+step
      endif
```

```
c     APPENDIX L
      ttheta=tan(theta)
      z=sqrt(((a**2)*(b**2))/(a**2+((b**2)*(ttheta**2))))
      y=ttheta*z
      iyy(i)=iyy(i)+((z**2)*al)
      izz(i)=izz(i)+((y**2)*al)
      iyz(i)=iyz(i)+(y*z*al)
 10   continue
 5    continue
c
      write(9,*) 'Enter output file name'
      read(9,100) filnm
      open(unit=40, file=filnm, status='new')
      step=(step/pi)*180.
      write(40,110) yem, nl, step
      write(40,*)
      write(40,*)
      write(40,*) 'Eccentricity      IYY      IZZ      IYZ'
      write(40,*)
      e=yem+yes
      do 15 i=1,n+1
      e=e-yes
      b=sqrt(usa/(2.*e))
      a=b*e
      xa=4.*e*(((a**2)*(b**2))/((e**2)*(b**2)+a**2))
      write(40,120) e,iyy(i), izz(i), iyz(i)
      write(40,170) a,b,xa
 15   continue
      write(40,*)
      write(40,*)
      do 25 i=1,4
      write(40,*)
      e=yem+yes
      do 30 j=1,n+1
      e=e-yes
      if(i .eq. 1) then
      write(40,130) e
      elseif(i .eq. 2) then
      write(40,140) iyy(j)
      elseif(i .eq. 3) then
      write(40,150) izz(j)
      else
      write(40,160) iyz(i)
      endif
 30   continue
 25   continue
      close(unit=40)
 100  format(a20)
 110  format('Max eccent.=',f8.6,tr5,'# long=',i2,tr5,'step=',f10.6)
```

```
c     APPENDIX L
 120  format(tr2,f6.4,tr10,f10.4,tr3,f10.4,tr3,f10.4)
 130  format(f8.6)
 140  format(f10.4)
 150  format(f10.4)
 160  format(f10.4)
 170  format(tr2,f18.8,tr2,f18.8,tr2,f18.8)
      stop
      end
```